THE JOURNAL
OF
CHEMICAL PHYSICS

VOLUME 9 JULY, 1941 NUMBER 7

The Infra-Red Absorption Spectrum of Propane

VIOLET L. WU* AND E. F. BARKER
Harrison M. Randall Laboratory of Physics, University of Michigan, Ann Arbor, Michigan

(Received April 17, 1941)

Of the twenty-seven internal degrees of freedom of propane, all nondegenerate, twenty-two may appear as fundamental absorption bands. These bands fall into three symmetry classes, designated A_1, B_1 and B_2, and distinguishable by their characteristic contours. Because of overlapping, however, it is impossible in many cases to determine their positions precisely. This is especially true in the regions of the C−H valence and deformation frequencies. Some ten or twelve fundamental bands may be identified with confidence as well as a number of combinations. An A_1 band at 870 cm^{-1} and a B_2 band at 748 cm^{-1} have been partially resolved, the line spacing being about 1.47 cm^{-1} in agreement with predictions based upon electron diffraction measurements. The fine structure of the B_1 bands has not been observed (the predicted spacing is 0.5 cm^{-1}) but the interval between maxima of the P and R branches is approximately 26 cm^{-1} as expected. With 24 cm-atmospheres of gas no bands were observed between 15μ and 35μ, although the symmetrical C−C deformation might be expected to produce a band of appreciable intensity within these limits. This frequency has apparently been observed in Raman spectra at 375 cm^{-1}.

SOME years ago the infra-red absorption spectrum of propane was investigated with a prism spectrometer by Bartholomé.[1] He found eleven bands between 14μ and 3.2μ, and eleven others, generally weaker, at wave-lengths below 3.2μ. They were not resolved sufficiently, however, to determine the characters of the associated motions. Several measurements of the Raman spectrum have also been reported,[2] and the distances between carbon atoms have been determined by means of electron diffraction.[3] This molecule belongs to the symmetry group C_{2v}, with the three carbon atoms forming an isosceles triangle whose vertex angle is obtuse. Twenty-seven internal degrees of freedom are indicated, without degeneracies. All the fundamental frequencies are permitted in Raman scattering, and twenty-two of the twenty-seven should be infra-red active.

Because of the relatively large moments of inertia, complete resolution of the rotational structure of the bands cannot be expected. Certain ones may be partially resolved, however, and for the others band envelopes may yield valuable information concerning the directions of oscillation of the electric moment, as has been shown by Dennison,[4] by Nielsen,[5] and by Badger and Zumwalt.[6] The last named authors have described the three different shapes of band envelopes to be expected for oscillations in different directions within the molecule. For propane $S \cong -0.90$ and $\rho \cong 2.7$ in their notation.** When the direction of oscillation of the electric moment

* Now at Hwa Nan College, Nanping, Fuchien, China.

[1] E. Bartholomé, Zeits. f. physik. Chemie **B23**, 152 (1933).

[2] P. Daure, Ann. de physique **12**, 375 (1929); S. Bhagavantam, Ind. J. Phys. **6**, 595 (1932); K. W. F. Kohlrausch and F. Köppl, Zeits. f. physik. Chemie **B26**, 209 (1934).

[3] L. Pauling and L. O. Brockway, J. Am. Chem. Soc. **59**, 1223 (1937).

[4] D. M. Dennison, Rev. Mod. Phys. **3**, 280 (1931).

[5] H. H. Nielsen, Phys. Rev. **38**, 1432 (1931).

[6] R. M. Badger and L. R. Zumwalt, J. Chem. Phys. **6**, 711 (1938).

** $S=(2b-a-c)/(a-c)$ and $\rho=(a-c)/b$, where a, b, and c are reciprocals of the principal moments of inertia, with $a>b>c$.

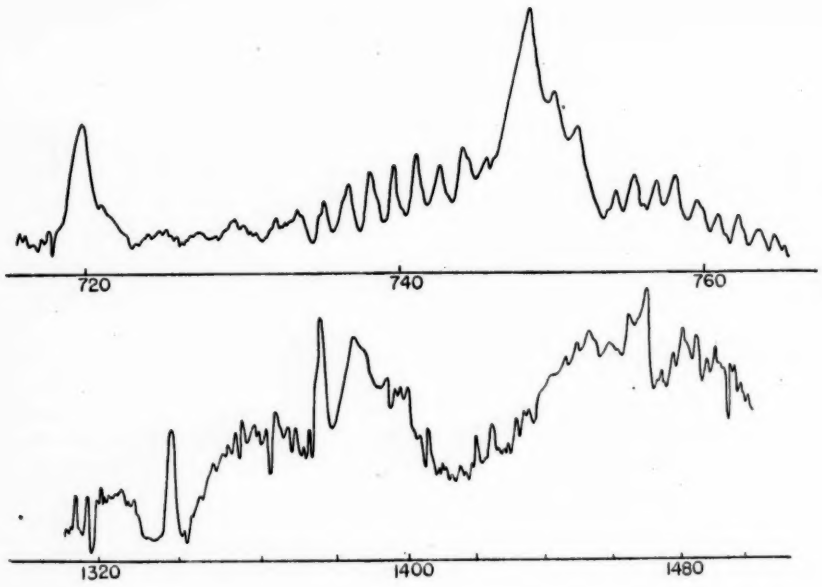

FIG. 1. The pair of B_2 bands near 13μ, and the δ_{CH} bands near 7μ.

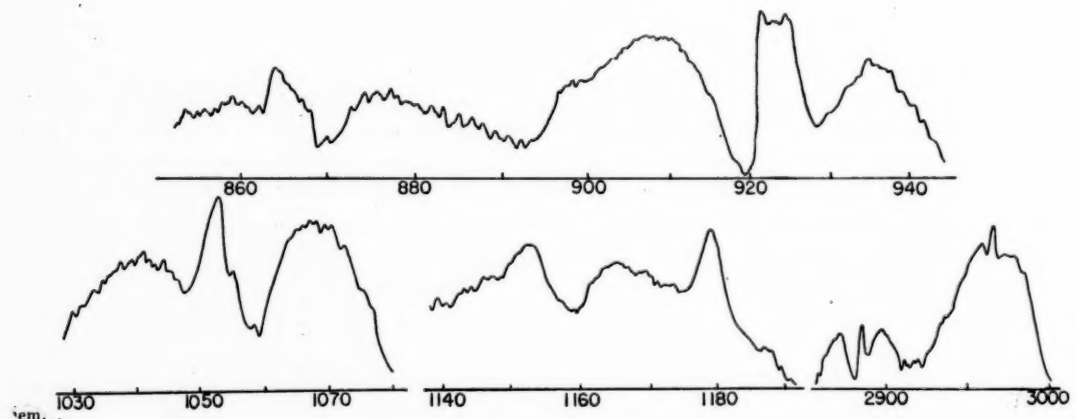

FIG. 2. Contours of several fundamental bands including the partially resolved A_1 band at 870 cm^{-1} and the B_1 combination band at 864 cm^{-1} (11.5μ).

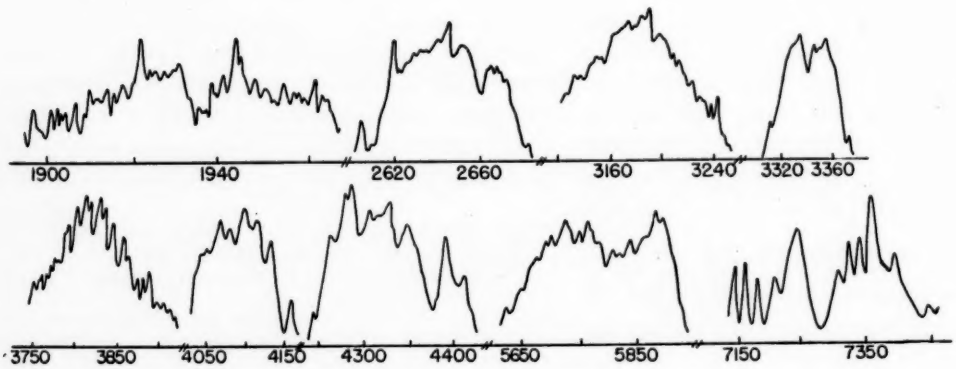

FIG. 3. Contours of harmonic and combination bands.

is along the twofold axis (the axis of the intermediate moment) the symmetrical motion falls in the class A_1, which includes nine modes of vibration. These bands are without obvious Q branches. The seven different motions in symmetry class B_1 are parallel to the plane of the carbon atoms but antisymmetric with respect to the twofold axis, hence the changes in electric moment are along the axis of minimum moment of inertia. The resulting bands have P, Q and R branches of comparable intensities, the Q branch being rather broad. The symmetry class B_2 includes six oscillations in which the changes of electric moment are along the axis of maximum moment of inertia, i.e., normal to the plane of the three carbon atoms. They give rise to bands with narrow and intense Q branches. A fourth symmetry class A_2 includes five symmetrical vibrations, none of which yield infra-red bands since they involve no change in electric moment.

Another rough but convenient classification of bands places them in three groups depending upon which particular atoms are principally involved in the motion. Only limiting cases are considered, and it must be remembered that the actual oscillations are not so simple; in general they involve linear combinations of the limiting cases. The first group includes motions primarily associated with the CH_2, the second includes the CH_3 oscillations, and the third those vibrations of the triangular structure formed by the three radicals each considered as rigid. This third group consists of nine torsional oscillations, three for each radical, and the three vibrations analogous to those of a symmetrical nonlinear triatomic molecule XY_2. The masses of the radicals being 15, 14 and 15, these last three frequencies should all lie below 1200 cm^{-1}. Dadieu and Kohlrausch[7] have predicted that the lowest one, corresponding to the symmetrical deformation, should occur at approximately 400 cm^{-1}. Subsequently Bhagavantam observed a Raman displacement at 377 cm^{-1}, and Kohlrausch and Köppl reported 373 cm^{-1}. There is in the Raman spectrum one sum band (1278 cm^{-1}) which seems to involve this frequency, but the corresponding difference has not been observed. Bartholomé failed to find any infra-red band near 375 cm^{-1}, and our own results are equally negative. It is interesting to note that the δ_{CC} vibration in propane appears to be so nearly inactive, since the corresponding infra-red band is very strong in nonlinear triatomic molecules.

[7] A. Dadieu and K. W. F. Kohlrausch, Akad. Wiss. Wien. 139, 165 (1930).

Experimental

We have examined the spectrum of propane between 1.35μ and 35μ with a prism grating spectrometer, using an absorption cell 25 cm in length. The windows were either of NaCl or of KBr. Since the instrument is not completely enclosed, atmospheric water and carbon dioxide interfere appreciably with the measurements in some regions. Three bands have been partially resolved, the contours for several others have been determined, and a number of new bands have been located. No absorption of measurable intensity was found between 13μ and 35μ. Figures 1 to 3 present the observed results. The effective slit widths and the amount of gas used in each case are indicated in Table I, while Table II lists the positions of the various bands, their apparent symmetry characters, and possible assignments. It must be emphasized that a completely unique scheme of assignments would require more information than is as yet available. Moreover, in regions where several bands overlap it is not always possible to identify the components without ambiguity; hence the precise positions must be uncertain in some cases. This is particularly true around 1400 cm^{-1} and 3000 cm^{-1} where the C—H vibrations occur. Some assistance in the interpretation of various bands is provided by data already available upon

Table I.

Spectral Region λ in Microns	Gas Pressure in cm 25-cm Cell	Effective Slit Widths in cm^{-1}
35–15	72	0.60
13.0	25	0.43
11.5	72	0.50
10.8	72	0.84
9.5–8.5	65	0.84
7.0	5	0.50
5.1	72	0.70
3.8	65	1.85
3.4	0.5	1.28
3.0	65	1.65
2.6	72	2.0
2.4–2.3	65	3.0
1.7–1.3	65	4.5

TABLE II. *Classification of the propane bands.*

	Symmetry Classes				Ethane	Analogs Ethylene	Cyclopropane
	A_1	A_2	B_1	B_2			
CH_2							
ν_σ				2980		3107, *3069*	3090
ν_π	2960					*3020*, 2988	
δ_π	*1450*					*1343*, 1444	*1453*, 1430
τ_σ			1152	1179		948, *943*	1020
						1015, *1035*	
τ_π		——				815	
CH_3							
ν_σ	*2966*	——	2968	2968	2980, *2965*		
ν_π	*2914*		*2942*		*2900*, 2955		
$2\delta_\sigma$	*2872*		2885	2885			
$2\delta_\pi$	*2722*						
δ_σ	1468	——	1465	1470	1461, *1463*		
δ_π	1370		1375		1375,* 1380		
τ_σ	*1149*	——	922	748	1170,* 831		
τ_π		——		——	275*		
C−C−C							
ν_σ			*1053*				
			1053				
ν_π	*867*				*993*	*1626*	*1184*, 865
	870						
δ_π	*375*						

* Not observed directly. Italics indicate Raman measurements. Subscripts π and σ indicate oscillations parallel to or perpendicular to the geometric axis of the group involved.

the analogous motions in ethane, ethylene and cyclopropane. These are also included in Table II.

Most of the A_1 frequencies are determined by Raman observations only, and for the liquid state. Two of the B_1 class also appear in Raman scattering as rather broad lines. The A_1 infra-red bands, lacking Q branches, are difficult to locate precisely unless isolated, as at 870 cm^{-1}. The methyl C−H valence vibrations apparently are complicated by resonance interaction, so that in class A_1 there are four Raman lines near 3000 cm^{-1}, and in each of the classes B_1 and B_2 at least two infra-red bands. These, of course, cannot be assigned individually to specific motions.

It is suggested that the B_2 band at 748 cm^{-1} arises from a rocking motion of the methyl radicals in a direction normal to the C_3 plane. For the corresponding motion parallel to the plane, the B_1 band at 922 cm^{-1} is proposed. Such specific assignments are perhaps hardly justified since both motions involve oscillations of the methylene also: in fact the pair of B_1 bands at 1152 and 922 cm^{-1}, and the pair of A_1 bands at 1179 and 748 cm^{-1}, are each combinations of the two limiting cases to which they have been assigned. The two normal frequencies in either case may have been quite close together, with the observed separation due to interaction.

The torsional motions τ_π of the methyl radicals around their own symmetry axes (in and out of phase) are of particular interest, but have not been identified. Their frequencies are probably low, and in consequence the excited states should be well populated. The transitions corresponding to any of the τ_σ oscillations may have somewhat different frequencies when the initial state is one of the τ_π excited levels. This would explain the broadening of the observed Q branches, particularly that of the 922 cm^{-1} band, which exhibits a second intense maximum at 925 cm^{-1}. Another possible interpretation, which, however, seems less probable, is to assign the frequencies 922 and 925 to the two infra-red τ_σ bands, and the frequency 748 to the τ_π band of type B_2.

The doublet type band at 870 cm^{-1} may be assigned with confidence to the symmetrical

TABLE III. *Observed values of $\Delta\nu_m$ for B_1 bands.*

ν	$\Delta\nu_m$	ν	$\Delta\nu_m$
923	27	1375	26
1053	26	1470	28
1152	26	2885	25

valence vibration of the C_3 framework. Apparently a second band, either of class B_1 or B_2, is superposed upon it, the Q branch appearing at 864 cm^{-1}. In the neighborhood of 1936 cm^{-1} a band is observed which, though only partially resolved, appears to be of the doublet (A_1) type, with a very irregular contour. This is probably a combination of the two B_1 bands at 922 and 1053 cm^{-1}. One other combination, observed as a Raman line, has already been mentioned; it is $1278=922(B_1)+375(A_1)$. Two moderately intense bands remain to be considered. They both have prominent Q branches, one at 1338 cm^{-1} and the other at 720 cm^{-1}; and they appear to belong to type B_2. No positive assertion regarding their origin can be made. Even the lower frequency seems much too high for the fundamental τ_π. It also seems too intense to represent the difference transition 1468–748. A possible explanation is that these two bands are sum and difference combinations of a low frequency A_2 band (τ_π) with the B_1 band at 1053. This would indicate a frequency of 333 cm^{-1} for one of the τ_π levels.

A number of other infra-red absorption regions have been observed, mostly at higher frequencies, representing multiple and combination bands. These are displayed in Fig. 3. Although some resolution is indicated, it seems hardly feasible at present to assign band centers, or to make definite assertions regarding their interpretation.

The B_2 band at 748.0 cm^{-1}, shown in Fig. 1, has been resolved into a fairly regular set of some twenty lines, almost equally spaced, as would be expected for a molecule having two nearly equal moments of inertia. By isolating the normal state a value of 1.475 cm^{-1} has been obtained for $h(a-d)/4\pi^2$, where a is the reciprocal of the smallest moment of inertia, and d is the mean of the reciprocals of the other two. The A_1 band at 870 cm^{-1} has also been partially resolved, with an average line interval in the R branch of 1.40 cm^{-1}. These frequency differences compare favorably with the value 1.47 computed for A_1 and B_2 bands using the C–C distances obtained by electron diffraction, and the C–H distance from methane. The corresponding line interval in the B_1 bands should be about 0.5 cm^{-1}, which could be observed only under very advantageous circumstances. The interval $\Delta\nu_m$ between maxima of the P and R branches in B_1 bands may be computed approximately, following Gerhard and Dennison,[8] its value being 26 cm^{-1}. Table III lists the values of $\Delta\nu_m$ observed for various B_1 bands. In Table IV the positions are given for the observed fine structure lines in the bands at 748 cm^{-1} and 870 cm^{-1}, and also for a number of the maxima appearing in the complex band near 1936 cm^{-1}.

TABLE IV. *Positions of observed lines in partially resolved bands.*

Band at 748 cm^{-1}		Band at 870 cm^{-1}		Band at 1936 cm^{-1}	
P	R	P	R	P	R
733.1	749.6	862.4	872.0	1914.9	1937.6
734.7	751.0	864.0	874.2	1916.8	1940.5
736.4	753.5	867.0	875.6	1918.7	1943.5
737.8	754.7		877.1	1922.3	1945.0
739.2	756.3		878.7	1924.5	1949.0
740.9	757.7		880.2	1926.0	1951.9
742.2	759.1		881.6	1927.7	1954.0
743.5	760.3		883.0	1930.6	1956.0
745.1	761.8		884.5	1934.0	
	763.4				

[8] S. L. Gerhard and D. M. Dennison, Phys. Rev. **43**, 197 (1933).

The Structure of Black Carbon

ADDISON H. WHITE AND LESTER H. GERMER
Bell Telephone Laboratories, 463 West Street, New York, New York

(Received April 10, 1941)

This paper is concerned with the structure of extremely small crystallites of carbon deposited upon silica by the pyrolysis of methane. Electron diffraction patterns have been obtained from more than 100 carbon films, from some by the reflection method, and from others by transmission after removing the films from their supports with hydrofluoric acid. In some of the specimens the individual crystallites are strongly oriented and reflection patterns obtained from these are approximations to rotation patterns from single crystals. From these patterns we have concluded that the films are made up of pseudo-crystals in each of which the carbon atoms are hexagonally arranged in planes as they are in graphite, but successive parallel atomic layers are displaced so that no regularities exist other than the uniform separation of the planes and the regular arrangement of atoms in each of them.

THE structure of what was formerly called amorphous carbon has been the subject of study by x-ray diffraction for many years, the first pattern from carbon having been obtained by Debye in 1916. Only powder patterns from randomly oriented small crystals have been studied.[1] From these it has been inferred that the structure of black carbon resembles that of graphite with discrepancies which increase with decreasing crystal size until, when the mean linear dimensions of the crystals are of the order of 20A, the pattern consists of only three distinguishable rings and resembles that of an amorphous material.[2] One can see that the number of measurable parameters is so limited that on the basis of such a pattern alone no deductions as to the arrangement of atoms in the smallest carbon crystallites can be confidently made. Nevertheless, structures have been assigned to the crystallites of such carbons by a sort of extrapolation from the results obtained from other carbons whose structures degenerate progressively from that of graphite.

We have obtained electron diffraction patterns from which the structures of such extremely small crystals can be reliably inferred without reference to any other carbon. In our experiments a marked degree of preferential orientation is observed, and the diffraction patterns are approximations to those which would be produced by a single crystal rotated about a principal axis. Such patterns yield evidence which is not available in the previously reported patterns from unoriented crystallites.

Representative electron diffraction patterns are reproduced in Figs. 1–3. The three films from which these patterns were obtained were prepared by deposition of carbon upon flat fused silica surfaces in a furnace containing methane and nitrogen[3] maintained at about 1000°C. The pattern of Fig. 1 was produced by electrons scattered by reflection from the surface of the deposited carbon. The thin films which gave the other two patterns were first removed by means of hydrofluoric acid from the silica plates on which they were formed, and each was then supported across a narrow slit in such a way that an electron beam could pass directly through it. The pattern of Fig. 2 was produced with the film normal to the electron beam, and that of Fig. 3 with the film rotated from a position normal to the beam by an angle of 45° about a horizontal axis.

On the original plate of the pattern of Fig. 1 one can observe six uniformly spaced diffuse spots or arcs lying along the center line. The best estimate of the separation between these is $s=6.4(0)$ mm, and from this the equivalent crystallographic spacing d can be calculated by

[1] X-ray diffraction patterns from oriented carbon crystallites were, however, obtained by M. Pirani and W. Fehse, Zeits. f. Elektrochemie **29**, 168–174 (1923).

[2] The most thorough investigation is that of V. Hoffman and D. Wilm, Zeits. f. Elektrochemie **42**, 504 (1936).

[3] The degree of orientation of the crystallites in the surface of the film which gave the pattern of Fig. 1 had been increased by mild oxidation in air, subsequent to the original deposition of the film.

FIG. 1. Electron diffraction pattern obtained by the reflection method from the surface of a film of carbon deposited upon fused silica by the pyrolysis of methane. (Reproduced 0.6 full size, $L\lambda = 2.34 \times 10^{-8}$ cm^2.)

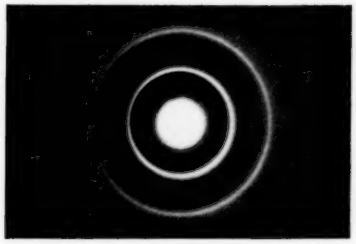

FIG. 2. Pattern by transmission at normal incidence from a carbon film deposited upon silica and subsequently removed with hydrofluoric acid.

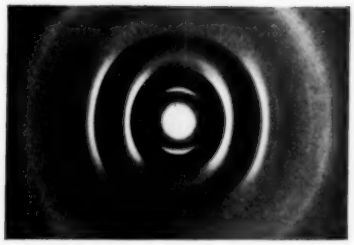

FIG. 3. Pattern from a carbon film inclined 45° to the primary beam, by rotation about a horizontal axis.

means of the relation $d = L\lambda/s$, where L is the distance from specimen to photographic plate and λ is the electron wave-length. Substituting for $L\lambda$ the independently determined value 2.34×10^{-8} cm^2, one obtains $d = 3.6(6)$A which is about 9 percent larger than $c_0/2 = 3.35$A, the separation between adjacent hexagonal planes in graphite. From the result of this comparison it is natural to infer that the pattern of Fig. 1 was produced by graphite-like crystallites oriented with their hexagonal planes predominantly parallel to the supporting quartz surface. If this inference is correct there must be features in Fig. 1 along a horizontal line through the primary beam position, insofar as the shadow of the specimen permits, which correspond to reflections having Miller indices of the form $(hk0)$, and perhaps also features at other positions corresponding to general indices (hkl). Crystallographic planes of the hexagonal system for which the third Miller index is zero make up a set having spacings inversely proportional to the square roots of the whole numbers 1, 3, 4, 7, 9, 12, 13$\cdots$ etc., and the radii of electron diffraction rings corresponding to these separations must be directly proportional to these square roots. Actually one can observe in Fig. 1 five features lying approximately along the horizontal line through the primary beam position, and the radii of these, as closely as they can be measured, are proportional to the square roots of the integers 1, 3, 4, 7 and 9. The calculated edge of the hexagonal cell is $a_0 = b_0 = 2.4(6)$A, which is just the corresponding value for graphite. There are, however, no traces whatsoever of features other than the $(00l)$ and $(hk0)$ reflections. The diffraction pattern thus gives no evidence of regularities in the structure of the individual crystallites in this specimen of black carbon other than in the arrangement of carbon atoms in the hexagonal planes and in the separation between these planes. The relative intensities of the different $(hk0)$ features correspond furthermore, as closely as we can estimate, to intensities to be expected from parallel but otherwise unrelated planes of carbon atoms, and not to intensities from crystallites having the complete graphite structure; relative to a corresponding pattern from oriented graphite crystals the "arcs" corresponding to the integers 3 and 9 are much too weak, although, of course, much stronger than similar features which would be produced by parallel but otherwise unrelated planes of atoms having a close packed arrangement. The separations and relative intensities of the $(hk0)$ features would have enabled us to deduce directly the arrangement and spacing of atoms in the separate planes, quite independently of knowledge of the graphite structure.

These deductions in regard to the structure of the carbon film are borne out by a more detailed consideration of the diffraction pattern. One can deduce very simply the pattern to be expected from an array of parallel and uniformly spaced but otherwise completely independent planes of carbon atoms. The lattice reciprocal to such a set of cross gratings is made up of the $(00l)$ spots of the graphite reciprocal lattice, and the surfaces of cylinders normal to the hexagonal planes and generated by (hk) lines which pass

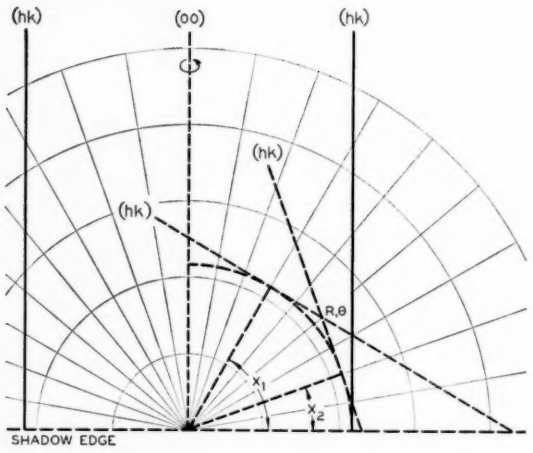

FIG. 4. Diagram illustrating the production of an (*hk*) diffraction feature of Fig. 1 by preferentially oriented cross gratings of carbon atoms.

through the points (*hk*0) of the graphite reciprocal lattice. For the case of hexagonal planes parallel to the surface and to the primary beam, the sphere of reflection, which is approximately a plane, intersects these cylinders in straight lines normal to the shadow edge. If the various pseudocrystallites are imperfectly aligned, with the hexagonal planes of many of them making small angles with the general surface, then the resulting diffraction lines will be distributed over an angular range about the normal to the shadow edge. The superposition of many such lines will be expected to give to each of the (*hk*) diffraction features the shape of a fountain, or narrow fan, appearing to diverge approximately from its intersection with the horizontal line through the primary beam position; one observes just this shape for those (*hk*0) features of Fig. 1 whose form can be clearly made out.

It is not difficult to calculate roughly the distribution of scattering intensity to be expected in one of the (*hk*) features of the pattern of Fig. 1. This distribution is quite approximately the same as it would be if the carbon planes were completely unrelated, and the calculation is carried out on that basis. Let χ represent the angle between the general plane of the surface and the planes of a set of parallel cross gratings, and assume that the number of gratings having normals lying in the element of solid angle $d\omega$ is proportional to $f(\chi)d\omega$. In Fig. 4 the plane of the paper is chosen to represent the sphere of reflection and the horizontal line through the origin its intersection with the plane of the specimen surface. The lattice reciprocal to each cross grating is the set of (*hk*) lines described earlier, and the reciprocal lattices of many planes parallel to each other form coaxial (*hk*) cylinders. The reciprocal lattice cylinders of those sets of parallel planes, which are parallel to the primary beam, will intersect the plane of Fig. 4 in straight lines. The broken reciprocal lattice lines (*hk*) correspond to the two orientations χ for which sets of cross gratings parallel to the primary beam contribute to the intensity at the point R, θ. The total intensity at R, θ is made up of increments from all sets of cross gratings whose normals are parallel to the tangents drawn from R, θ to the sphere of radius $R_0 = L\lambda/d$, where d is the spacing between the cross-grating lines which correspond to the feature under consideration. By assuming for the distribution function $f(\chi) = \exp(b\cos^2\chi)$ and integrating over all values of χ corresponding to gratings whose normals are parallel to these tangents, one finds that the number of gratings contributing to the intensity at R, θ is proportional to

$$(1-R_0^2/R^2)^{\frac{1}{2}}\int_{-1}^{+1}\exp\left[bB(x+A)^2\right]dx/(1-x^2)^{\frac{1}{2}}, \quad (1)$$

where

$$A=(R^2-R_0^2)^{\frac{1}{2}}(\tan\theta)/R_0 \text{ and } B=R_0^2(\cos^2\theta)/R^2.$$

One represents random orientation of cross gratings by setting $b=0$, and the number of gratings contributing to the intensity at R, θ for this case is proportional to $(1-R_0^2/R^2)^{\frac{1}{2}}$ as one sees by evaluating the integral. One can expect that the actual intensity at R, θ for $b\neq 0$ will be given by the ratio of these two quantities multiplied into the intensity at R, θ for random orientation. The latter as calculated by v. Laue[4] is $E^2/R(R^2-R_0^2)^{\frac{1}{2}}$. Here E, the atomic form factor, can be replaced[5] by $(Z-f)/R^2$ which, in the range with which we are concerned, is approximately proportional to $1/R$. In this way one finds that the intensity at R, θ will be approxi-

[4] M. v. Laue, Zeits. f. Krist. **82**, 133 (1932). This expression is infinite at $R=R_0$, due to the assumed unlimited extent of each grating. We understand that Dr. B. E. Warren has carried through the v. Laue calculation for the case of randomly oriented gratings of limited extent.

[5] N. F. Mott, Proc. Roy. Soc. **A127**, 658 (1930).

mately, $J=$ Expression (1)$/R^2(R^2-R_0^2)$. In order to determine the value of the constant b we have estimated that, for the (10) feature, the intensity in Fig. 1 is about one-tenth as great at $R=R_0$, $\theta=30°$, as at $R=R_0$, $\theta=0°$, and by numerical integration we have found that $b=8$ corresponds to a value of this intensity ratio of 9.4. Using this value ($b=8$) the intensity has been calculated[6] at various points within the (10) feature, and the values obtained are plotted as a contour diagram in Fig. 5. (The numbers on the contour lines of Fig. 5 are J multiplied by 50.) Except for the region close to $R=R_0$, where the assumption of unlimited extension of each grating introduces serious error, the calculated intensity distribution of Fig. 5 is similar to that which is apparent in Fig. 1. This seems to us to confirm the assumption that the various cross gratings of which each crystallite is composed are unrelated except for their parallelism and uniform separation. (One cannot, however, determine from the experiments whether or not successive atomic layers are merely displaced laterally in random fashion from their positions in the graphite lattice, or are both displaced and rotated.)

We believe that the considerable vertical breadths of the (00l) features in Fig. 1 arise from poor resolving power of the individual crystallites due to small dimensions parallel to their c axes. Some of the breadth of these features might, conceivably, be attributed to non-uniform separation of atomic planes, but this would result in progressive increase in breadth with increasing order of reflection. As closely as we can estimate the breadths at half-maximum of the various orders are about the same, and we therefore conclude that the planes in each crystallite are uniformly spaced and that the spacing is the same in different crystallites. From the vertical breadths we estimate that the mean dimension in the direction parallel to the c axes is 8A, indicating that on the average the crystallites are made up of only three planes of carbon atoms. With this fact in mind the striking contrast between the character of the (00l) and the (hk) reflections is especially significant, as it offers further confirming evidence that there is no regularity in the way the uniformly spaced planes of atoms lie upon each other in each crystallite, even as regards one plane and its next neighbor.

This conclusion is supported by diffraction patterns obtained by the transmission method. Measurements of the features of the patterns of Figs. 2 and 3 indicate that all of them, as in Fig. 1, have indices of the form (hk0) or (00l).

The rings in the pattern obtained at normal incidence (Fig. 2) have radii proportional to the square roots of the whole numbers 1, 3, 4, 7, 9 and 12 and thus correspond to cross-grating reflections of the form (hk). There are no traces of (00l) reflections, and we know therefore that the cross gratings in this film are strongly oriented, as is the case in the film which produced the pattern of Fig. 1. Microphotometer curves obtained from the (10), (11) and (20) rings of Fig. 2 are reproduced as Fig. 6, the ordinates being the differences between the logarithms of the light intensity I transmitted through the photographic plate and the logarithms of the intensity I_B corresponding to the estimated background curve. These microphotometer curves are more satisfactory than similar curves previously obtained from x-ray diffraction patterns of black carbon, because strong (00l) diffraction rings are

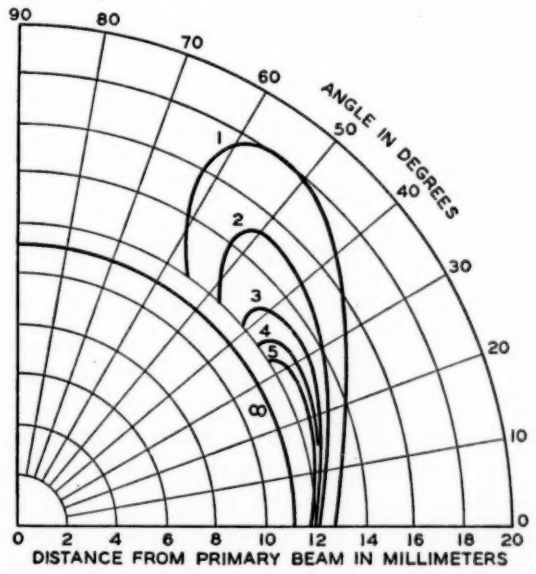

FIG. 5. Calculated intensity distribution in a (10) diffraction feature of Fig. 1, plotted as a contour diagram.

[6] We are indebted to Dr. L. A. MacColl for advice and assistance in the numerical integrations.

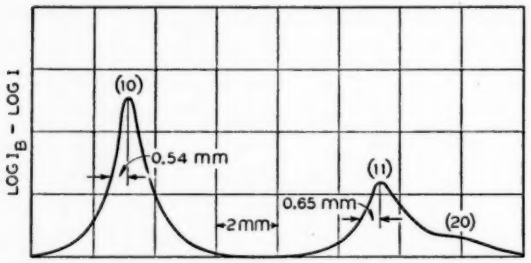

FIG. 6. Microphotometer curves of the (10), (11) and (20) diffraction rings of the pattern of Fig. 2.

present in the latter and overlap the (*hk*) reflections. The maxima of Fig. 6 are asymmetrical in the manner to be expected from imperfectly oriented cross gratings,[4] and we cannot calculate the mean breadth of the cross gratings directly from the widths of the curves at half-maximum. A fair estimate can, however, be obtained by substituting, for the ring broadening in the Scherrer formula for crystal size, twice the difference between the radius of a particular ring at maximum intensity and that at half-maximum on the inner side. This will not yield exactly the mean linear dimension but the error will not be important. Estimated in this way, the widths at half-maximum, ΔR, of the (10) and (11) peaks of Fig. 6 are 2(0.54) mm and 2(0.65) mm. These correspond to average linear dimensions, ϵ, of the cross gratings of 22A and 18A, respectively, as calculated from the Scherrer formula in the form $\epsilon = L\lambda/\Delta R$. The reason for the discrepancy between these estimates is not clear; similar disagreement has been observed in x-ray determinations.[2] Microphotometer curves were taken upon another pattern through the (10), (11), (21) and (30) rings, and an attempt was made to account in some simple fashion for the variation in half-breadth which was observed. In this we have been unsuccessful.

The diffraction features which appear on the pattern of Fig. 3 are (002), (004) and the (*hk*) reflections corresponding to the whole numbers 1, 3, 4, 7, 9 and 12. The (00*l*) reflections are those which appear most strongly along the vertical center line, and the (*hk*) reflections along the horizontal. The fact that even along the horizontal line the (002) reflection appears weakly, whereas this reflection is entirely absent in the pattern of Fig. 2, is evidence that the crystallites in the film which produced the pattern of Fig. 3 were less sharply oriented than those in the film which gave the latter pattern. Except for this quantitative difference the orientation was, however, the same in the two films. The difference between the character of the (00*l*) and the (*hk*) reflections is brought out almost as clearly in Fig. 3 as in Fig. 1. One observes in Fig. 3 that the locus of (002) reflections is a circle, whereas the (10) and the (11) features are not true circular arcs but flare outward above and below the center line. The contour diagram of Fig. 5 can be used to estimate very crudely the intensity distribution to be expected within these features. To accomplish this one imagines this diagram reflected through the line $\theta = 0°$ and both parts then rotated through 360° about $\theta = 90°$ as an axis, resulting in an appropriate volume density distribution in reciprocal space. Intensities in the pattern of Fig. 3 are then represented by the intersection of this solid with a plane normal to the plane of the paper and inclined 45° to $\theta = 0$. The horizontal radial distribution through an (*hk*) feature of Fig. 3 will be represented by the contour lines at $\theta = 0$ in Fig. 5, and the vertical radial distribution approximately by the contour lines at $\theta = 45°$ in the same diagram. One should realize, of course, that the diagram of Fig. 5 was calculated by assuming cross gratings of infinite extent, whereas the gratings are actually only about 20A wide; furthermore, the diagram corresponds to more strongly oriented crystallites than was the case in the film which gave the pattern of Fig. 3.

It has been pointed out that the degree of preferential orientation is different in different films (for example, those which produced the patterns of Figs. 2 and 3). More than a hundred films have been investigated and it has been discovered that the degree of orientation is considerable in some and slight in others. The patterns chosen for consideration here have been selected from those showing a high degree of orientation.

SUMMARY

We have shown that these films of pyrolytically deposited carbon consist of pseudo-crystals each made up of 3 or 4 parallel and uniformly spaced but otherwise randomly disposed atomic

planes in each of which the carbon atoms are hexagonally arranged as in graphite. This structure is just that inferred from x-ray studies[7] of similar carbons, but in our experiments evidence is obtained which is not available in the previously reported patterns from unoriented crystallites and the deductions are made without reference to any other carbon.

[7] For example, V. Hoffman and D. Wilm, reference 2; H. L. Riley, Sci. J. Roy. Coll. Sci. **10**, 10–20 (1940).

JULY, 1941 JOURNAL OF CHEMICAL PHYSICS VOLUME 9

Spectroscopic Studies of the Simpler Porphyrins

III. The Absorption Spectra of *ms*-Tetraphenylporphine and a Series of Its Metal Complex Salts

V. M. Albers and H. V. Knorr
The C. F. Kettering Foundation for the Study of Chlorophyll and Photosynthesis, Antioch College, Yellow Springs, Ohio

(Received April 14, 1941)

The molecular absorption coefficients of *ms*-tetraphenylporphine and the Cu, Ag_2, Mg, Zn, Cd, Hg, $SnCl_2$, Pb, MnCl, FeCl, Co and Ni complex salts have been measured over the visible region of the spectrum. The curves representing the absorption coefficients as a function of the wave-length are shown. The variations in the spectra of the metal salts of this one *ms*-tetrasubstituted porphine are much greater than those which have been found in the spectra of the different *ms*-tetrasubstituted porphines which so far have been studied.

Introduction

THE two previous publications in this series have been concerned with absorption spectra of synthetic porphines which were not metal complex salts. The first[1] was a study of the spectra of porphine and four *ms*-tetrasubstituted porphines, of which *ms*-tetraphenylporphine was one. The second[2] was a study of the spectra of the two isomeric forms of those porphines for which the two isomers were available. At the time of the first investigation the *ms*-tetraphenylporphine was the most difficult of the series to prepare and not enough of the substance was available to perform a separation of the isomers, consequently the material used in that investigation of the spectrum of *ms*-tetraphenylporphine contained a mixture of the two isomers. Since that time, a procedure for the synthesis of this porphine has been discovered[3] which yields quantitatively only the isomer of HCl number 13.5.* This is a

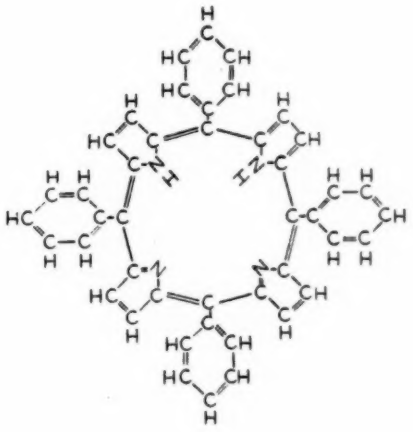

Fig. 1. Structural formula of *ms*-tetraphenylporphine.

[1] V. M. Albers and H. V. Knorr, J. Chem. Phys. **4**, 422–425 (1936).
[2] H. V. Knorr and V. M. Albers, J. Chem. Phys. **9**, 197–203 (1941).
[3] Rothemund and Menotti, J. Am. Chem. Soc. **63**, 267–270 (1941).
* The HCl number of a porphyrin is defined as the concentration of HCl which will extract two-thirds of the porphyrin from an equal volume of ether solution on thorough shaking.

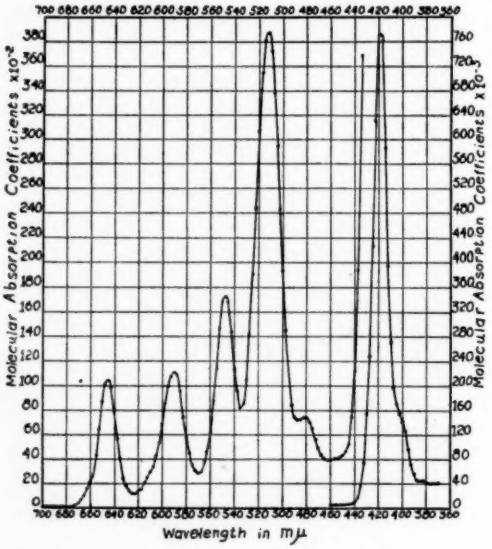

FIG. 2. Absorption spectrum of *ms*-tetraphenylporphine in benzene solution.

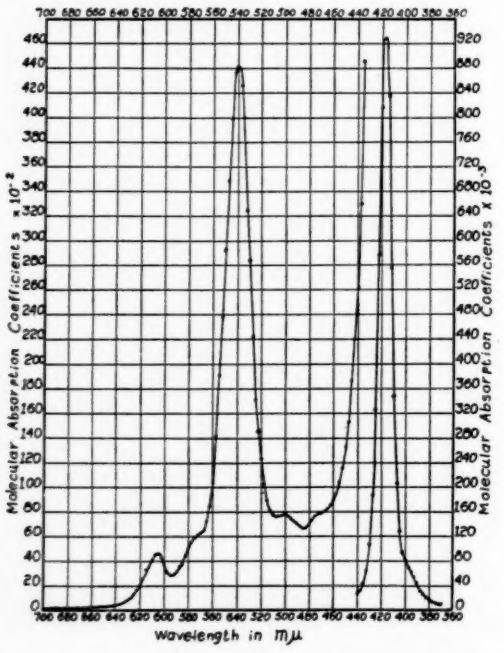

FIG. 3. Absorption spectrum of the *ms*-tetraphenylporphine Cu complex salt in benzene solution.

very important discovery, since the separation of the isomers of these substances involves a tedious process of HCl fractionation from ether solutions. Accordingly, this porphine was chosen as one from which a long series of metal complex

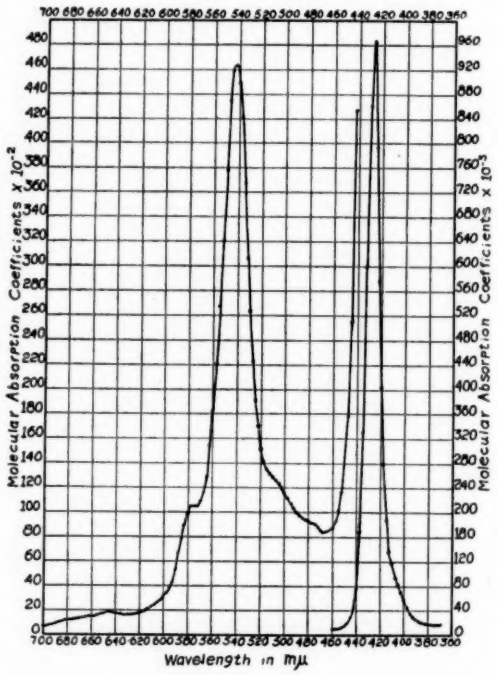

FIG. 4. Absorption spectrum of the *ms*-tetraphenylporphine Ag_2 complex salt in benzene solution.

salts was prepared[4] in order to study the variations of the properties with the substituted metal.

All of the preparations were purified by recrystallization and their composition verified by analysis. In the case of the magnesium complex salt there is still some question about the structure; the analyses were consistent with the structure in which the magnesium goes into the molecule as MgOH but this structure has not yet been definitely proved.[4]

The formula for *ms*-tetraphenylporphine is shown in Fig. 1. The metal complex salts are prepared by substituting the metal for the hydrogens which are attached to the nitrogen atoms in the pyrrole rings. When the metal is monovalent, as is the case with the silver salt, two metal atoms replace the two hydrogen atoms. When the metal is divalent the two valences of the metal are linked to the two nitrogen atoms and, in the case of trivalent and tetravalent metals, the extra valences are usually satisfied with chlorine atoms.

[4] Rothemund and Menotti, J. Am. Chem. Soc. In process of publication.

Experimental

The spectra were measured with a recording spectroradiometer which has been previously described.[5] The spectra were examined, in all cases, from 900 mμ to 370 mμ. Since none of the substances showed characteristic absorption above 700 mμ, only the region between 700 mμ and 370 mμ was actually measured.

The spectra were all measured for benzene solutions and the absorption coefficients were calculated from Beer's law in the form of Eq. (1),

$$I_T/I_0 = e^{-acx}, \qquad (1)$$

where I_T/I_0 is the ratio of transmission of the absorption cell filled with solution to its transmission when filled with the pure solvent, c is the concentration of the solution in moles per liter, x is the thickness of the absorption cell in cm and a is the molecular absorption coefficient of the substance.

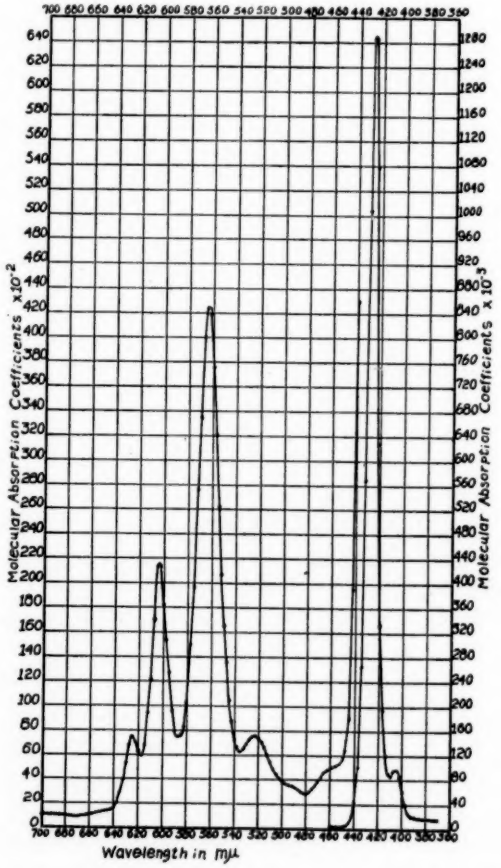

FIG. 5. Absorption spectrum of the *ms*-tetraphenylporphine Mg complex salt in benzene solution.

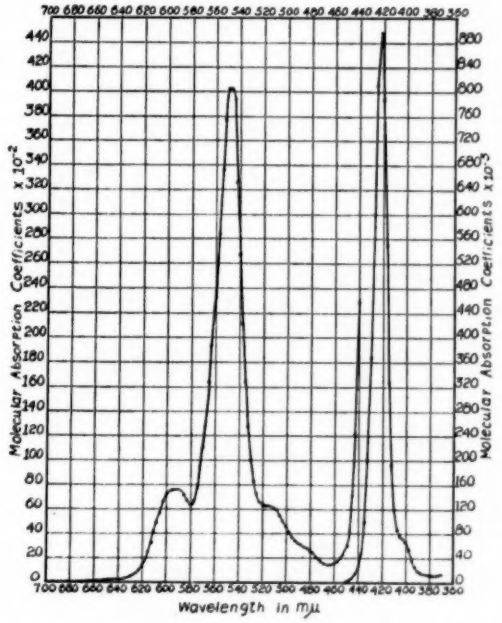

FIG. 6. Absorption spectrum of the *ms*-tetraphenylporphine Zn complex salt in benzene solution.

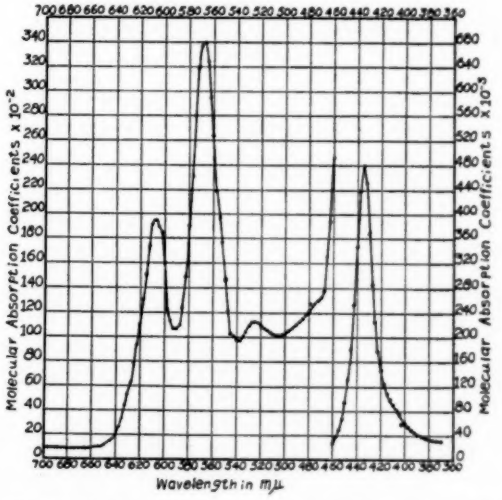

FIG. 7. Absorption spectrum of the *ms*-tetraphenylporphine Cd complex salt in benzene solution.

In measuring these spectra with the spectroradiometer, a 108-watt spiral filament lamp was used as a source to illuminate the entrance slit of the Hilger Quartz Monochromator. The absorption cell was placed between the exit slit of the monochromator and a photoelectric cell.

[5] V. M. Albers and H. V. Knorr, J. Opt. Soc. Am. **28**, 121–123 (1938).

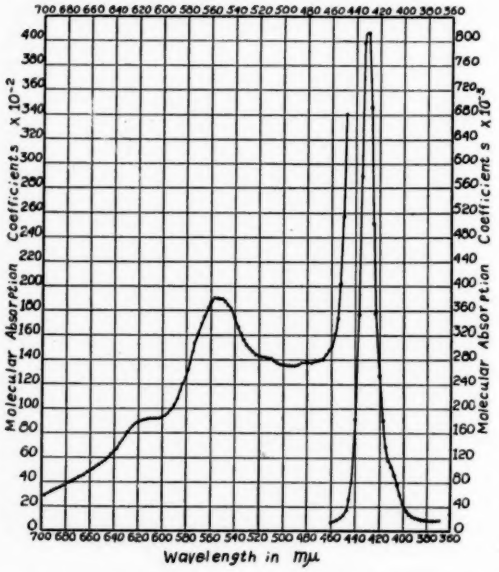

FIG. 8. Absorption spectrum of the *ms*-tetraphenylporphine Hg complex salt in benzene solution.

The photoelectric cell current was amplified with a d.c. amplifier whose output was fed to a Leeds and Northrup Speedomax recorder. Records were made by driving the wave-length drum of the monochromator and the record paper in the recorder with synchronous motors operating from the same a.c. line. In order to obtain I_T/I_0 as a function of wave-length it was necessary to have a record made with the absorption cell filled with pure solvent and another record made with the cell filled with the solution. The deflections of the recorder pen were then measured at 2.5-mμ intervals and the ratio $d_T/d_0 = I_T/I_0$, where d_T was the deflection when the cell was filled with solution and d_0 was the deflection when the cell was filled with solvent, since it has been shown that the deflection of the recorder pen at any given wave-length is proportional to the light intensity on the photoelectric cell at that wave-length.[5] Since it is necessary that the temperature of the lamp filament and the gain of the amplifier remain constant throughout the making of the records for d_T and d_0, the following procedure was used for each solution concentration. Four records were made, the first and fourth were made with the absorption cell filled with the solvent and the second and third were made with the cell filled with the solution. At the beginning and

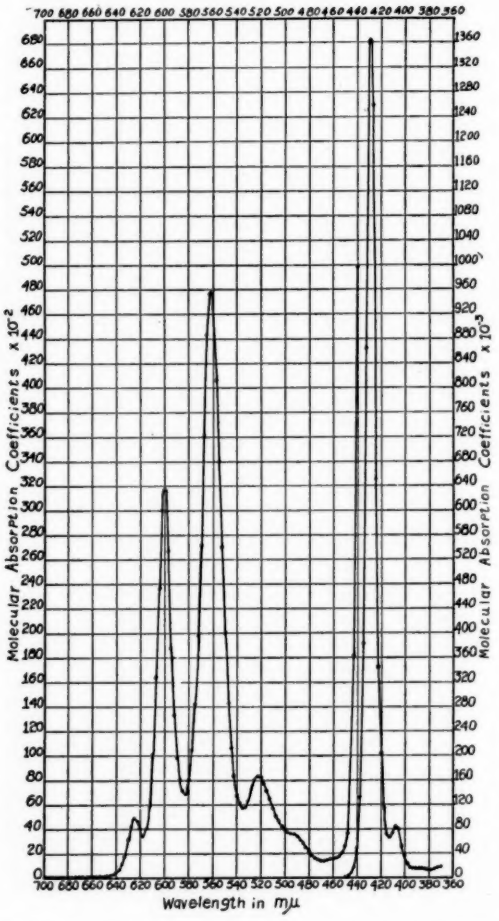

FIG. 9. Absorption spectrum of the *ms*-tetraphenylporphine $SnCl_2$ complex salt in benzene solution.

end of each record the zero position, i.e., the position of the pen when no light was allowed to pass through the system, was obtained. By this means any variation of the lamp or amplifier could be detected and, in addition, two independent determinations for d_T and d_0 were available at each wave-length, the mean values of which were used to compute the values of I_T/I_0.

The value of a was determined at 2.5-mμ intervals between 700 mμ and 370 mμ. It was found that a concentration of from five to seven milligrams of material in ten cc of solvent was sufficient for the regions of lower absorption. A series of concentrations made by diluting a given volume of solution with an equal volume of solvent was made up and records for each

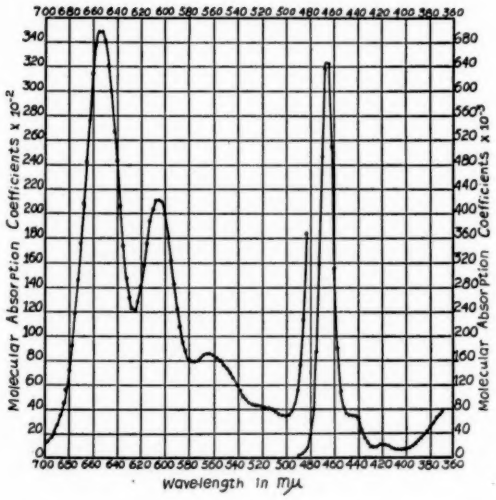

FIG. 10. Absorption spectrum of the *ms*-tetraphenylporphine Pb complex salt in benzene solution.

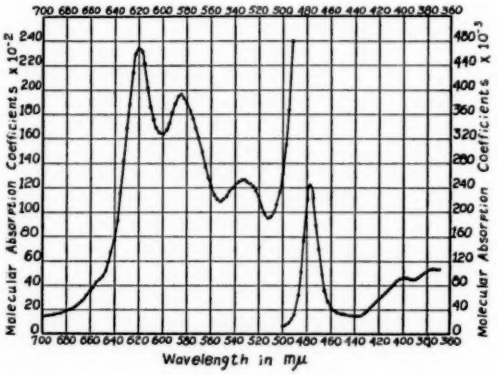

FIG. 11. Absorption spectrum of the *ms*-tetraphenylporphine MnCl complex salt in benzene solution.

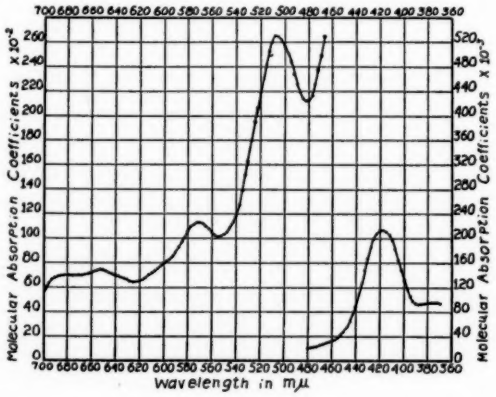

FIG. 12. Absorption spectrum of the *ms*-tetraphenylporphine FeCl complex salt in benzene solution.

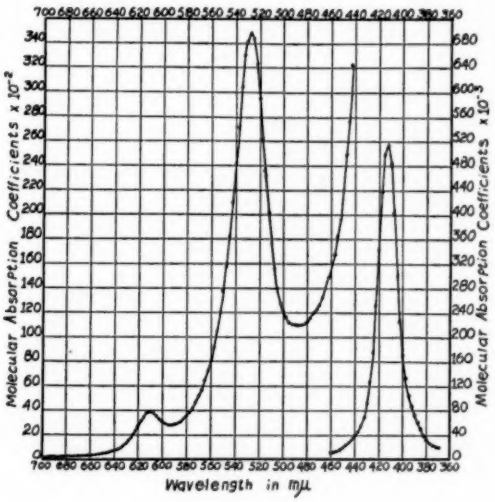

FIG. 13. Absorption spectrum of the *ms*-tetraphenylporphine Co complex salt in benzene solution.

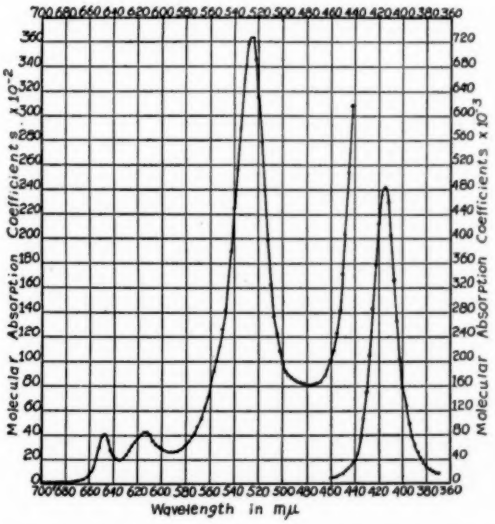

FIG. 14. Absorption spectrum of the *ms*-tetraphenylporphine Ni complex salt in benzene solution.

concentration were made until a solution of sufficient dilution was obtained to determine with maximum accuracy the value of a in the region of greatest absorption. An analysis of the propagation of errors in calculating a from the values of I_T/I_0 indicates that only values of I_T/I_0 between 0.15 and 0.50 should be used in order to prevent the errors involved in reading the deflections from producing excessive errors in a. Whenever the values of I_T/I_0 for two concentrations of solution fell within this range

TABLE I.

NAME	WAVE-LENGTH ($m\mu$)	a
ms-Tetraphenylporphine	418	772.0×10^3
	481	7.4
	512	38.7
	547	17.3
	590	11.0
	645	10.4
ms-Tetraphenylporphine Cu complex salt	417	930.0
	500	7.8
	540	44.0
	605	4.6
ms-Tetraphenylporphine Ag_2 complex salt	427	966.0
	543	46.4
	577	10.5
ms-Tetraphenylporphine Mg complex salt	427	1292.0
	523	7.6
	565	42.5
	604	21.5
	625	7.4
ms-Tetraphenylporphine Zn complex salt	422	896.0
	548	40.3
	591	7.6
ms-Tetraphenylporphine Cd complex salt	434	480.0
	525	11.2
	568	34.0
	607	19.5
ms-Tetraphenylporphine Hg complex salt	431	814.0
	555	19.0
ms-Tetraphenylporphine $SnCl_2$ complex salt	429	1360.0
	522	8.4
	562	47.7
	600	31.7
	625	4.8
ms-Tetraphenylporphine Pb complex salt	465	643.0
	563	8.6
	604	21.0
	653	34.9
ms-Tetraphenylporphine MnCl complex salt	477	245.0
	533	12.7
	585	19.7
	620	23.4
ms-Tetraphenylporphine FeCl complex salt	418	214.0
	507	26.5
	570	11.3
ms-Tetraphenylporphine Co complex salt	412	498.0
	528	34.8
	610	4.0
ms-Tetraphenylporphine Ni complex salt	415	485.0
	526	34.6
	613	4.3
	647	4.1

at any one wave-length, both were used in determining the value of a and a mean of the two values of a was used. The values of a at the tops of the bands and in the regions between bands are accurate to about ± one or two percent. The monochromator slits were operated at about 0.001-inch width. Under these conditions the two yellow lines of mercury are just resolved.

Figs. 2–14 show the spectra of the substances studied. In all cases, the absorption in the violet end of the spectrum is much greater than that in the rest of the region so the curves are broken at the point where this heavy absorption sets in and the strong band is plotted on a scale 1/20 as large. The ordinates for the part of the curves to the left of the break are indicated at the left edge of the graphs and those for the part of the curves to the right of the break are indicated at the right edge of the graphs.

DISCUSSION

In comparing these data with those previously obtained from *ms*-tetrasubstituted porphines, one is impressed by the fact that the variations in the spectra of the different metal salts of *ms*-tetraphenylporphine are much greater than those which have been found in the spectra of the different *ms*-tetrasubstituted porphines. Seven of the salts (Cu, Ag_2, Zn, Hg, FeCl, Co and Ni) have spectra with two principal bands while five of them (MnCl, Pb, $SnCl_2$, Cd and Mg) have three principal bands. In addition to the principal bands all of these substances have one or more weak bands. In Table I the wave-lengths and absorption coefficients of all of the bands in the spectra of these substances between 700 mμ and 370 mμ are tabulated.

Beer's law apparently holds throughout the visible region for all of these substances, since absorption coefficients for different solution concentrations at the same wave-length agree very well.

Helium Repulsive Potential from Collision Cross Section Measurements*

I. AMDUR AND H. PEARLMAN
Research Laboratory of Physical Chemistry, Massachusetts Institute of Technology, Cambridge, Massachusetts

(Received April 23, 1941)

Total collision cross sections have been measured for fast helium atoms, having velocities corresponding to 300–1000 electron volts, scattered in room temperature helium gas. Using classical theory, attempts were made to find a repulsive intermolecular potential which could account for the experimental results. A hard sphere model or a Lennard-Jones type potential were both unsatisfactory, whereas exponential type potentials of the form $V(r)=A\exp(-ar^n)$ seemed promising. For the distances involved in the scattering experiments, 0.55 to 1.05A, the specific repulsive potential which predicted total collision cross sections within the experimental error was $V(r)=11.3\exp(-4.63r^4)\times10^{-10}$ erg.

THE elastic scattering of high velocity neutral particles by slow moving neutral particles affords a method for experimentally determining intermolecular repulsive forces. If the fast particles have energies of the order of 100 electron volts or greater, scattering beyond about one degree results from interactions over very small distances where only repulsive forces are of significance. The calculations are further simplified by the fact that the scattering particles, whose velocity seldom reaches one percent of that of the fast particles, may be regarded as initially at rest.

In the present experiments, beams of helium atoms with energies from 300 to 1000 electron volts were scattered by helium gas at room temperature. The apparatus and experimental procedure have been previously described[1] in connection with the determination of total collision cross sections of high velocity hydrogen atoms scattered in room temperature molecular hydrogen. As in the earlier experiments, total collision cross sections for the helium atoms scattered in helium gas were computed from the ratio of axis beam intensities after passage through helium at two different pressures. The average angular aperture of the detecting system was, as before, 2.25 degrees. The accuracy of the cross sections, computed from 11 individual runs, is estimated at 15 percent. The values are listed in Table I as a function of beam particle voltage.

TABLE I. *Total collision cross sections of helium atoms scattered in helium.*

Voltage	300	400	500	600	700	800	900	1000
Cross section (A^2)	3.3	2.8	1.7	1.3	1.1	1.2	1.0	0.9

As pointed out by Massey and Mohr,[2] it is permissible to use classical theory to describe collisions in which the beam particle is scattered through a relative angle greater than a critical value Θ_c. Θ_c is approximately equal to $\lambda/2r_0$ where λ is the de Broglie wave-length of the colliding system and r_0, the equivalent hard sphere radius, that is (cross section/π)$^{\frac{1}{2}}$. The use of classical theory is definitely justified in the present calculations since the calculated Θ_c values are nearly constant at the various voltages, with a value close to 0.5°, whereas all measured scattering occurred at relative angles greater than 4.5° (2.25° in apparatus coordinates).

Kennard[3] has derived the equations applicable to the classical scattering by a fixed scatterer of a beam of particles homogeneous in velocity, and has indicated the changes required when the scatterer, although initially at rest, is free to move after collision, as in the present experiments. In this case the equations remain formally unchanged if relative coordinates are used throughout. The mass of the beam particle is replaced by the reduced mass of the system; the angular deflection of the beam particle with respect to the beam axis, by the relative angle of scattering; and the initial beam velocity, by

* Contribution from the Research Laboratory of Physical Chemistry, Massachusetts Institute of Technology, No. 478. Presented before the American Physical Society at the Cambridge Meeting, February 22, 1941.

[1] Amdur and Pearlman, J. Chem. Phys. **8**, 7 (1940).

[2] Massey and Mohr, Proc. Roy. Soc. **A141**, 434 (1933).

[3] Kennard, *Kinetic Theory of Gases* (McGraw-Hill Book Company, Inc., 1938), Chapter III.

the relative initial velocity of the system. For the particular case under consideration, the relative initial velocity of the system is virtually the same as the initial velocity of the high energy beam particle, the reduced mass of the system is equal to half the mass of the beam or scattering particle and the relative angle of scattering is twice the angular deflection of the beam particle with respect to the beam axis.

For deflections of 10 degrees or less, the relative angle of scattering is given by

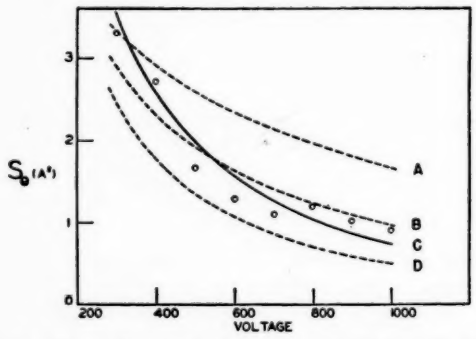

FIG. 1. Dependence of cross section on voltage as calculated for various assumed potentials: A, 8.71 exp$(-4.63r)$; B, 8.71 exp$(-4.63r^4)$; C, 11.3 exp$(-4.63r^4)$; D, 8.71 $\times$exp$(-4.63r^4)$ (units, 10^{-10} erg). Circles represent experimental points.

$$\Theta=\frac{2r_0}{\mu v^2}\int_{r_0}^{\infty}\frac{[V(r_0)-V(r)]rdr}{(r^2-r_0^2)^{\frac{1}{2}}}, \qquad (1)$$

where $V(r)$ is the intermolecular potential expressed as a function of the distance r between centers of the beam particle and the scatterer; r_0, the distance of closest approach of the center of the beam particle to the center of the scatterer; μ, the reduced mass; and v, the relative initial velocity of the colliding system. The total collision cross section, for a given average angular aperture Θ, is given by

$$S_\Theta=\left|2\pi\int_\Theta^\pi G(\Theta)\sin\Theta d\Theta\right|=\left|2\pi\int_\Theta^\pi b_\Theta db_\Theta\right|=\pi b_\Theta^2, \qquad (2)$$

where $G(\Theta)$ is the scattering function and b_Θ, the impact parameter defined by

$$\left(1-\frac{V(r_0)}{\frac{1}{2}\mu v^2}\right)r_0^2=b_\Theta^2. \qquad (3)$$

Relations (1), (2) and (3) are sufficient to predict total collision cross sections, consistent with an assumed intermolecular potential, for comparison with experimental values. The actual method of calculation is as follows:

(A) A potential function $V(r)$ is assumed. This permits the calculation from Eq. (1) of points for a curve of $\frac{1}{2}\mu v^2$ *versus* r_0 for a constant value of Θ (in the present case equal to 0.0785 radian, the relative average angular aperture of the detecting system). From this curve, it is possible to find the r_0 values which correspond to the experimental atom gun voltages as expressed in terms of $\frac{1}{2}\mu v^2$.

(B) Using the assumed potential form, the value of the impact parameter b_Θ, corresponding to a given combination of r_0 and $\frac{1}{2}\mu v^2$, is computed from Eq. (3).

(C) From this value of b_Θ the total collision cross section, for a given relative average angular aperture and beam particle energy, is directly computed from Eq. (2).

It is therefore possible, in principle, to predict a curve of S_Θ *versus* voltage for any assumed intermolecular potential. Two general forms of repulsive potential were assumed, for both of which the integral in Eq. (1) may be evaluated without great difficulty. The first of these was the Lennard-Jones type which may be represented by $V(r)=C/r^s$ where s is a positive integer. In this case, it is possible, as shown by Kennard,[3] to integrate Eq. (1) and obtain an expression for Θ in closed form. The second general form of potential used was $V(r)=A\exp(-ar^n)$. In this case, it can be shown that if $2/n$ is a positive integer, an asymptotic expansion of Eq. (1) exists from which Θ may be calculated with high accuracy. The general method is as follows:

If $V(r)=A\exp(-ar^n)$, Eq. (1) may be written

$$\Theta=\frac{2r_0}{\mu v^2}\int_{r_0}^{\infty}\frac{A\exp(-ar_0^n)rdr}{(r^2-r_0^2)^{\frac{1}{2}}}-\frac{2r_0}{\mu v^2}\int_{r_0}^{\infty}\frac{A\exp(-ar^n)rdr}{(r^2-r_0^2)^{\frac{1}{2}}}.$$

Integrating the first term directly, the second term by parts and simplifying, gives

$$\Theta=\frac{2r_0Aan}{\mu v^2}\int_{r_0}^{\infty}\frac{\exp(-ar^n)r^{n-1}dr}{(r^2-r_0^2)^{\frac{1}{2}}}.$$

If y is a new variable such that $y=a(r^n-r_0^n)$, then

$$\Theta=\frac{2A\exp(-ar_0^n)}{\mu v^2}\int_0^\infty \frac{\exp(-y)\,dy}{\left[\left(\frac{y}{ar_0^n}+1\right)^{2/n}-1\right]^{\frac{1}{2}}}.$$

When $2/n$ is a positive integer $[(y/ar_0^n)+1]^{2/n}$ may be expanded into a polynomial, after which the denominator of the integrand may be expanded according to the binomial theorem. The final result is an infinite series whose terms are Γ functions multiplied by known numerical coefficients. The binomial expansion is valid only for $(y/ar_0^n)<1$, so that the series does not converge. However, by taking only the first four or five terms, Θ may be computed to one part in several thousand since the first part of the series is an asymptotic expansion for Θ. This expansion is very satisfactory for values of ar_0^n from 3 to 6, the range encountered in the present calculations.

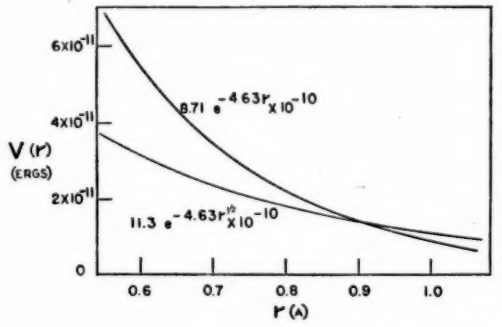

FIG. 2. Comparison of repulsive potential deduced from present experiments with Buckingham modification of Slater-Kirkwood potential.

The repulsive potential which was first tried was the Lennard-Jones type suggested by de Boer and Michels,[4] $V(r)=4.45/r^{12}\times10^{-10}$ erg (r in A units). The resulting theoretical curve of S_Θ *versus* voltage for this assumed potential was unsatisfactory both with respect to average magnitude and slope. The predicted cross sections decreased slowly from 6.6A² at 300 volts to 5.4A² at 1000 volts. Since satisfactory agreement could not be obtained with this potential form by any change of constants, it was decided to use "softer" potentials of the form $V(r)=A\exp(-ar^n)$. The modified Slater-Kirkwood repulsive potential proposed by Buckingham,[5] $V(r)=8.71\exp(-4.63r)\times10^{-10}$ erg gave results which, although better than those obtained by using the potential of de Boer and Michels, were still unsatisfactory. Changing the value of n in the generalized potential expression from 1 to $\frac{1}{2}$ and $\frac{2}{3}$ while keeping A and a constant at 8.71 and 4.63, respectively, did not materially improve the agreement, but did serve to point out that if the S_Θ curve resulting from the assumption, $V(r)=8.71\exp(-4.63r^{\frac{1}{2}})\times10^{-10}$ erg, were laterally displaced in the direction of increasing voltage, the new curve would fit the experimental points quite well. This lateral displacement merely involves changing the assumed potential by a multiplicative constant which eventually multiplies the predicted voltage consistent with a given S_Θ. Applying this procedure in the present case, it is found that the repulsive potential which predicts collision cross sections in agreement with experiment may be represented by $V(r)=11.3\exp(-4.63r^{\frac{1}{2}})\times10^{-10}$ erg. Figure 1 illustrates the agreement between the experimental points and the predictions resulting from assumption of the various exponential type repulsive potentials.

The present results indicate that, for separation distances of 0.55 to 1.05A, the repulsive potential is considerably softer than the Slater-Kirkwood or slightly modified Slater-Kirkwood potentials which are usually used for larger distances. Figure 2 compares the potential deduced from the present experiments with Buckingham's modification of the Slater-Kirkwood potential, at the distances involved in the scattering of the 300- to 1000-volt helium atoms.

Margenau[6] states that the original calculation of Slater and Kirkwood[7] neglected second-order exchange forces which have the effect of softening the repulsion. Near the minimum (2.9A) the magnitude of the repulsive energy is decreased about 9 percent by taking into account these

[4] de Boer and Michels, Physica **6**, 409 (1939).

[5] Buckingham, Proc. Roy. Soc. **168**, 264 (1938).
[6] Margenau, Phys. Rev. **56**, 1000 (1939).
[7] Slater and Kirkwood, Phys. Rev. **37**, 682 (1931).

second-order effects. Although Margenau's calculations do not apply to smaller distances, it appears that the correction would be very much larger at such distances.

The results of this paper show that the measurement of total collision cross sections of high velocity particles can be used as a sensitive method for determining intermolecular repulsive potentials if the experimental results reveal a large dependence of cross section on velocity. In such cases it is found that the greater the slope of the cross section *versus* velocity curve, the softer will be the potential required to reproduce the experimental points. An extreme illustration of this point is found in the collision cross section for rigid spheres, which has no velocity dependence and is the result of an infinitely steep repulsive potential.

JULY, 1941 JOURNAL OF CHEMICAL PHYSICS VOLUME 9

The Efficiency of the Primary Photochemical Process in Solution

KENTON ATWOOD AND G. K. ROLLEFSON
Department of Chemistry, University of California, Berkeley, California

(Received April 14, 1941)

A study has been made of the effect of an inert solvent on the efficiency of the primary process in the photolysis of oxalyl bromide and nitrosyl chloride. The oxalyl bromide was studied at the wave-lengths 2650, 3130, 3650, 4047, and 4358A, the nitrosyl chloride at 3650, 4047, 4358, 5461, and 5790A. In order to eliminate the back reaction between nitric oxide and chlorine, oxygen was introduced which converted the nitric oxide into nitrogen dioxide. The solvent used was carbon tetrachloride. Quantum yields for nitrosyl chloride showed only a slight trend ranging from 0.7 at 3650A to 0.5 at 5790A as compared to approximately 2 at all wave-lengths in the gas phase. Oxalyl bromide gave approximately the same quantum yield in solution as in the gas phase at 2650A, i.e., ~0.9, and the values in solution decreased to ~0.3 at 4358A with most of the change occurring between 3130 and 3650A. The results are discussed in terms of the Franck-Rabinowitch hypothesis and it is pointed out that they are most readily accounted for by assuming a deactivating action of the solvent rather than a high efficiency of recombination. A new quartz capillary arc of high intensity is described. The equilibrium $N_2O_4=2NO_2$ has been studied in carbon tetrachloride solution and the equilibrium constant at 25°C found to be 6.4×10^{-5}, concentrations expressed in mole fractions.

THE effect of a solvent on the efficiency of a primary photochemical process has been discussed by Franck and Rabinowitch.[1] According to their view the quantum yield of the initial step should be lower in a solvent than in the gas phase because of (1) deactivation by solvent molecules, or (2) a higher efficiency of recombination due to the fragments of the original molecule being held together by a "cage" of solvent molecules. The chief difficulty in applying these views to most systems lies in the fact that secondary processes are involved and it is impossible to determine how much of an observed solvent effect is caused by a modification of the secondary reactions. In order to avoid such complications we have studied two systems in which the fragments produced by photodissociation of the absorbing molecule do not react with the solvent molecules and any secondary reactions are unaffected by the solvent or do not affect the yield of the primary process. The reactions are (1) the photolysis of oxalyl bromide and (2) the photo-oxidation of nitrosyl chloride. Both were studied in carbon tetrachloride solution and some experiments were performed with nitrosyl chloride in hexane solution in which case action with the solvent had to be considered.

[1] Franck and Rabinowitch, Trans. Faraday Soc. **30**, 120 (1934).

EXPERIMENTAL METHODS AND APPARATUS

The light source (Fig. 1) used in most of the experiments was a thick-walled capillary arc. Quartz capillary of about 1.5 mm wall thickness and internal diameter between 2.7 and 3.3 mm has been used on various arcs; a bore of around 3 mm and a length of about 4.5 cm for the working part seemed to give the best results. The bottom tungsten lead is sealed into the large quartz tube with De Khotinsky cement, and the

arc filled with mercury to the upper bulb. The tube is pumped on to remove most of the gas trapped on the walls, though there is no need for great care in removing air, since gas bubbles do not tend to collect in the capillary. After the rest of the tube is filled with mercury and the screw clamp tightened on the rubber tubing, mercury may move slowly through it, but sudden oscillations are prevented. The upper part of the holder into which the arc is screwed may be filled with water, so that the rubber and upper part are kept cold. The arc was operated on 220 d.c. (the top is connected to the negative side of the line) with a resistance in series. The resistance is adjusted to give a current of around 10 amperes, and the arc struck by breaking the mercury column near the bottom bulb with a small flame. A brisk stream of cooling water should be turned on immediately and the jacket (a quartz tube for filter work—a metal tube with a quartz window for the monochromator) screwed up so that the arc is entirely surrounded by flowing water. During operation, the resistance in series is varied between 10 and 15 ohms, depending on the arc's characteristics and the intensity desired. Around a kilowatt was the average power used, though arcs have been operated on as much as 1500 watts for several hours. They will not operate well on 110 d.c. with little or no resistance in series. After forty or fifty hours of operation it is advisable to clean the capillary with hydrofluoric acid and repair any small cracks which may develop. None of these arcs have ever broken down violently except when the water supply failed. One was operated (with perhaps a dozen or more cleanings) almost 1000 hours on about 900 watts. A tungsten lead which has been used for a long time in the bottom of an arc seems to help prevent blackening of the capillary.

Zeiss monochromat filters *A*, *B*, and *C* were used for the 5790, 5461, and 4358A mercury lines, respectively, Corning 586 filter (8 mm) for 3650A, and Corning 587 (3.9 mm) with Corning 330 (noviol 0, 2 mm) for the 4047 A line. A large fused quartz prism monochromator was used to separate the 2650 and 3130A radiations.

Nitrogen dioxide was prepared by heating C. P. lead nitrate. The gas was passed through phosphorus pentoxide and freed from gaseous impurities by repeated freezings and pumpings. The solid nitrogen tetroxide was colorless. Apiezon grease "L" was not attacked noticeably by short exposures to nitrogen dioxide. A weighed ground joint with a small bulb attached was pumped out in the vacuum line. A known volume and pressure of nitrogen dioxide was condensed into the bulb which was then sealed off and weighed, along with the rest of the ground joint. Weights of nitrogen dioxide thus obtained checked to within less than 1 percent of the weights calculated from the volume-pressure measurements, using the equilibrium constants for nitrogen dioxide and nitrogen tetroxide of Verhoek and Daniels.[2]

Chlorine was prepared from tank chlorine, which was bubbled into water at 0°C until a considerable amount of chlorine hydrate had formed. On warming to 10°C the gas was evolved and passed through calcium chloride and phosphorus pentoxide. The chlorine was distilled in a vacuum line, the first and last fractions being discarded.

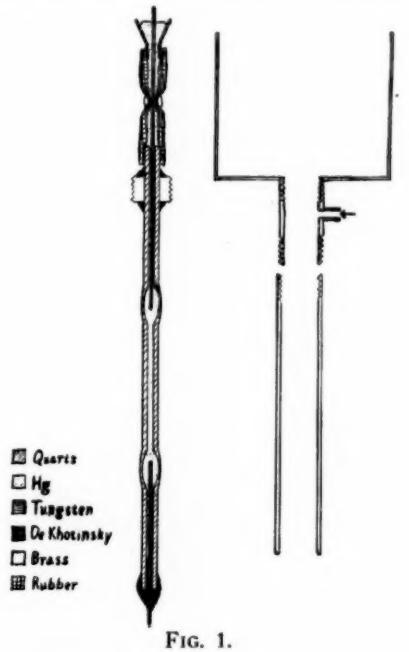

FIG. 1.

Nitric oxide was prepared by a modification of the method of Johnston and Giauque.[3]

[2] Verhoek and Daniels, J. Am. Chem. Soc. **53**, 1250 (1931).

[3] Johnston and Giauque, J. Am. Chem. Soc. **51**, 3194 (1929).

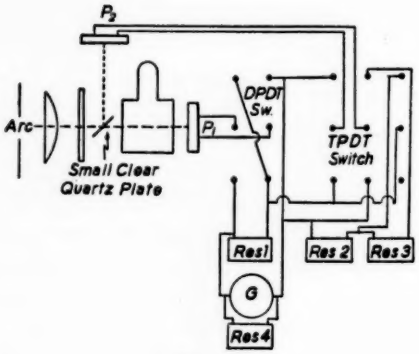

FIG. 2.

Nitrosyl chloride was prepared by a method similar to that of Taylor and Denslow.[4]

Nitric oxide (in excess) and chlorine were allowed to react in a three-liter flask. When the chlorine was practically all used up the gases were repeatedly condensed in liquid air and evaporated until pressure measurements showed complete reaction. Then the gases were condensed in liquid oxygen and non-condensible nitric oxide pumped off, the operation being repeated until no gas was uncondensed by liquid oxygen. Finally the nitrosyl chloride was distilled, with the first and last fractions discarded. Some preparations were made in a system using greaseless glass valves; others were made in a system containing stopcocks greased with Apiezon grease "L." The grease, which was protected from light when in contact with nitrosyl chloride, was not affected visibly. No effect of stopcock grease on the gas photolysis was found. Weights of nitrosyl chloride were checked against pressure-volume measurements by the method used with nitrogen dioxide. These different values checked to within about $\frac{1}{2}$ percent.

Oxalyl bromide, prepared from oxalyl chloride and hydrogen bromide in a system using greaseless glass valves, was kindly supplied by Dr. Tuttle. Titration of the acid formed on hydrolysis of oxalyl bromide checked within about 3 percent of the pressure-volume measurements. Free halogen in the material amounted to less than 0.1 percent.

Sulfur-free carbon tetrachloride, saturated with chlorine, was exposed to sunlight for several days, but was found to produce acid on illumination with chlorine even after such treatment. Finally chlorine dioxide was bubbled through and the solution illuminated with a 150-watt bulb for five days, chlorine dioxide being renewed as it was used up. Chlorine dioxide was prepared by the method of Bray.[5] Finally the carbon tetrachloride was washed with alkali and distilled from phosphorus pentoxide, the end fractions being discarded.

Crude hexane was shaken with small amounts of concentrated sulfuric acid until the acid took up no color. Then the hexane was shaken several times with 0.1 *N* potassium permanganate in 10 percent sulfuric acid, and a few times with 0.1 *N* potassium permanganate in 10 percent sodium hydroxide solution. The fraction distilling between 65–70°C was used.

Pressures of the corrosive gases were measured with a click gauge connected to a sulfuric acid manometer. Samples of the various gases were condensed and sealed off in small bulbs which could be broken by shaking in the reaction cells. Two cells were used—one cylindrical Pyrex cell 40 mm in diameter and 30.4 mm long, the other a rectangular quartz cell 30 by 40 mm and 24.2 mm long, used in the work below 3650A.

The experimental set-up is shown in Fig. 2. Absorption of substances in the cell could be measured in two ways. Direct reading of currents from photo-cell P_1 with the cell in and out of the light path may be made, or both photo-cells may be used in a potentiometric arrangement. The beam reflected from the quartz plate to photo-cell P_2 measures the incident light intensity; the voltage of P_2 is applied across the full resistance of the potentiometer (resistance boxes 2 and 3). The two methods gave identical results, but it was more convenient to use the first method

TABLE I. *Calibration of the sensitivity of the photronic cell.*

Wave-Length, A	(Moles/min. × mm) × 10^6		
	Nitrosyl Chloride	Uranyl Oxalate	Thermopile
3650	0.57	0.49	0.59
4358	1.22	1.44	1.08
5461	5.0	—	6.8
5790	7.8	—	7.3

[4] Taylor and Denslow, J. Phys. Chem. **31**, 374 (1927).

[5] Bray, Zeits. f. physik. Chemie **54**, 463 (1906).

when the cell could be moved rapidly back and forth from the light path. When the cell could not be moved, it was necessary to use the latter method, since it corrects for fluctuations in the intensity of the arc. When absorption measurements were used for analytical purposes dense screens, cutting out about 97 percent of the light, were used, so that photochemical reaction during the measurement would be negligible. Analytical measurements were often made at one or two wave-lengths on a reaction initiated by light of another wave-length.

The absolute number of quanta entering the reaction cell was determined from current outputs of photo-cell P_1, which was calibrated against actinometers and a thermopile. Uranyl oxalate[6] was used as an actinometer between 2537 and 4358A. This actinometer alone was used at 2650 and 3131A. Nitrosyl chloride gas, assuming a quantum yield of 2.0, was used between 3650 and 5790A, and those calibrations checked against a Moll large surface thermopile. Photocell sensitivities from these actinometers and the large surface thermopile calibrated against a standard lamp are compared in Table I. The nitrosyl chloride gas values were used in calculating the nitrosyl chloride solution yields, while uranyl oxalate values were used for the oxalyl bromide quantum yields.

TABLE II. *Oxalyl bromide absorption coefficients in carbon tetrachloride solution.*

WAVE-LENGTH, A	$M\times10^3$	K
2650	1.8	~200
3130	2.3	~120
3650	2.1– 8.3	30.9±1.7
4047	6.0–18.0	5.9±0.2
4358	2.3–18.0	1.78 (2.43–1.58)

M = concentration of oxalyl bromide in moles/liter.
l = length of cell.
$K = 1/lM \times \log_{10} I_0/I$.

TABLE III. *Quantum yields for the photolysis of oxalyl bromide in carbon tetrachloride solution.*

WAVE-LENGTH	OBSERVED VALUES	AVERAGE
2650	0.94, 0.91, 0.82, 0.91, 0.87	0.89
3130	0.81, 0.79, 0.81, 0.74	0.79
3650	0.37, 0.39, 0.34, 0.38, 0.38, 0.35	0.37
4047	0.29, 0.23	0.26
4358	0.22, 0.32, 0.33, 0.30, 0.26	0.29

[6] Leighton and Forbes, J. Am. Chem. Soc. **52**, 3139 (1930).

TABLE IV.

STOICHIOMETRIC MOLE FRACTION OF $NO_2\times10^5$	$K=\frac{(N_{NO_2})^2}{N_{N_2O_4}}\times10^5$ $T=25°C$
1.1	5.65
3.3	5.69
9.7	5.55
19.3	6.18
29.0	6.15
38.6	6.34
48.3	6.42
58.1	6.41
77.3	6.40
96.5	6.49
145.0	5.68
173.9	5.73
4250	1.4*

Henry's law constants $= \frac{\text{fugacity (atmos.)}}{\text{mole fraction}}$ $T=25°C$

$NO_2 = 74.6$
$N_2O_4 = 2.5$

* Cundall, J. Chem. Soc. **51**, 1076 (1891); **67**, 794 (1895).

PHOTOCHEMICAL DECOMPOSITION OF OXALYL BROMIDE IN CARBON TETRACHLORIDE SOLUTION

The decomposition of oxalyl bromide was followed by bromine absorption measurements, and iodometric titration of the bromine liberated. Since oxalyl bromide has a much smaller absorption coefficient than bromine at 4358A, light absorption at that wave-length was used for analysis in the work at all wave-lengths. Titration and absorption measurements gave checks within 5 percent, except in runs at 2537 and 2650A. At these wave-lengths the carbon tetrachloride itself absorbs light and liberates oxidizing material. As the concentration of oxalyl bromide is increased, the discrepancy decreases, since the solvent then absorbs a smaller fraction of the light. If a correction is made for oxidizing material produced from the solvent the two methods of analysis are brought into good agreement, even at low oxalyl bromide concentrations. The photolysis of oxalyl bromide appears to be unaffected by the accompanying carbon tetrachloride decomposition, except insofar as the solvent acts as an inner filter. The inner filter action of the bromine at the longer wave-

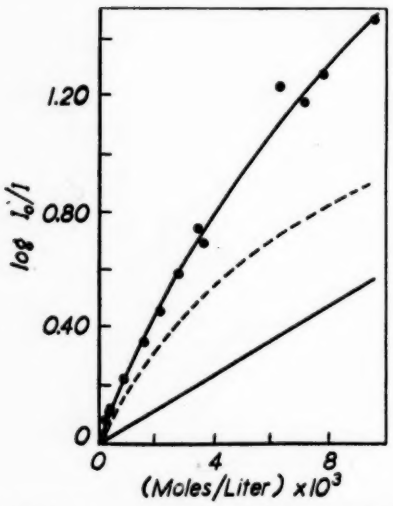

FIG. 3. 3650A. -·-·-·- ($\Delta \log I_0/I)_1$ *vs.* stoichiometric NO_2 conc.; ———— ($\Delta \log I_0/I)_{2+3}$ *vs.* NOCl conc.; - - - - - - $\Delta \log I_0/I$ *vs.* NOCl conc. decrease.

lengths was eliminated by using initial rates for the calculation of quantum yields.

Two runs were made at 2537A, using a low pressure, gas-filled mercury arc which furnishes over 90 percent of its radiation at 2537A. The set-up in these two experiments was different from that in the others. A lower limit for the quantum yield was about 0.6; the geometry of the system indicated an upper limit of 1.2.

Errors in the 4358A measurements are larger than those at the other wave-lengths, since the absorptions are small and the quantum yield is low. There appears to be a slight change in absorption coefficient with concentration at 4358A, though the errors in measurement at the low concentrations are large. Table II shows the absorption coefficients of oxalyl bromide in solution, Table III summarizes the quantum yield data.

Illumination of a solution of nitrosyl chloride in carbon tetrachloride caused no measurable amount of decomposition. Experiments with mixtures of nitric oxide and chlorine in solution in the same solvent showed that the back reaction was so fast (at least 100 times as fast as in the gas phase) that the photostationary state which could be set up by our light source was not measurable. In order to eliminate this back reaction oxygen was introduced into the system. Control experiments showed that oxygen reacts very much faster than chlorine with nitric oxide in carbon tetrachloride. With oxygen present the net reaction on illumination is $2NOCl+O_2=2NO_2+Cl_2$. This reaction can be followed readily by measurement of the increase in the absorption of light by the solution. The presence of any water in the carbon tetrachloride interfered with this measurement by reacting with the nitrogen dioxide. In order to eliminate this difficulty it was necessary to distill the carbon tetrachloride through fluffy phosphorus pentoxide and condense it directly in the reaction vessel which was then sealed off.

The nitrogen dioxide exists in the solutions in equilibrium with the tetroxide. From absorption measurements in very dilute solutions, in which the dissociation of the tetroxide is essentially complete, it was possible to determine the absorption coefficients for the dioxide at the wave-lengths 4358 and 3650A. Since only the dioxide absorbs at 4358A, it is possible to obtain the data necessary for the calculation of equilibrium constants by measuring the absorption and the total amount of dissolved oxides at higher concentrations. The constants obtained in this way are tabulated in Table IV.

In order to follow the course of the oxidation of nitrosyl chloride by light absorption it is necessary to set up a relationship between the change in the light absorption and the amount of the nitrosyl chloride which has reacted. The change in log I_0/I may be written

$$\Delta \log I_0/I = k_1 \Delta C_{NO_2} + k_2 \Delta C_{Cl_2} + k_3 \Delta C_{NOCl}.$$

From the stoichiometry of the net reaction $\Delta C_{Cl_2} = -\frac{1}{2}\Delta C_{NOCl}$. The correlation between ΔC_{NO_2} and ΔC_{NOCl} is not so simple because of the equilibrium between the dioxide and tetroxide. However, if we speak of the total tetravalent nitrogen as a stoichiometric C_{NO_2} then the ΔC_{NO_2} corresponding to this is numerically equal to ΔC_{NOCl}. Thus the above equation can be reduced to a function of ΔC_{NOCl}. The simplest way to use this expression for analytical purposes is to prepare a graph of $\Delta \log I_0/I$ against ΔC_{NOCl}. Each term of the equation is plotted; the last two give straight lines but the first gives a curve because of the equilibrium between the dioxide and tetroxide. The contribution of each term for a given ΔC_{NOCl} is read from the graph and the three are combined to give a point for the

desired curve. The curve obtained with λ4358A could be used only for small values of ΔC_{NOCl} because $\Delta \log I_0/I$ changed very little at the higher values. The curve obtained for λ3650A was quite satisfactory and was used in most of the analyses with checks against the one for λ4358A. The agreement between the two was found to be satisfactory. Figure 3 shows the curves for λ3650A. In this figure the contributions of the second and third terms have been combined into the single straight line.

The quantum yields for the oxidation reaction are listed in Table V. It was found that unless the oxygen pressure over the solution was controlled considerable variation was noted in the results. The effect of varying the oxygen pressure is shown in the values for 3650A. High oxygen pressures apparently have some inhibiting action although oxygen must be present for the reaction to go. At the other wave-lengths the oxygen pressure was fixed at one atmosphere.

The recombination of the nitric oxide and chlorine atoms formed in the photolysis of nitrosyl chloride may be prevented by carrying out the reaction in a solvent which reacts with chlorine atoms. Hence some experiments were performed with hexane as a solvent. No nitrogen dioxide was formed in this system under any conditions and the absorption decreased as the reaction proceeded. The reaction could not be run to completion since the solution became cloudy due to the separation of some hexane-insoluble product. Some experiments were tried with a solution of hexane in carbon tetrachloride and in these the reaction was carried to completion; the absorption dropped to zero. The quantum yields for these experiments are contained in Table VI.

TABLE V. *Quantum yields for the oxidation of nitrosyl chloride in carbon tetrachloride solution.*

WAVE-LENGTH	OXYGEN PRESSURE	OBSERVED VALUES	AVERAGE
3650	0.2 atmos.	0.70	0.70
	1	0.66, 0.67, 0.67, 0.68, 0.64	0.66
	1.5	0.56	0.56
	2	0.48, 0.45	0.47
4358	1	0.68, 0.76	0.72
5461	1	0.48, 0.51, 0.42, 0.43, 0.50	0.47
5790	1	0.48, 0.44, 0.58	0.50

TABLE VI. *Quantum yields for the photolysis of nitrosyl chloride in hexane solution.*

WAVE-LENGTH	OBSERVED VALUES	AVERAGE
3650	0.91, 0.87, 0.96, 1.19, 1.10	1.0
4358	0.69	0.69
5790	0.27, 0.30, 0.33, 0.32, 0.37	0.32
3650 Solvent 0.05 mole fraction of hexane in CCl_4	0.50, 0.60	0.55

DISCUSSION

According to the hypothesis of Franck and Rabinowitch[1] the quantum yield of simple reactions such as are considered here should be less in liquids than in the gaseous state. Our results show that this is true at all wave-lengths in the case of nitrosyl chloride and at long wave-lengths with oxalyl bromide but not at short wave-lengths where our results are essentially the same as found by Tuttle in the gas phase.[7] If the decrease in yield of the primary process is caused by a high efficiency of recombination of the molecular fragments brought about by a "cage" action of the solvent molecules it might be expected that the yield would vary with wave-length since at high frequencies the large kinetic energies possessed by the separating fragments would favor escape from the cage. The excess energy in the case of nitrosyl chloride amounts to 41 kcal. at 3650A and 11 at 5790A.[8] The products are the same at all wave-lengths except possibly that the chlorine atom may or may not be raised to the $P_{\frac{1}{2}}$ state, a difference of 2.5 kcal. The estimate of the excess energy for the oxalyl bromide depends upon what values are chosen for the carbon-carbon and carbon-bromine bonds. If we assume that the primary process is the same between 3650A and 4358A, the range in which an effect was noted, the variation in energy amounts to 13 kcal. Inspection of our results shows that in carbon tetrachloride solution there is only a slight trend in the yield with nitrosyl chloride and with oxalyl bromide the only change of importance occurs in a rather narrow wave-length range. Nitrosyl chloride in the presence of hexane shows a much greater variation. In this case a reaction with the solvent

[7] J. E. Tuttle, Ph.D. Thesis, University of California, 1940.

[8] Dixon, Zeits. f. physik. Chemie **B24**, 328 (1934).

occurs and it is possible that the excess energy supplied at the shorter wave-length is required to supply an activation energy for such a reaction. A point in favor of this view is supplied by the experiments in the dilute solution of hexane in carbon tetrachloride. Under these conditions some of the excess energy could be taken up by the carbon tetrachloride before a reaction with hexane could occur and actually we find a quantum yield only half as great as in pure hexane at the same wave-length.

The results which have been presented are more readily accounted for by assuming a deactivating action of the solvent rather than a high efficiency of recombination. Such a deactivation need not involve a change of electronic state in the photoactivated molecule but only the removal of vibrational energy. Usually the absorption of light produces a strongly vibrating molecule; if vibrational energy is removed from such a molecule until the amount left is less than that required for the dissociation of that particular electronic state the molecule will remain intact. If the potential energy curve which could be drawn to represent the excited state has no minimum or only a very slight one it may not be possible to remove enough energy to prevent dissociation. Apparently such a situation is found with hydrogen iodide in hexane solution.[9] If we consider oxalyl bromide from this standpoint the difference in behavior at long and at short wave-lengths corresponds to excitation to two different electronic states. The one produced at short wave-lengths has no minimum in its potential energy function, hence the solvent cannot prevent the dissociation and the quantum yield is the same in solution and in the gas phase. At long wave-lengths two-thirds of the molecules in solution lose so much vibrational energy that they cannot dissociate and the quantum yield drops accordingly. In the case of nitrosyl chloride between two-thirds and three-fourths of the molecules are deactivated. The slight trend in the results is such that it could be said that with the larger energies there is a little less chance of the energy being lowered below the dissociation limit. According to Goodeve and Katz[10] the potential energy curves for the upper states of the nitrosyl chloride involved in the absorption process at all the wave-lengths we have used except 5790A are repulsion curves. However, these curves intersect one which does have a minimum and transfers of the type which are involved in predissociation occur between the states. If this set of energy levels is assumed to be correct then the deactivating action of the solvent would involve removal of vibrational energy plus this transfer to an excited state with a minimum in its potential energy function. Ultimately the molecule is deactivated further to the lowest state but the dissociation is prevented in the first action of the solvent.

The arguments which have been presented do not exclude the possibility that a great many cases may exist in which a low quantum yield in solution is due to recombination. That effect has probably been overemphasized in the literature. A deactivation by the removal of vibrational energy is better suited to account for some of the specific effects observed and the small or absent trends with wave-length. It also offers a possibility of predicting the effect of a solvent if any information is available concerning the potential energy function of the excited state.

[9] Warburg and Rump, Zeits. f. Physik **47**, 305 (1928). They found the quantum yield the same in the gas phase and in solution at 2820A. At shorter wave-lengths their results were complicated by absorption of the solvent they used.

[10] Goodeve and Katz, Proc. Roy. Soc. London **A172**, 432 (1939).

The Unmixing Effect of Sound Waves on Liquid Mixtures

KARL F. HERZFELD
Catholic University of America, Washington, D. C.

(Received May 13, 1941)

The equations for sound waves passing through liquid mixtures are given. The amount of unmixing and the increase in sound absorption are calculated and found to be too small for observation.

G. W. WILLARD[1] has found that the absorption of ultrasonic waves in liquid mixtures may have a maximum for a certain concentration. In a discussion of Willard's paper at the May, 1940, meeting of the American Physical Society, the writer proposed an explanation, which Willard has kindly mentioned in his paper, namely that sound waves produce a partial unmixing.[2]

Unfortunately, the detailed calculation shows that both the unmixing and the increase in absorption are much too small to be of interest, and therefore only a short report is given here.

The liquid mixture is assumed to consist of two substances of molecular weight M_1 and M_2, and concentrations (mole per cc) c_1 and c_2. The particle velocity is called u_1 and u_2.

Let a plane sound wave, of frequency ν and pressure amplitude P travel through the medium in the z direction. Let μ_1 and μ_2 be the chemical potentials of the two components in the mixture. The equation of motion of the component one is then for one mole.

$$M_1\frac{\partial u_1}{\partial t}=-\left(\frac{\partial \mu_1}{\partial z}\right)_T - Rk_T\frac{c_1+c_2}{c_1}\frac{\partial T}{\partial z}+\frac{\Gamma_1}{(u_1-u_2)}. \quad (1)$$

Here k_T is the coefficient of the thermal diffusion, as defined by Chapman.[3] The last term is the force of friction resisting the relative motion of the two components.

Introducing the mole fraction x

$$x=c_1/(c_1+c_2),$$

this can be written, together with the equation for the second component

$$M_1\frac{\partial u_1}{\partial t}=-\left(V_1-\frac{RT}{c_p}\beta\frac{k_T}{x}\right)\frac{\partial p}{\partial z}-\frac{\partial \mu_1}{\partial x}\frac{\partial x}{\partial z} + \frac{2RT}{D}(1-x)(u_1-u_2), \quad (2)$$

$$M_2\frac{\partial u_2}{\partial t}=-\left(V_2+\frac{RT}{c_p}\beta\frac{k_T}{1-x}\right)\frac{\partial p}{\partial z}+\frac{x}{1-x}\frac{\partial \mu_1}{\partial x}\frac{\partial x}{\partial z} - \frac{2RT}{D}(u_1-u_2)x. \quad (2')$$

Here, V_1, V_2 are the partial mole volumes in the mixture, β the expansion coefficient and c_p the specific heat at constant pressure of 1 cc of the mixture, so that

$$\partial T/\partial z=(T\beta/c_p)\partial p/\partial z. \quad (3)$$

On the right side of (2) the first term is the driving force of the pressure gradient, the second that of the thermal diffusion, the third that of the concentration gradient and the last that of friction. The normal effect of viscosity has been omitted, as at first approximation the effects are additive. D is defined so that the flow due to a concentration gradient is

$$-\frac{D}{RT(1-x)}\frac{\partial \mu_1}{\partial z}.$$

Furthermore, the energy equation is written

$$c_p\frac{\partial T}{\partial t}=T\beta\frac{\partial p}{\partial t}+K\frac{\partial T}{\partial z}-\frac{\partial H}{\partial x}\frac{\partial x}{\partial t}. \quad (4)$$

The first term on the right is the useful work done, the second is the heat evolved in connection with thermal diffusion, the last one is due to a possible deviation from the law of ideal solutions,

[1] G. W. Willard, Phys. Rev. **57**, 1057 (1940); J. Acous. Soc. Am. **12**, 438 (1941).
[2] Y. Rocard, J. de phys. et rad. **1**, 426 (1930).
[3] S. Chapman, Proc. Roy. Soc. **177**, 38 (1940).

representing a (negative) heat of dilution. Heat conductivity and slow energy exchange terms have been omitted.

However, in the integration we neglect, in the energy equation, the last term, and in the equation of motion the effect of the concentration gradient.

We call the sound velocity W, the value without unmixing W_0, $2\alpha'$ the increase of the absorption coefficient 2α, defined so that the intensity diminishes proportional to $\exp(-2\alpha z)$, Δx the change of x at its maximum.

We also introduce the notation

$$\rho_1 = M_1/V_1, \quad \rho_2 = M_2/V_2.$$

Then

$$\frac{1}{W^2} = \frac{1}{W_0^2} - \frac{K}{W_0}\beta^2\rho T \frac{1}{c_p^2}\left(1+\frac{K}{W_0 c_p}\right)^{-1} \quad (\nu = 0), \tag{5}$$

$$\frac{2\alpha'}{\nu^2} = \frac{2\pi^2}{W}\frac{M_1^2 M_2^2 c_1 c_2}{xM_1+(1-x)M_2}\frac{D}{RT}\frac{\rho_2-\rho_1}{\rho_1\rho_2} \times\left[\frac{\rho_2-\rho_1}{\rho_1\rho_2} - \frac{RT\beta}{c_p}\frac{k_T}{x(1-x)}\left(\frac{1-x}{M_1}+\frac{x}{M_2}\right)\right], \tag{6}$$

$$\Delta x = x(1-x)\frac{P}{W^2}\frac{\pi\nu D}{RT}\left(\frac{1-x}{M_1}+\frac{x}{M_2}\right)^{-1} \times\left[\frac{\rho_2-\rho_1}{\rho_1\rho_2} - \frac{RT\beta}{c_p}\frac{k_T}{x(1-x)}\left(\frac{1-x}{M_1}+\frac{x}{M_2}\right)\right]. \tag{7}$$

Equations (6) and (7) are given in first approximation. The phase of Δx is 90° ahead of the pressure.

Numerically, $2\alpha/\nu^2$ is, for a reasonable case, about 10^{-18}, $\Delta x/x$, for P one atmosphere pressure, $1\cdot 10^{-18}\nu$.

JULY, 1941 JOURNAL OF CHEMICAL PHYSICS VOLUME 9

Statistical Mechanics of Fusion

JOHN G. KIRKWOOD AND ELIZABETH MONROE
Baker Laboratory, Cornell University, Ithaca, New York

(Received April 2, 1941)

A statistical mechanical theory of fusion based upon the use of local free energies is presented. An integral equation is formulated for the distribution function of average density in a region occupied by a system of molecules. Periodic solutions characteristic of a crystalline phase are found for certain ranges of values of a set of parameters depending upon temperature and volume. When the parameters decrease below certain critical values, all terms of the Fourier series representing the distribution function vanish with the exception of the constant term. A uniform density distribution characteristic of a fluid phase is then obtained. The melting parameters of argon at several pressures are calculated with the aid of the theory and compared with experiment.

INTRODUCTION

IN recent investigatious of the fusion process by the methods of statistical mechanics, two different points of view have been advanced. Lennard-Jones and Devonshire have proposed a very interesting theory based upon the idea of an order-disorder transformation in the distribution of molecules between normal and interstitial sites of a basic lattice.[1,2] Born[3] has proposed a theory of a different type in which the liquid-solid transition is attributed to the vanishing of the rigidity modulus of the solid and a resulting instability of the lattice under shear. Although the two points of view may not be mutually exclusive, that of Lennard-Jones and Devonshire is intuitively the more attractive. From the diffraction of x-rays, it is known that a crystalline solid is characterized by a periodic density distribution extending over domains of macroscopic dimensions. In the scattering of x-rays by liquids, there is no evidence of long range

[1] J. E. Lennard-Jones and A. F. Devonshire, Proc. Roy. Soc. **A170**, 464 (1939).
[2] G. H. Wannier, J. Chem. Phys. **7**, 810 (1939).
[3] M. Born, J. Chem. Phys. **7**, 591 (1939).

crystalline order, but only of a rapidly damped local order in the density distribution around each molecule. However, the Lennard-Jones-Devonshire theory leaves something to be desired in the details of its formulation, since it allows the disordered phase a residual long range order rather than requiring a complete destruction of the lattice in the fusion process. This is due to the limitations of the formalism of the order-disorder theory, which is designed for the solution of problems involving a finite set of configurations such as superlattice formation in alloys.

We shall present a theory of fusion similar in its physical aspects to that of Lennard-Jones and Devonshire. It is based upon the use of local free energies in a classical canonical ensemble. With aid of a device based upon the introduction of coupling parameters into the potential of intermolecular force, an integral equation is formulated for a distribution function $\rho_1(\mathbf{R})$ specifying the average density at a point $\mathbf{R}$ in a region occupied by a system of molecules. The kernel of the integral equation contains, in addition to the potential energy of a molecular pair, a correlation function $g(\mathbf{R}, \mathbf{R}')$ which determines the local order in the density at a point $\mathbf{R}'$ established by a molecule situated at the point $\mathbf{R}$. The correlation function is approximated by the radial distribution function, to which it reduces in a liquid phase. For density distributions with the period of a specified space lattice, the integral equation is shown to be equivalent to a set of transcendental equations for the Fourier coefficients of the distribution function $\rho_1(\mathbf{R})$. As parameters in the set of transcendental equations there enter the Fourier transforms of the potential energy of a molecular pair and the correlation function. For certain ranges of values of the parameters, it is found that all terms of the Fourier series representing the distribution function $\rho_1(\mathbf{R})$ vanish except the constant term. When $\rho_1(\mathbf{R})$ reduces to a constant, the average density becomes uniform with no residue of crystalline long range order. A disordered density distribution of this type is characteristic of a liquid phase. For values of the parameters exceeding certain critical values, the transcendental equations determining the Fourier coefficints of $\rho_1(\mathbf{R})$ have non-vanishing solutions, and a non-trivial periodic density distribution characteristic of a crystalline phase exists. The stable periodic structure is selected as the one of minimum work content. Since the parameters determining the distribution function $\rho_1(\mathbf{R})$ depend upon temperature and volume, areas in the temperature-volume plane corresponding to the liquid and solid phases are determined. Since it is convenient to calculate the distribution functions under the restraint of macroscopic homogeneity, areas corresponding to coexistence of the liquid and solid phases are determined with the aid of the thermodynamic criteria of heterogeneous equilibrium.

The melting parameters of argon are calculated with the aid of the theory and compared with experiment. An interesting inference from the theory is the absence of a critical point for fusion for certain crystal structures, among them the face-centered cubic structure characteristic of argon.

The Distribution Functions

In a system of N molecules confined within a volume v, the average molecular density at a point $\mathbf{R}$ in this region is equal to $(N/v)\rho_1(\mathbf{R})$, where $\rho_1(\mathbf{R}_i)dv/v$ is the probability that any specified molecule i occupies dv at the point $\mathbf{R}_i$. According to classical statistical mechanics, the distribution function is determined by the local free energy $W_1(\mathbf{R})$ of the system when a molecule is fixed at the point $\mathbf{R}$.

$$\rho_1(\mathbf{R}) = \exp\{-(1/kT)[W_1(\mathbf{R}) - W_0]\},$$

$$\exp[-W_n(\mathbf{R}_k \cdots \mathbf{R}_l)/kT]$$

$$= v^n \int^v \cdots \int^v \exp(-V_N/kT) dv_1 \cdots dv_{N-n}, \quad (1)$$

where kT is the product of Boltzmann's constant and the temperature, V_N is the potential of intermolecular forces, and $W_n(\mathbf{R}_k, \cdots \mathbf{R}_l)$ is the local free energy of the system when a set of n specified molecules $k \cdots l$ are fixed at the points $\mathbf{R}_k, \cdots \mathbf{R}_l$.

A crystalline phase is characterized by a periodic distribution function $\rho_1(\mathbf{R})$ with the period of a certain space lattice possessing maxima at specified points within the elementary cell Δ of the lattice. A liquid phase, on the

other hand, is characterized by a constant distribution function equal to unity everywhere in the region v. Coexistent phases would correspond to distribution functions $\rho_1(\mathbf{R})$ with physical discontinuities at the phase boundary.

A theoretical investigation of the properties of the distribution function $\rho_1(\mathbf{R})$ might be based upon a direct evaluation of the integrals, Eq. (1) defining the local free energies $W_1(\mathbf{R})$ and W_0. Since this is an almost prohibitively difficult procedure in condensed phases, we shall employ a device, previously proposed by one of us,[4] which involves the introduction of coupling parameters into the potential of intermolecular force. We assume that V_N can be expressed as a sum of the potential energies $V(|\mathbf{R}_k-\mathbf{R}_l|)$ of molecular pairs, each term of which depends only on the distance $|\mathbf{R}_k-\mathbf{R}_l|$ between the members of the pair.

$$V_N=\sum_{k<l} V(|\mathbf{R}_k-\mathbf{R}_l|). \tag{2}$$

We may define a potential $V_N(\xi_i)$,

$$\begin{aligned} V_N(\xi_i)&=V_{N-1}+\xi_i V_i,\\ V_{N-1}&=\sum_{k<l\neq i} V(|\mathbf{R}_k-\mathbf{R}_l|),\\ V_i&=\sum_k V(|\mathbf{R}_k-\mathbf{R}_i|), \end{aligned} \tag{3}$$

corresponding to a hypothetical system in which all terms in the potential energy associated with a specified molecule i are multiplied by a parameter ξ_i. By allowing ξ_i to assume values between zero and unity, the coupling between molecule i and the other molecules may be varied from zero to its value in the actual system. Corresponding to the potential $V_N(\xi_i)$, we define the local free energies

$$\begin{aligned} &\exp[-W_n(\mathbf{R}_k,\cdots\mathbf{R}_l,\xi_i)/kT]\\ &=v^n\int^v\cdots\int^v \exp[-V_N(\xi_i)/kT]dv_1\cdots dv_{N-n}, \end{aligned} \tag{4}$$

where the integral extends over the coordinates of all molecules except those of the set of n fixed molecules $k\cdots l$. According to Eq. (1), the distribution function $\rho_1(\mathbf{R},\xi)$ in the partially coupled system becomes

$$\rho_1(\mathbf{R},\xi)=\exp\{-(1/kT)[W_1(\mathbf{R},\xi)-W_0(\xi)]\}, \tag{5}$$

[4] J. G. Kirkwood, J. Chem. Phys. **3**, 300 (1935).

where the parameter ξ is understood to refer to a specified molecule fixed at the point $\mathbf{R}$. For the determination of the distribution function $\rho_1(\mathbf{R},\xi)$, and for the calculation of the thermodynamic functions of the system, we shall need to consider the following distribution functions for molecular pairs,[5]

$$\begin{aligned} &\rho_2(\mathbf{R},\mathbf{R}',\xi)\\ &=\exp\{-(1/kT)[W_2(\mathbf{R},\mathbf{R}',\xi)-W_0(\xi)]\},\\ &{}^{(1)}\rho_2(\mathbf{R},\mathbf{R}',\xi)\\ &=\exp\{-(1/kT)[W_2(\mathbf{R},\mathbf{R}',\xi)-W_1(\mathbf{R},\xi)]\},\\ &g(\mathbf{R},\mathbf{R}',\xi)=\exp\{-(1/kT)[W_2(\mathbf{R},\mathbf{R}',\xi)\\ &\qquad+W_0(\xi)-W_1(\mathbf{R},\xi)-W_1(\mathbf{R}',\xi)]\}, \end{aligned} \tag{6}$$

where ξ is understood to refer to a molecule at the unprimed position $\mathbf{R}$. The probability that the partially coupled molecule is situated in dv at $\mathbf{R}$ and another specified molecule in dv' at $\mathbf{R}'$ is $(1/v^2)\rho_2(\mathbf{R},\mathbf{R}',\xi)dvdv'$. The probability that a specified molecule is situated in dv' at $\mathbf{R}'$ when the partially coupled molecule is fixed at $\mathbf{R}$ is $(1/v)^{(1)}\rho_2(\mathbf{R},\mathbf{R}',\xi)dv'$. From Eqs. (5) and (6), the following relations between the distribution functions are evident,

$$\begin{aligned} \rho_2(\mathbf{R},\mathbf{R}',\xi)&=\rho_1(\mathbf{R},\xi)\rho_1(\mathbf{R}')g(\mathbf{R},\mathbf{R}',\xi),\\ {}^{(1)}\rho_2(\mathbf{R},\mathbf{R}',\xi)&=\rho_1(\mathbf{R}')g(\mathbf{R},\mathbf{R}',\xi), \end{aligned} \tag{7}$$

where it is understood that ξ has the value unity when not indicated explicitly. Properly, $\rho_1(\mathbf{R}',\xi)$ should appear in Eqs. (7), but it may be shown that $\rho_1(\mathbf{R}',\xi)$ differs from $\rho_1(\mathbf{R}',1)$ by terms of negligible order when ξ does not refer to the molecule fixed at $\mathbf{R}'$. We shall refer to the distribution function $g(\mathbf{R},\mathbf{R}')$ as the correlation function, since it determines the correlation, $\langle f_1(\mathbf{R})f_2(\mathbf{R}')\rangle_{Av}-\langle f_1(\mathbf{R})\rangle_{Av}\langle f_2(\mathbf{R}')\rangle_{Av}$, of any two functions $f_1(\mathbf{R})$ and $f_2(\mathbf{R}')$ of the positions of two molecules. The correlation,

$$\begin{aligned} \langle f_1f_2\rangle_{Av}-\langle f_1\rangle_{Av}\langle f_2\rangle_{Av}&=\frac{1}{v^2}\int^v\int^v f_1(\mathbf{R})f_2(\mathbf{R}')\\ &\times[g(\mathbf{R},\mathbf{R}')-1]\rho_1(\mathbf{R})\rho_1(\mathbf{R}')dvdv', \end{aligned} \tag{8}$$

would vanish if $g(\mathbf{R},\mathbf{R}')$ were identically unity

[5] The distribution functions are similar to those defined by J. E. Mayer and E. Montroll, J. Chem. Phys. 9, 2 (1941).

everywhere. In a liquid phase for which $\rho_1(\mathbf{R})$ is unity everywhere, the correlation function $g(\mathbf{R}, \mathbf{R}')$ reduces to the radial distribution function $g_0(|\mathbf{R}'-\mathbf{R}|)$ of the liquid, which has been extensively investigated from the experimental standpoint by x-ray scattering. By virtue of their definitions, the several distribution functions satisfy the following conditions,

$$\begin{gathered}\frac{1}{v}\int^{v}\rho_1(\mathbf{R},\,\xi)dv=1,\\ \frac{1}{v}\int^{v}g(\mathbf{R},\,\mathbf{R}',\,\xi)\rho_1(\mathbf{R}')dv'=1,\\ \rho_1(\mathbf{R},\,0)=1\,;\quad g(\mathbf{R},\,\mathbf{R}',\,0)=1\,;\\ {}^{(1)}\rho_2(\mathbf{R},\,\mathbf{R}',\,0)=\rho_1(\mathbf{R}').\end{gathered}\tag{9}$$

We shall now undertake the formulation of an integral equation for $\rho_1(\mathbf{R})$. Differentiation of both sides of Eq. (5) with respect to ξ and reference to Eqs. (3), (4) and (6) lead to the result,

$$\begin{gathered}\frac{\partial \log \rho_1(\mathbf{R},\,\xi)}{\partial\xi}=-\frac{N}{kT}[\langle {}^{(1)}V(\mathbf{R},\,\xi)\rangle_{Av}-\langle V(\xi)\rangle_{Av}],\\ \langle {}^{(1)}V(\mathbf{R},\,\xi)\rangle_{Av}=\frac{1}{v}\int^{v}V(|\mathbf{R}'-\mathbf{R}|)\\ \qquad\times {}^{(1)}\rho_2(\mathbf{R},\,\mathbf{R}',\,\xi)dv',\\ \langle V(\xi)\rangle_{Av}=\frac{1}{v^2}\int\int V(|\mathbf{R}'-\mathbf{R}|)\\ \qquad\times\rho_2(\mathbf{R},\,\mathbf{R}',\,\xi)dvdv'.\end{gathered}\tag{10}$$

Integration of Eq. (10) and substitution from Eq. (7) yields

$$\begin{gathered}\log\lambda\rho_1(\mathbf{R})=\int^{v}K(\mathbf{R},\,\mathbf{R}')\rho_1(\mathbf{R}')dv',\\ K(\mathbf{R},\,\mathbf{R}')=-(N/vkT)V(|\mathbf{R}'-\mathbf{R}|)L(\mathbf{R},\,\mathbf{R}'),\\ L(\mathbf{R},\,\mathbf{R}')=\int_0^1 g(\mathbf{R},\,\mathbf{R}',\,\xi)d\xi,\\ \log\lambda=-(N/vkT)\int_0^1\langle V(\xi)\rangle_{Av}d\xi.\end{gathered}\tag{11}$$

The constant λ is fixed by the normalization condition, Eq. (9). If the correlation function $g(\mathbf{R}, \mathbf{R}', \xi)$ is known for all values of ξ between zero and unity, $L(\mathbf{R}, \mathbf{R}')$ can be calculated and the kernel $K(\mathbf{R}, \mathbf{R}')$ of the integral equation constructed. A formal investigation of the properties of the correlation function leads to an integral equation for this function, similar in form to Eq. (11), with a kernel involving $\rho_1(\mathbf{R})$ and in addition the correlation function for sets of three molecules. Since the simultaneous integral equations obtained by a continuation of this process are extremely complicated and their solution prohibitively difficult, we shall base the further development of the present theory on approximations to $g(\mathbf{R}, \mathbf{R}', \xi)$ suggested by certain reasonable physical hypotheses.

The long range order characteristic of crystalline structure is determined by the distribution function $\rho_1(\mathbf{R})$. The local order imposed by a molecule fixed at a point $\mathbf{R}$ on its environment is determined by the correlation function $g(\mathbf{R}, \mathbf{R}')$, which may conveniently be regarded as a function of $\mathbf{R}$ and $\mathbf{R}'-\mathbf{R}$. The average density at a point $\mathbf{R}'-\mathbf{R}$ from a molecule fixed at $\mathbf{R}$ is proportional to $g(\mathbf{R}, \mathbf{R}'-\mathbf{R})\rho_1(\mathbf{R}')$. Thus the dislocation of the lattice by a molecule fixed at an arbitrary point $\mathbf{R}$ is determined by the correlation function. On physical grounds, one is led to attribute the following properties to the correlation function

$$\begin{gathered}\lim_{|\mathbf{R}'-\mathbf{R}|\to\infty} g(\mathbf{R},\,\mathbf{R}'-\mathbf{R})=1,\\ \lim_{|\mathbf{R}'-\mathbf{R}'|\to 0} g(\mathbf{R},\,\mathbf{R}'-\mathbf{R},\,\xi)=0\,;\quad \xi>0.\end{gathered}\tag{12}$$

The first of these relations implies that the correlation in position between two molecules vanishes at large intermolecular distances. The second implies the existence of large repulsive forces at small distances, excluding molecular interpenetration. The first of the relations (12) requires careful examination. In a three-dimensional system, it is true in the liquid phase, as we know from the properties of the radial distribution function to which it reduces. It can also be shown to be true in the well-ordered crystal with harmonic lattice vibrations. However, it is not valid for the linear chain or for the surface grating, in which the correlation in position between two molecules remains finite at infinite separation.* It is interesting to remark

* We are indebted to Professor P. Debye and Professor J. E. Mayer for illuminating discussions on this point.

that the approximation of $g(\mathbf{R}, \mathbf{R}'-\mathbf{R})$ by unity everywhere is equivalent to assuming an Einstein crystal.

From another point of view, the correlation function may be regarded as a functional $g(\mathbf{R}', \mathbf{R}, [\rho])$ of the distribution function ρ_1 in the sense of Volterra.[6] Though we shall not make extensive use of this property, we remark again that for the disordered phase, $\rho_1(\mathbf{R})=1$,

$$g(\mathbf{R}', \mathbf{R}, [1])=g_0(|\mathbf{R}'-\mathbf{R}|), \tag{13}$$

where $g_0(|\mathbf{R}'-\mathbf{R}|)$ is the liquid radial distribution function, which depends only on the distance $|\mathbf{R}'-\mathbf{R}|$. We shall base the further development of our theory on the approximation of $g(\mathbf{R}', \mathbf{R}, [\rho])$ by $g(\mathbf{R}, \mathbf{R}', [1])$, that is by the radial distribution function $g_0(|\mathbf{R}'-\mathbf{R}|)$ of the disordered liquid phase, perhaps metastable. The existence of undercooled liquid phases makes this approximation physically meaningful. Its adequacy from a quantitative standpoint is difficult to estimate by theoretical criteria, but can be judged *a posteriori* in the applications of the theory which are to follow. With this approximation, the integral equation (11) becomes

$$\log \lambda\rho_1(\mathbf{R})=\int K_0(|\mathbf{R}'-\mathbf{R}|)\rho_1(\mathbf{R}')dv',$$

$$K_0(|\mathbf{R}'-\mathbf{R}|)=-(N/vkT) \times V(|\mathbf{R}'-\mathbf{R}|)L_0(|\mathbf{R}'-\mathbf{R}|). \tag{14}$$

$$L_0(|\mathbf{R}'-\mathbf{R}|)=\int_0^1 g_0(|\mathbf{R}'-\mathbf{R}|, \xi)d\xi,$$

where due to the short range character of $V(|\mathbf{R}-\mathbf{R}'|)$ the integral may be extended to all of space, except in the immediate vicinity of the boundaries of the region v.

We shall be interested in those solutions of Eq. (14) with the period of a specified space lattice. Among the possible lattices and distribution functions, the one corresponding to a minimum value of the work content at constant temperature and volume is to be selected as appropriate to thermodynamic equilibrium. The periodic distribution function and its logarithm may be expanded in the Fourier series,

$$\rho_1(\mathbf{R})=\sum_{\substack{h_1, h_2, h_3 \\ =-\infty}}^{+\infty} s(\mathbf{h}) \exp (2\pi i\mathbf{h}\cdot\mathbf{R}),$$

$$\log \lambda\rho_1(\mathbf{R})=\sum_{\substack{h_1, h_2, h_3 \\ =-\infty}}^{+\infty} q(\mathbf{h}) \exp (2\pi i\mathbf{h}\cdot\mathbf{R}), \tag{15}$$

$$\mathbf{h}=h_1\mathbf{b}_1+h_2\mathbf{b}_2+h_3\mathbf{b}_3,$$

where h_1, h_2, h_3 are integers and $\mathbf{b}_1$, $\mathbf{b}_2$, $\mathbf{b}_3$ are the basic vectors of the reciprocal lattice of the assumed structure. Substitution of the Fourier series (15) into the integral equation (14) yields the relations

$$q(\mathbf{h})=\alpha(\mathbf{h})\cdot s(\mathbf{h}),$$

$$\alpha(\mathbf{h})=(2/h)\int_0^\infty rK_0(r) \sin (2\pi hr)dr, \tag{16}$$

$$h=|\mathbf{h}|.$$

For periodic solutions, the normalization condition, Eq. (9) becomes

$$\frac{1}{\Delta}\int^\Delta \rho_1(\mathbf{R})dv=1, \tag{17}$$

where the integration extends over the elementary cell Δ of the lattice. Substitution of the second of the series (15) into Eq. (17) yields†

$$\lambda=(1/\Delta)\int^\Delta \exp [\sum_h q_h \exp (2\pi i\mathbf{h}\cdot\mathbf{R})]dv, \tag{18}$$

which determines λ as a function of the variables q_h. Calculation of the Fourier coefficient s_h from the second of the series (15) gives

$$s_h=\frac{1}{\lambda\Delta}\int^\Delta \exp (-2\pi i\mathbf{h}\cdot\mathbf{R}) \times\exp [\sum_{h'} q_{h'} \exp (2\pi i\mathbf{h}'\cdot\mathbf{R})]dv$$

or

$$s_h=\partial \log \lambda/\partial q_h^*, \tag{19}$$

where q_h^* is the conjugate of q_h, equal to q_{-h}, since both $\rho_1(\mathbf{R})$ and its logarithm must be real. Combination of Eqs. (16) and (19) gives

$$q_h=\alpha_h G_h(q_0, \cdots),$$

$$G_h(q_0\cdots)=\partial \log \lambda/\partial q_h^*, \tag{20}$$

[6] V. Volterra, *Theory of Functionals and of Integral and Integro-Differential Equations* (Blackie and Son, Ltd., 1930).

† *Note.*—For simplicity in notation $\alpha(\mathbf{h})$, $q(\mathbf{h})$, and $s(\mathbf{h})$ will occasionally be written as α_h, q_h and s_h.

an infinite set of transcendental equations for the Fourier coefficients q_h of the logarithm of the distribution function. Thus the determination of real periodic solutions of the integral equation (14) is equivalent to determining the solutions of the set of transcendental equations (20) as functions of the transforms $\alpha(\mathbf{h})$ of the kernal $K_0(r)$. From Eqs. (20) and the normalization condition (17) we remark that

$$q_0=\alpha_0, \quad s_0=1, . \tag{21}$$

where we write q_0 and s_0 for q_{000} and s_{000}. By inspection, one finds that Eqs. (20) always have the solutions $q_h=0$ for $h>0$, according to which $\rho_1(\mathbf{R})$ has the constant value unity everywhere, corresponding to a disordered phase. We shall not undertake at the present time the difficult mathematical investigation of the infinite set of equations (20). However, when the transforms α_h vanish for h greater than some finite h_0, the equations reduce to a finite set of transcendental equations. It may then be shown that for specified lattices, non-trivial periodic solutions $\rho_1(\mathbf{R})$, with non-vanishing Fourier coefficients s_h for $h>0$, exist for sufficiently large values of the transforms α_h, and correspond to lower work content than the solution $\rho_1(\mathbf{R})=1$. Since the transforms α_h are functions of temperature and volume, the Fourier coefficients s_h of $\rho_1(\mathbf{R})$ become discontinuous functions of volume, all except s_{000} vanishing when the volume exceeds a critical value v^* at a specified temperature. We shall postpone the detailed discussion of the approximate solutions of Eqs. (20) to a later section of the article.

The Thermodynamic Functions and Heterogeneous Equilibrium

We shall undertake the formulation of expressions for the thermodynamic functions of the system in terms of the Fourier coefficients s_h of the distribution function $\rho_1(\mathbf{R})$, under the restraint of homogeneity according to which the periodic solution of the structure of minimum work content at the specified average density and temperature is assumed valid throughout the region v occupied by the system. The lowest work content may actually be realized with different periodic solutions in different domains of the region v, corresponding to the coexistence of two or at most three distinct phases. Although this situation can be treated explicitly by minimizing the work content with respect to the masses of the several homogeneous parts, it is more convenient to employ the thermodynamic criteria of heterogeneous equilibrium in conjunction with the theoretical expressions for the thermodynamic functions calculated with the restraint of homogeneity.

We refer to Eq. (18) of the article "Statistical Mechanics of Fluid Mixtures" by one of us.[4] From this equation and the last of Eqs. (11) of the present article, we find for the molar Gibbs free energy F, identical with the chemical potential in a one-component system,

$$\begin{gathered} F/RT=-\log \lambda v+F^0(T)/RT, \\ F^0(T)/RT=-\log \frac{(2\pi mkT)^{\frac{3}{2}}}{Nh^3}, \end{gathered} \tag{22}$$

where v is the molar volume, N is Avogadro's number, m the molecular mass and h Planck's constant. The parameter λ is specified as a function of the Fourier coefficients q_h by Eq. (18) of the present article. The mean energy E of the system is

$$\begin{gathered} E/RT=\tfrac{3}{2}+(N/2kT)\bar{V}, \\ \bar{V}=(1/v)^2\int^v\int^v V(|\mathbf{R}'-\mathbf{R}|)g(\mathbf{R}',\mathbf{R}) \\ \times\rho_1(\mathbf{R})\rho_1(\mathbf{R}')dvdv', \end{gathered} \tag{23}$$

where $\bar{V}$ is the average potential energy of a molecular pair. Introducing the Fourier series, Eq. (15), into the integral of Eq. (23) and approximating the correlation function by the radial distribution function $g_0(|\mathbf{R}'-\mathbf{R}|)$, we obtain

$$\begin{gathered} E/RT=-(\tfrac{1}{2})\sum_h \beta_h|s_h|^2+\tfrac{3}{2}, \\ \beta_h=-(2N/vhkT)\int_0^\infty rV(r)g_0(r)\sin(2\pi hr)dr. \end{gathered} \tag{24}$$

If we define $\beta_h(\xi)$ as

$$\beta_h(\xi)=-(2N/vhkT)\int_0^\infty rV(r)g_0(r,\xi)\sin(2\pi hr)dr, \tag{25}$$

we remark from Eqs. (14) and (16) that the transforms α_h and $\beta_h(\xi)$ are related in the following manner

$$\alpha_h = \int_0^1 \beta_n(\xi) d\xi. \tag{26}$$

In order to obtain the equation of state, we differentiate Eq. (22) with respect to volume at constant temperature and refer to Eqs. (16) and (18)

$$-\frac{v}{RT}\left(\frac{\partial p}{\partial v}\right)_T = \frac{1}{v} + \frac{1}{2}\sum_h \frac{1}{\alpha_h}\left(\frac{\partial q_h^2}{\partial v}\right)_T. \tag{27}$$

We shall assume that the stable solutions of Eqs. (20) are continuous functions of the volume except at a point v^* and that $q_h = 0$ for $v > v^*$ and $h > 0$. Integration of Eq. (27) under these conditions with a minor transformation based upon partial integration yields

$$pv/RT = 1 - \Delta\Omega^* + \tfrac{1}{2}\sum_h{}' \left\{ \alpha_h |s_h|^2 + v\int_{v^*}^{v} (1/v')^2 \frac{\partial(\alpha_h v')}{\partial v'} |s_h|^2 dv' \right\} - v\int_{\infty}^{v} \frac{\alpha_0}{v'^2} dv', \tag{28}$$

$$\Omega = \log \lambda' - \tfrac{1}{2}\sum_h{}' \alpha_h |s_h|^2; \quad \lambda' = \lambda \exp(-\alpha_0),$$

$$\Delta\Omega^* = \Omega(v^* - 0) - \Omega(v^* + 0),$$

where the prime denotes the omission of the term for $h = 0$ in the sums and the discontinuity $\Delta\Omega^*$ in pv/RT is determined by the requirement that the work content $F - pv$ be continuous at v^*. For volumes not differing greatly from v^*, the integrals

$$v\int_{v^*}^{v} (1/v')^2 \frac{\partial(\alpha_h v')}{\partial v'} |s_h|^2 dv'$$

can be neglected without great error since they can be shown to be bounded in absolute value by $[\alpha_h - (v^*/v)\alpha_h^*]|s_h|^2$ if $\alpha_h v$ is monotonic function of the volume.

If we denote by F', A' and E' the excesses $(F - F_0)$, $(A - A_0)$, and $(E - E_0)$ of the free energy, work content, and energy over their disordered values F_0, A_0 and E_0 at the specified temperature and volume, we may write from Eqs. (22), (24) and (28)

$$\begin{aligned} F'/RT &= -\log \lambda', \\ A'/RT &= -\log \lambda' + \tfrac{1}{2}\sum_h{}' \alpha_h |s_h|^2 + \Delta\Omega^*, \\ E'/RT &= -\tfrac{1}{2}\sum_h{}' \beta_h |s_h|^2, \\ p'v/RT &= -\tfrac{1}{2}\sum_h{}' \alpha_h |s_h|^2 - \Delta\Omega^*, \end{aligned} \tag{29}$$

where the last two formulas involve the neglect of the volume integrals between v^* and v in Eq. (28).

The conditions for heterogeneous equilibrium between the liquid phase (disordered) and the crystalline phase (ordered), equality of the chemical potentials and pressures in the two phases, combined with Eqs. (29) lead to the relations

$$\begin{aligned} &\log \lambda' = -\Delta F_0/RT, \quad p' = \Delta p_0, \\ &\Delta F_0 = F_0(T, v_l) - F_0(T, v_s), \\ &\Delta p_0 = p_0(T, v_l) - p_0(T, v_s), \end{aligned} \tag{30}$$

where F_0 and p_0 are the free energy and pressure of the undercooled disordered phase. Since λ' and p' are functions of the q_h, which depend upon temperature and volume through the transforms α_h, Eqs. (30) provide two relations between v_l and v_s at a specified temperature, from which, in principle, the liquid and solid volumes may be determined, and from them the other fusion parameters calculated. The increments in the thermodynamic functions of the disordered phase may be approximated in the following manner,

$$\begin{aligned} &\Delta F_0 = -\Delta v/\kappa_0, \\ &\Delta p_0 = -(1/\kappa_0)\log v_l/v_s, \\ &\Delta E_0 + p\Delta v = \frac{T\gamma_0}{\kappa_0} + \frac{v_s}{\kappa_0}\left[\log\frac{v_l}{v_s} - \frac{\Delta v}{v_s}\right], \\ &\Delta v = v_l - v_s, \end{aligned} \tag{31}$$

if the compressibility κ_0 and the thermal expansion coefficient γ_0 are treated as constant in the volume interval Δv. With the aid of Eqs. (29) and (31), Eqs. (30) may be put into the

somewhat more convenient form,

$$\log \lambda' = \Delta v/\kappa_0 RT,$$

$$\Omega = \Delta\Omega^* + \frac{v_s}{\kappa_0 RT}\left\{\frac{\Delta v}{v_s} - \log\left(\frac{v_l}{v_s}\right)\right\}, \quad (32)$$

$$\Omega = \log \lambda' - \tfrac{1}{2}\sum_h{}' \alpha_h |s_h|^2.$$

The entropy of fusion, ΔS, equal to $\Delta H/T$, is calculated from Eqs. (29) and (31) to be

$$\Delta S/R = \tfrac{1}{2}\sum_h{}' \beta_h |s_h|^2 + \Delta S_0/R,$$

$$\Delta S_0/R = \frac{\gamma_0 \Delta v}{\kappa_0} + \frac{v_s}{\kappa_0 RT}\left\{\log\left(\frac{v_l}{v_s}\right) - \frac{\Delta v}{v_s}\right\}. \quad (33)$$

Eqs. (32) and (33) will be employed to determine the fusion parameters Δv and ΔS in a later section of the article.

The Transforms α_h and β_h

The transform β_h defined in Eq. (24) may be computed by numerical integration from the potential energy $V(r)$ of a molecular pair and the experimental radial distribution function $g_0(r)$, extrapolated if necessary to the undercooled liquid region. The calculation of $\beta_h(\xi)$ and α_h is considerably more difficult, since it demands a knowledge of the radial distribution function $g_0(r, \xi)$ for intermediate degrees of intermolecular coupling not realized in the actual system. However, certain approximate results can be stated without entering into a detailed theory of the radial distribution function.

It is convenient to employ the impenetrable sphere approximation to intermolecular repulsion, at small distances, according to which the molecules are assigned a diameter a_0. This may be accomplished by introducing a potential of intermolecular force,

$$V(r) = V_0; \quad 0 < r < a_0, \quad (34)$$

where V_0 is a positive constant which is allowed to approach infinity in the partition function and the distribution functions derived from it. If we divide the interval of integration in Eq. (25) defining $\beta_h(\xi)$, we may write

$$\beta_h(\xi) = \tau_0 \beta_h{}^{(0)}(\xi) + \beta_h{}^{(1)}(\xi),$$

$$\beta_h{}^{(0)}(\xi) = \frac{-2N}{vh}\int_0^{a_0} r g_0(r, \xi)\sin(2\pi hr)dr, \quad (35)$$

$$\beta_h{}^{(1)}(\xi) = \frac{-2N}{vhkT}\int_{a_0}^{\infty} r V(r) g_0(r, \xi)\sin(2\pi hr)dr,$$

where τ_0 is equal to V_0/kT and $V(r)$ is the potential of intermolecular attraction in the interval $a_0 \leqslant r < \infty$. Examination of the phase integrals defining the correlation function, here approximated by the radial distribution function, shows that it depends upon the coupling parameter ξ in the form $g_0(r, \xi\tau_0, \xi/T)$. We shall need to consider the following limits

$$\lim_{\tau_0 \to \infty} g_0(r, \xi\tau_0, \xi/T) = \bar{g}_0(r, \xi/T); \quad \xi > 0$$
$$\lim_{\tau_0 \to \infty} g_0(r, \tau, \tau/\tau_0) = g_0(r, \tau). \quad (36)$$

The function $\bar{g}_0(r, \xi/T)$ corresponds to full repulsive coupling and partial attractive coupling of one molecule of the pair with the other molecules of the system, whereas $g_0(r, \tau)$ corresponds to partial repulsive coupling and vanishing attractive coupling. Substitution of the $\beta_h(\xi)$ of Eq. (35) into Eq. (26), change of variable in the first integral and passage to the limit $V_0 \to \infty$ yields

$$\alpha_h = \alpha_h{}^{(0)} + \alpha_h{}^{(1)},$$

$$\alpha_h{}^{(0)} = \frac{-2N}{vh}\int_0^{a_0} r L^{(0)}(r)\sin(2\pi hr)dr,$$

$$\alpha_h{}^{(1)} = \frac{-2N}{vhkT}\int_{a_0}^{\infty} r V(r) L^{(1)}(r)\sin(2\pi hr)dr, \quad (37)$$

$$L^{(0)}(r) = \int_0^{\infty} g_0(r, \tau)d\tau,$$

$$L^{(1)}(r) = \int_0^1 \bar{g}_0(r, \xi/T)d\xi.$$

If $\bar{g}_0(r, \xi/T)$ for $r > a_0$ is assumed to be an analytic function of ξ/T, $\bar{g}_0(r, \xi/T)$ differs from the radial distribution function $g_0(r)$ for complete intermolecular coupling, $\xi = 1$ by terms of order $1/T$ and we may write, remembering

Eq. (26),

$$\alpha_h^{(1)} = \beta_h\{1+O(1/T)\}, \tag{38}$$

where the neglected terms of order $1/T$ represent the effect of intermolecular attraction on the radial distribution function. Since β_h is of the order $1/T$, we may write

$$\alpha_h = \alpha_h^{(0)} + \beta_h + O(1/T^2), \tag{39}$$

where $\alpha_h^{(0)}$ depends upon both volume and temperature, but reduces to a function of volume only, for a system of impenetrable spheres with vanishing intermolecular attraction.

In order to get a clearer idea of the properties of the function $L^0(r)$ from which the transform $\alpha_h^{(0)}$ is calculated, we shall examine the thermodynamic functions of the disordered phase alone. From Eqs. (22) and (28) we may write for the work content

$$A_0/RT = -\log(ev) + v\int_\infty^v (\alpha_0/v^2)dv + F^0/RT. \tag{40}$$

If on the other hand the work content is expanded in the moments of the potential of intermolecular attraction, we obtain

$$A_0/RT = -\log(ev_f) - \beta_0/2 + O(1/T^2) + F^0/RT, \qquad v_f = (Z_N{}^0)^{1/N}, \tag{41}$$

where $Z_N{}^0$ is the phase integral appropriate to impenetrable spheres with no attractive forces, and v_f is a free volume of the type introduced by Eyring[7] or by Lennard-Jones and Devonshire[8] in their theories of the liquid state. Comparison of Eqs. (40) and (41) yields

$$\alpha_0 = -\log(v/v_f) - \frac{\partial \log(v_f/v)}{\partial \log v} - \frac{1}{2}\left(\frac{\partial(\beta_0 v)}{\partial v}\right)_T + \beta_0 + O\left(\frac{1}{T^2}\right). \tag{42}$$

From Eqs. (14), (15) and (39), we obtain

$$\frac{4\pi N}{v}\int_0^{a_0} r^2 L^{(0)}(r)dr = \log\left(\frac{v}{v_f}\right) + \frac{\partial \log(v_f/v)}{\partial \log v} + \frac{1}{2}\frac{\partial(\beta_0 v)}{\partial v}. \tag{43}$$

If $L^0(r)$ is approximated by a constant in the sphere a_0, the transform $\alpha_h^{(0)}$ becomes

$$\alpha_h^{(0)} = \frac{\sigma(v,T)}{(2\pi h a_0)^2}\left\{\cos 2\pi h a_0 - \frac{\sin 2\pi h a_0}{2\pi h a_0}\right\}, \qquad \sigma(v,T) = 3\left\{\log\left(\frac{v}{v_f}\right) + \frac{\partial \log(v_f/v)}{\partial \log v} + \frac{1}{2}\frac{\partial(\beta_0 v)}{\partial v}\right\}. \tag{44}$$

As we shall later see, the term $\alpha_h^{(0)}$ in the transform α_h leads to the prediction that a system of hard spheres without attraction must crystallize at sufficiently small volumes.

Approximations for the Face-Centered Cubic Lattice

We shall investigate the solutions of Eq. (14) for a cubic lattice with a unit cell of volume $\Delta = 4v/N$, having an average content of four atoms. The lattice vectors $\mathbf{a}_1$, $\mathbf{a}_2$, $\mathbf{a}_3$ are orthogonal and of the same length a equal to $\Delta^{\frac{1}{3}}$. The reciprocal vectors $\mathbf{b}_1$, $\mathbf{b}_2$, $\mathbf{b}_3$ are also orthogonal and of equal magnitude $1/a$. We denote by x, y, and z the components $\mathbf{R}\cdot\mathbf{b}_1$, $\mathbf{R}\cdot\mathbf{b}_2$, and $\mathbf{R}\cdot\mathbf{b}_3$. If we approximate the Fourier transform α_h by zero for values of h greater than or equal to $2/a$, we conclude from Eqs. (20) that all q_h vanish for $h > \sqrt{3}/a$, and the infinite set of transcendental equations reduces to a finite set determining the twenty-six variables q_h in the distribution function*

$$\log \lambda' \rho_1(x,y,z) = \sum_{h_1,h_2,h_3}{}^{\prime}{}^{+1}_{-1} q(h_1,h_2,h_3) \times \exp[2\pi i(h_1 x + h_2 y + h_3 z)], \tag{45}$$

the constant term in the Fourier series being absorbed in the parameter λ' defined as $\lambda \exp(-q_0)$. Since the transforms α_h depend only on the absolute value of h, it is evident that Eqs. (20) have solutions depending only on the absolute value of h, in which case the twenty-six variables $q(h)$ reduce to three q'', q' and q corresponding to values of h of $1/a$, $\sqrt{2}/a$ and $\sqrt{3}/a$, respectively. Since the origin to which $\rho_1(x,y,z)$ is referred is arbitrary, from one set of solutions q_h other sets $q_h \exp 2\pi i \mathbf{h}\cdot\mathbf{R}_0)$, with $\mathbf{R}_0$ an arbitrary constant

[7] H. Eyring and J. O. Hirschfelder, J. Phys. Chem. **41**, 249 (1937).

[8] J. E. Lennard-Jones and A. F. Devonshire, Proc. Roy. Soc. **A163**, 53 (1937).

* The vanishing of the coefficient q_h for $h \geq 2/a$ is due to the neglect of the α_h and does not imply the vanishing of the corresponding s_h.

TABLE I. *The transcendental equation.*

$8q$ $2.82=8q^*$	α $0.9730=\alpha^*$	s $0.36_2=s^*$	$\log\lambda'$ $0.506=\log\lambda'(q^*)$
3.00	0.9734	0.3853	0.5738
3.50	0.9783	.4472	0.7819
4.00	0.9897	.5052	1.0203
4.50	1.0082	.5579	1.287
5.00	1.0325	.6053	1.578
5.50	1.0633	.6466	1.892
6.00	1.0991	.6824	2.223
6.50	1.1400	.7127	2.572
7.00	1.1848	.7385	2.936
7.50	1.232	.7609	3.312
8.00	1.283	.7794	3.696

q^*, α^*, and s^* are the critical values of q, α, and s.

vector, may be constructed. If we place the origin at the point (0, 0, 0) in any cell and employ the solutions q'', q' and q, the distribution function, Eq. (45), becomes

$$\begin{aligned}
\rho_1(x,y,z)&=\frac{1}{\lambda'}f''(x,y,z)f'(x,y,z)f(x,y,z),\\
f''(x,y,z)&=\exp\left[6q''(\cos 2\pi x\right.\\
&\qquad\left.+\cos 2\pi y+\cos 2\pi z)\right],\\
f'(x,y,z)&=\exp\left[12q'(\cos 2\pi x\cos 2\pi y\right.\\
&\qquad+\cos 2\pi y\cos 2\pi z\\
&\qquad\left.+\cos 2\pi z\cos 2\pi x)\right],\\
f(x,y,z)&=\exp\left[8q(\cos 2\pi x\cos 2\pi y\cos 2\pi z)\right].
\end{aligned}\tag{46}$$

The factor $f''(x, y, z)$ has the symmetry of a simple cubic structure, $f'(x, y, z)$ that of a body-centered structure, and $f(x, y, z)$ that of a face-centered structure. The transcendental equations (20) reduce to

$$\begin{aligned}
q''&=\frac{\alpha''}{6}\frac{\partial\log\lambda'}{\partial q''},\\
q'&=\frac{\alpha'}{12}\frac{\partial\log\lambda'}{\partial q'},\\
q&=\frac{\alpha}{8}\frac{\partial\log\lambda}{\partial q},
\end{aligned}\tag{47}$$

$$\lambda'=\int_0^1\int_0^1\int_0^1 f''(x,y,z)f'(x,y,z)\times f(x,y,z)\,dxdydz,$$

where α'', α' and α are the values of the Fourier transform α_h for $1/a$, $\sqrt{2}/a$, and $\sqrt{3}/a$. Since it may be verified that $\partial\log\lambda'/\partial q''$ and $\partial\log\lambda'/\partial q'$ vanish for all values of q when $q'=q''=0$, special solutions of Eqs. (48) are obtained with $q'=q''=0$. Corresponding to these solutions, is the distribution function

$$\begin{aligned}
\rho_1(x,y,z)&=(1/\lambda')\exp\left[8q(\cos 2\pi x\right.\\
&\qquad\left.\times\cos 2\pi y\cos 2\pi z)\right],\\
\lambda'&=\int_0^1\int_0^1\int_0^1\exp\left[8q\cos 2\pi x\cos 2\pi y\right.\\
&\qquad\left.\cos 2\pi z\right]dxdydz,
\end{aligned}\tag{48}$$

which, for positive q, has congruent maxima at the points (0, 0, 0), $(\frac{1}{2}, \frac{1}{2}, 0)$, $(\frac{1}{2}, 0, \frac{1}{2})$, and $(0, \frac{1}{2}, \frac{1}{2})$, that is at the lattice points of a face-centered structure of cell Δ. Properly, it should be demonstrated that the face-centered distribution, Eq. (48), corresponds to the lowest work content consistent with the specified temperature and volume, before accepting it as the equilibrium distribution. For the present, we shall assume this to be true without proof. A proof would have to be based upon the specific form of the potential of intermolecular forces from which the transforms α_h are calculated. For the distribution function, Eq. (48), the transcendental equations (47) reduce to a single equation

$$\begin{aligned}
q&=\alpha G(q),\\
G(q)&=\tfrac{1}{8}(\partial\log\lambda'/\partial q)_{q''=q'=0}.
\end{aligned}\tag{49}$$

Development of the exponential in the expression for λ', Eq. (48) leads to the following expressions for λ' and $G(q)$

$$\begin{aligned}
\lambda'(q)&=\sum_{n=0}^{\infty}\frac{[(2n)!]^2}{[n!]^3}q^{2n},\\
G(q)&=\frac{q}{8\lambda'}\sum_{n=0}^{\infty}\frac{(2n+2)[(2n+2)!]^2q^{2n}}{[(n+1)!]^3}
\end{aligned}\tag{50}$$

from which λ' and G may be computed as functions of q. For α less than 0.973,[9] it is found that the only real solution of Eq. (49) is $q=s=0$. For α greater than 0.973, there are two non-vanishing positive solutions, the larger of which

[9] *Note.*—Due to certain modifications in the theory, this critical value of α differs slightly from the one stated in our preliminary report, J. G. Kirkwood and E. Monroe, J. Chem. Phys. **8**, 845 (1940).

TABLE II. *Reduced radial distribution function for liquid argon from data of Eisenstein and Gingrich.*

x	$4\pi x^2 g_0(x)$	x	$4\pi x^2 g_0(x)$
0.7847	1.96	1.3732	17.88
0.8828	16.64	1.4713	25.73
0.9809	21.86	1.5694	32.30
1.0790	14.30	1.6675	38.10
1.1771	16.21	1.7656	44.27
1.2751	18.14		

represents the equilibrium distribution, since it may be shown to correspond to the least work content. Corresponding to each positive solution q of Eq. (49), there is also a negative solution $-q$. Since the negative solutions merely imply a change in origin from the point (0, 0, 0) to the point $(\frac{1}{2}, \frac{1}{2}, \frac{1}{2})$, we need only consider the positive solutions. In Table I, the stable solution q of Eq. (49) and certain important functions of q are presented as functions of the parameter α.

Subject to the approximations which have been described, Eqs. (32), expressing the conditions for equilibrium between the liquid phase and a face-centered crystalline phase, become

$$\log \lambda'(q) = \Delta v/\kappa_0 RT,$$
$$\log \lambda'(q) - \frac{4q^2}{\alpha} = 0.0043 + \frac{v_s}{\kappa_0 RT}\left\{\frac{\Delta v}{v_s} - \log\frac{v_l}{v_s}\right\} \tag{51}$$

and the entropy of fusion, Eq. (33), becomes

$$\Delta S/R = 4\beta s^2 + \Delta S_0/R, \tag{52}$$

where q, β and s denote the values of q_h, β_h and s_h for $h=\sqrt{3}/a$ at v_s, the β_h for $h \gtrsim 2/a$ being approximated by zero as in the case of the α_h. From Eq. (24), we may write

$$\beta = -\frac{4}{\sqrt{3}kT}\int_0^\infty x\, V(r_0 x) g_0(r_0 x) \sin(\sqrt{6}\pi x)dx, \tag{53}$$
$$x = r/r_0; \quad r_0 = a/\sqrt{2},$$

where r_0 is the distance between the lattice points of the face-centered structure of cell Δ equal to $4v/N$. An alternative expression for $\Delta S/R$ is

$$\Delta S/R = 4\beta s^2 - \Delta\beta_0/2 + p\Delta v,$$
$$\Delta\beta_0 = \beta_0(v_l) - \beta_0(v_s), \tag{54}$$

where β_0 is the value of the transform β_h for $h=0$. With the aid of Eq. (24), it may be written in the form,

$$\beta_0 = \frac{-4\pi\sqrt{2}}{kT}\int_0^\infty x^2 V(r_0 x) g_0(r_0 x)dx. \tag{55}$$

Were α known as a function of volume and temperature, Eqs. (49) and (51) would provide three relations from which to determine q, v_s and v_l at a specified temperature. From the values q and Δv so determined and values of β_0 and β, ΔS could then be calculated with the aid of Eq. (53), or Eq. (54). Although it is possible to calculate β_0 and β, deficiencies in the theory of the liquid state allow only rough estimates of the parameter α. Using a free volume of the Eyring type it is found with the aid of Eqs. (39) and (44) that α is of the order of magnitude unity at volumes intermediate between v_l and v_s in the case of argon, and thus approximates the critical value 0.973 in the fusion range. In the absence of adequate theoretical estimates of α, we can, however, calculate the fusion parameters Δv and ΔS if the volume of the liquid v_l is taken from experiment, by solving Eqs. (49) and (51) simultaneously for q, α and v_s. An estimate of the entropy of fusion alone may be obtained if both v_l and Δv are taken from experiment and Eqs. (49) and the first of Eqs. (51) solved simultaneously for q and α. Both methods will be employed in the next section for the calculation of the fusion parameters of argon.

THE FUSION PARAMETERS OF ARGON

The liquid-solid transition in argon provides a favorable case for testing theories of fusion. Not only has the transition been extensively studied from the experimental side, but also the intermolecular force between argon atoms is of a simple type and has been investigated in some

TABLE III. *The integrals β_0 and β.*

a (A)	v (CC/MOLE)	$\beta_0 T$ (DEGREES)	βT
5.2	21.3	1752	7.5
5.3	22.6	1667	32.0
5.4	23.9	1590	46.7
5.5	25.2	1542	56.1
5.6	26.6	1461	61.9
5.7	28.1	1402	

detail. In order to calculate the fusion parameters of argon on the basis of the present theory, information concerning the potential energy $V(r)$ and also of the radial distribution function $g_0(r)$ is necessary. For $V(r)$, the potential energy of a pair of argon atoms, we use the familiar two power expression due to Lennard-Jones, as modified by Rushbrooke[10] in accordance with the calculations of Corner.[11] In our notation, this potential is

$$\frac{V}{k}=\frac{3.273\times10^{10}}{(ax)^{11.4}}-\frac{6.487\times10^{6}}{(ax)^{6}},\qquad x=r/r_0;\quad r_0=a/\sqrt{2} \tag{56}$$

with the parameter a expressed in Angstrom units. Eisenstein and Gingrich[12] have determined the radial distribution function of liquid argon at 90°K under a pressure of about 5 atmos. from measurement of the angular distribution of intensity in x-ray scattering. In view of the small compressibility of liquid argon, the density of the liquid under the conditions of their measurements may be taken as 1.374 g/cc or 0.02085 atoms/A^3 as measured by Mathias, Onnes and Crommelin[13] for liquid argon under its own vapor pressure at 90°K. In order to extrapolate the Eisenstein-Gingrich function to other densities, we assume that the radial distribution function is a function only of the reduced radial distance r/r_0 without explicit dependence on density. Although this assumption lacks theoretical justification, we may expect it to be reasonably adequate for extrapolation over small density intervals. The radial distribution function $g_0(x)$ calculated from the data of Eisenstein and Gingrich is presented as a function of the reduced interatomic distance x in Table II. The integrals[14] β and β_0 of Eqs. (53) and (55) calculated by numerical integration with the interatomic potential (56) and the data of Table II are presented as functions of the molar volume v and the lattice parameter a in Table III. Since the energy of vaporization ΔE_v of the disordered phase is equal to $\beta_0 RT/2$, an experimental check on the calculated value of β_0 is possible. For liquid argon at 90°, $\Delta E_v/RT$ has the observed value 7.14, with which the calculated value of $\beta_0/2$ equal to 7.17 compares favorably.

TABLE IV. *Fusion parameters for argon.*

T_m DEGREES KELVIN	$\Delta S/R$ OBS.	Δv OBS. CC/MOLE	Δv CALC. CC/MOLE	$\Delta S/R$ CALC. (EQ. (52) WITH Δv (CALC.)	$\Delta S/R$ CALC. (EQ. (52) WITH Δv OBS.)	$\Delta S/R$ CALC. (EQ. (54) WITH Δv OBS.)
83.9	1.68	3.53	3.25	1.74	1.78	2.02
119.7	1.10	1.88	.62	.70	1.50	1.63
183.2	.71	.92	.33	.48	.97	1.06

TABLE V. *Observed properties of liquid argon at the melting point.*

T_m DEREES K	p_m KG/CM^2	v_l CC/GRAM	κ_0 (KG/CM^2)$^{-1}$	γ_0 (DEGREES)$^{-1}$
83.9	1	0.709	$2.3_4\times10^{-4}$	4.5×10^{-3}
119.7	1650	.661	6.1×10^{-5}	1.9×10^{-3}
183.2	5350	.631	2.1×10^{-5}	8.6×10^{-4}

Sources: At high pressures: v_l from Bridgman's[16] "best values for the volume..of the amorphous phase..on the melting curve"; γ_0 by extrapolation from his Table IV; κ_0 from γ_0, his v_l and dp_m/dT_m, using the relation, $\kappa_0=\gamma_0(dT_m/dp_m)-(1/v_l)(dv_l/dp_m)$. At one atmosphere pressure: v_l, γ_0 by extrapolation of liquid density data;[13] κ_0 from T, v_l, γ_0 and (C_p-C_v) for the liquid ($C_p-C_v=4.8$ cal./mol/degree—Eucken and Hauck, Zeits. f. physik Chemie **134**, 161 (1928)).

The theoretical fusion parameters of argon, ΔS and Δv, are presented in Table IV, calculated with the aid of the best available data (Table V) on the density, compressibility and thermal expansion coefficient of the liquid and compared with the experimental values at several pressures. The fusion parameters were calculated in three ways. Both ΔS and Δv were calculated with the aid of Eqs. (49), (51) and (52). In addition ΔS alone was calculated with use of the observed Δv, Eq. (49), the first of Eqs. (51) and with each of Eqs. (52) and (54). At one atmosphere, comparison is made with the data of Clusius and Weigand[15] and at the higher pressures with the data of Bridgman.[16] At one atmosphere the

[10] G. S. Rushbrooke, Proc. Roy. Soc. Edinburgh **60**, 182 (1940).

[11] J. Corner, Trans. Faraday Soc. **35**, 711 (1939).

[12] A. Eisenstein and N. S. Gingrich, Phys. Rev. **58**, 307 (1940). We are indebted to Dr. Gingrich for a private communication placing at our disposal certain data, some of which are used in Table II. The radial distribution function employed here does not represent the optimum function obtainable from their data (N. S. Gingrich, Phys. Rev. **59**, 290 (1941)), but small variations do not greatly affect the transforms β_0 and β.

[13] Mathias, Onnes and Crommelin, Proc. Acad. Sci. Amst. **15**, 667 (1913).

[14] *Note.*—We may anticipate that the radial distribution function of K. Lark-Horovitz and E. P. Miller, Nature **146**, 459 (1940), or the interatomic potential of O. K. Rice, J. Am. Chem. Soc. **63**, 3 (1941) would lead to somewhat higher values of the integrals β and β_0.

[15] K. Clusius, Zeits. f. physik. Chemie **B31**, 457 (1936); K. Clusius and K. Weigand, *ibid.* **B46**, 1 (1940).

[16] P. W. Bridgman, Proc. Am. Acad. Sci. **70**, 1 (1935).

TABLE VI. *Reduced melting parameters.*

SUBSTANCE	T_c DEGREES	v_c CC/MOLE	T_m/T_c	v_l/v_c	v/v_c	$\Delta S/R$
Ne	44.4	41.7	0.553	0.388	0.0513	1.64
A	150.6	75.2	.556	.376	.0470	1.68
Kr	209.4	92.1	.554	.371	.0487	1.69
Xe	289.7	113.7	.557	.375	.0493	1.71
N_2	126.0	90.1	.502	.358	.0286	1.24
CH_4	190.6	99	.475	.340	.0272	1.37
CCl_4	556.3	275.9	.451	.333	.0144	1.16
A (CALC.)					.0432	1.78

References: critical data:—except Kr—Int. Crit. Tab. (Pickering), Kr (reference a); latent heats and T_m: Ne, A, Kr—(reference 15; Xe (reference b); N_2 (reference c); CCl_4 (reference d); CH_4(reference e); v_l: A (reference 13); Ne (reference f); Kr (reference a); N_2 Int. Crit. Tab.; Xe CH_4 (see reference 15); CCl_4, Int. Crit. Tab. (extrapolated); Δv: A, Kr, Xe, CH_4 (reference 15), Ne (reference 15), N_2 (reference g), CCl_4, Int. Crit. Tab.

[a] Mathias, Crommelin and Meihuizen, Comptes rendus **204**, 630 (1937), or Proc. Acad. Sci. Amst. **40**, 259 (1937).
[b] K. Clusius and L. Riccoboni, Zeits. f. physik Chemie **B38**, 81 (1937).
[c] W. F. Giauque and J. O. Clayton, J. Am. Chem. Soc. **55**, 4875 (1933).
[d] D. R. Stull, J. Am. Chem. Soc. **59**, 2726 (1937).
[e] K. Clusius, Zeits. f. physik. Chemie **B3**, 41 (1929).
[f] Mathias, Crommelin and Onnes, Ann. d. Physik **19**, 231 (1923).
[g] W. H. Keesom and J. H. C. Lisman, Physica **1**, 737 (1934).

calculated fusion parameters agree remarkably well with the observed values. At the higher pressures the entropy increment agrees moderately well, the volume increment rather poorly, with the observed values. In view of the approximations which it is necessary to introduce into the theory in order to arrive at explicit numerical results, no more than semi-quantitative agreement with experiment is to be expected. We may therefore conclude that the experimental confirmation of our theory is adequate.

It has long been a matter of speculation whether a critical point for fusion analogous to that for vaporization exists. Our theory predicts no critical point for the face-centered lattice if the parameter α is a monotone increasing function of density, unbounded at infinite density. This property is consistent with the approximate Eq. (44), since with increasing density the free volume tends to zero and α becomes infinite as close packing of rigid spherical molecules is approached. The basis for this conclusion is to be found in the fact that the liquid-solid transition is of the first order at constant volume. If at an arbitrary temperature a volume exists for which the parameter α attains its critical value, 0.973, the pressure jumps discontinuously to a lower value, and by the criterion of equal areas, the pressure-volume isotherm must possess a flat. It is to be remarked that no experimental evidence for the existence of a critical point for fusion exists, even in Bridgman's extensive investigations of the liquid-solid transition at very high pressures.

Some general theoretical conclusions concerning the fusion parameters may be based upon a law of corresponding states. As has been pointed out by Pitzer,[17] the partition function and all quantities derivable from it can be expressed as functions of the reduced temperature T/T_c, and reduced volume v/v_c alone, if the potential of intermolecular force is a two parameter function of the distance, T_c and v_c being the critical temperature and critical volume. The two-power Lennard-Jones potential with fixed exponents is of this type. If such a potential is assumed, we would expect the transforms α_h and β_h of the present theory to depend only on the reduced temperature and reduced volume. The equations of the theory would thus involve only the reduced variables. As a consequence, the entropy increment ΔS and the reduced volume increment $\Delta v/v_c$ of fusion at the triple point would have to be identical with those of argon at its triple point for all substances which have potentials of intermolecular force differing from that of argon only in the magnitudes of the coefficients of the two terms in the Lennard-Jones formula. If the triple-point pressures are of the order of magnitude of one atmosphere, the comparison may equally well be made at one atmosphere, since the fusion parameters are not sensitive to changes in pressure of this order. Under these assumptions our calculations for argon should be applicable to the other rare gases. A summary of the reduced fusion data for these and for some other substances composed of approximately spherical molecules is given in Table VI. Since all of the substances included in the table except nitrogen crystallize in face-centered cubic lattices, and all enjoy uninhibited molecular rotation at the melting point, the observed deviations from the law of corresponding states are doubtless attributable to departures from the assumed form of the potential of intermolecular force.

[17] K. S. Pitzer, J. Chem. Phys. **7**, 583 (1939).

The Heat Capacity of Certain Halomethanes

GEORGE GLOCKLER AND WALTER F. EDGELL
Chemical Laboratory, State University of Iowa, Iowa City, Iowa

(Received April 30, 1941)

A semi-empirical method of calculating the heat capacities of the halomethanes is presented. It is based on additive contributions of the bonds and angles making up the molecule. Values obtained for eighteen molecules at three temperatures by this method are compared with those calculated by statistical means. The average deviation is 0.9 percent.

IN recent years the halomethanes have become increasingly important in industry; yet there exist reliable thermodynamical data for only a few of them.[1] On the other hand, these compounds are being extensively studied by Raman and infra-red spectroscopy. In some cases where thermal data are available the two have been combined to yield complete thermodynamic functions in the temperature range in which the rigid rotator-simple harmonic oscillator approximation is valid. Heat capacity and entropy have been calculated for some molecules for which no thermal data are available.[2] However, there exist a considerable number of halomethanes for which the fundamental vibrations are uncertain or unknown, and hence accurate calculations are not yet possible. Thus it seems worth while to investigate to what extent the existing data can be made to yield results of engineering value. The present investigation is concerned with a semi-empirical calculation of the heat capacity of certain halomethanes.

THEORETICAL CONSIDERATIONS

In all molecules of this type rotation has been excited to its classical value before room temperature has been reached; hence one is concerned only with the vibrational contribution. The vibration of a polyatomic molecule is a complicated process in which in each normal mode the motion of every atom is generally involved. Nevertheless, there exist certain modes in which the frequency is largely determined by the motion of only a few atoms. Thus in the molecule CXYZT there is a vibration, associated with the stretching of each valence bond, which remains nearly independent of the molecule in which the bond happens to be.[3] The remaining five vibrations result from the deformation of the six angles and are more or less characteristic of them. Thus one may write

$$C^0_p = 4R + \sum_1^4 C^0_{\nu_i} + \sum_1^5 C^0_{\delta_j}, \qquad (1)$$

where the first term is the contribution of translation and rotation (plus R for $C_p - C_v$), and $C^0_{\nu_i}$ and $C^0_{\delta_j}$ are Einstein functions for the stretching and deformation vibrations, respectively. By choosing values of ν_i which are most nearly consistent with a number of molecules it is possible to approximate the second term with considerable accuracy. Table I gives a summary of the characteristic C−X vibrations in some halomethanes and the values chosen for each bond.[3,4]

The deformation vibrations are, in general, more nearly functions of all the angles rather than any one, and hence the same kind of treatment cannot be followed. However, the third term may be satisfactorily approximated by expanding it into a summation over the six angles, weighted according to the total number of angles. Equation 1 then becomes

$$C^0_p = 4R + \sum_1^4 C^0_{\nu_i} + \frac{5}{6} \sum_j n_j C^0_{\delta_j}, \qquad (2)$$

[1] R. C. Lord, Jr. and E. R. Blanchard, J. Chem. Phys. **4**, 707 (1936); Egan and Kemp, J. Am. Chem. Soc. **60**, 2097 (1938); Messerly and Aston, J. Am. Chem. Soc. **62**, 886 (1940).

[2] See references in the review article by E. Bright Wilson, Jr., Chem. Rev. **27**, 17 (1940).

[3] G. R. Leader, "Studies in molecular structure," Ph.D. thesis, University of Minnesota (1940) and others.

[4] Ta-You Wu, *Vibrational Spectra and Structure of Polyatomic Molecules* (China Science Corporation, Shanghai, 1939).

TABLE I. *Characteristic* C−X *frequencies.*

C−H		C−F		C−Cl		C−Br	
$CHCl_3$	3020 cm^{-1}	CH_3F	1048	CH_3Cl	732	CH_3Br	610
$CHCl_2F$	3019	CH_2ClF	1046	CH_2BrCl	726	CH_2IBr	616
$CHBr_2F$	3017	$CHCl_2F$	1065	$CHBr_2Cl$	750	CH_2Br_2	637
$CHBrCl_2$	3020	CCl_3F	1067	CBr_3Cl	734	$CHCl_2Br$	610
$\nu = 3000$		$\nu = 1050$		$\nu = 730$		$\nu = 610$	

where n_j is the number of j angles and the summation is over all different angles. $C^0_{\delta j}$ is the Einstein function for the hypothetical characteristic deformation frequency δ_j, associated with each angle, which will be evaluated later. Thus, by Eq. (2) the heat capacity of any halomethane is solely determined by the bonds and angles which make up the molecule. The success of this treatment is indicated by the values in Table III.

This discussion does not apply to molecules of the type CX_4 since they have two stretching and two deformation vibrations separated widely enough to invalidate the above statements. This puts little restriction upon the general usefulness of Eq. (2).

Bennewitz and Rossner[5] have successfully applied a similar treatment to molecules containing C, H and O in which a deformation frequency was assigned to each bond rather than angle. This type of approximation is valid whenever the forces resisting deformation arise primarily from the directed nature of the valence bond or whenever the bond appears only in angles of the same kind as in those molecules treated by Bennewitz and Rossner. The forces between the atoms not joined by valence bonds are of considerable importance in halomethanes with several halogen atoms. This is clearly shown by the fact that the normal coordinate treatment of halomethanes with three or more halogen atoms has been successful only when based on a central force field, i.e., assumption of forces only along the lines joining the atoms in the molecule. Thus it is not surprising to find that the modification presented above is more successful in treating molecules containing several halogen atoms.

[5] Bennewitz and Rossner, Zeits. f. physik. Chemie **B39**, 126 (1938).

APPLICATION TO THE HALOMETHANES

In order to evaluate the third term in Eq. (2) it is necessary to calculate the hypothetical deformation frequencies to be associated with each angle. In view of the meager experimental data available these constants have been obtained from heat capacities evaluated statistically.[3, 6, 7] They are given in Table II, together with their contribution to heat capacities at several temperatures. For temperatures not included in Table II the contributions of the various frequencies may be found in tabulated values of the Einstein function.[2] The standard state is the usual one of unit fugacity and zero pressure. Corrections to finite pressures have been adequately discussed.[7, 8]

The most useful application of Eq. (2) is to molecules for which no data at all are available. Thus one may calculate the heat capacity of

TABLE II. *Contribution of angles and bonds to heat capacity.*

ANGLE OR BOND	δ OR ν	C^0_ν or C^0_δ 298.1	373.1	473.1°K
HCH	1893 cm^{-1}	0.0186	0.0738	0.213
HCCl	942	0.451	0.738	1.052
ClCCl	332	1.614	1.738	1.826
HCF	1191	0.214	0.438	0.740
FCF	483	1.292	1.503	1.668
FCCl	326	1.625	1.746	1.832
HCBr	883	0.530	0.825	1.132
BrCBr	242	1.777	1.849	1.901
FCBr	410	1.452	1.622	1.751
ClCBr	293	1.688	1.789	1.860
C−H	3000	0.0002	0.0026	0.0188
C−F	1050	0.330	0.595	0.910
C−Cl	730	0.778	1.073	1.344
C−Br	610	1.017	1.284	1.507

[6] (a) D. P. Stevenson and J. Y. Beach, J. Chem. Phys. **6**, 25 (1938); (b) Geo. Glockler and Walter F. Edgell, J. Chem. Phys. **9**, 224 (1941); (c) Walter F. Edgell and Geo. Glockler, J. Chem. Phys. **9**, 484 (1941); (d) C^0_p for CH_2Br_2 was taken from reference 6(c) rather than 6(a) for reasons cited in 6(c).

[7] R. D. Vold, J. Am. Chem. Soc. **57**, 1192 (1935).

[8] Fugassi and Rudy, Ind. Eng. Chem. **30**, 1029 (1938).

TABLE III. *Comparison between semi-empirical and statistical heat capacities.**

SUBSTANCES	298.1°K(CAL./°K/MOLE) C^0_p CALC.	C^0_p STAT.	% DEV.	373.1°K(CAL./°K/MOLE) C^0_p CALC.	C^0_p STAT.	% DEV.	473.1°K(CAL./°K/MOLE) C^0_p CALC.	C^0_p STAT.	% DEV.
CH_3Cl	9.9	9.7	2.1	11.1	11.1	—	12.5	12.8	−2.3
CH_2Cl_2	12.4	12.4	0	14.1	14.1	—	15.9	15.9	0
$CHCl_3$	15.4	15.7	−1.9	17.4	17.4	—	19.2	19.0	1.0
CH_3F	8.9	8.95	−0.6	9.8	10.1	−2.9	11.3	11.8	−4.2
CH_2F_2	10.4	10.4	0	11.9	11.9	—	13.8	13.8	0
CHF_3	12.7	12.7	0	14.6	14.6	—	16.7	16.7	0
CH_2FCl	11.5	11.5	0	13.1	13.1	—	14.9	14.9	0
$CHClF_2$	13.9	13.8	0.7	15.7	15.6	0.6	17.7	17.5	1.1
$CHCl_2F$	14.8	14.6	1.4	16.6	16.3	1.8	18.5	18.1	2.2
$CFCl_3$	18.7	18.7	0	20.5	20.4	0.5	22.0	22.0	0
CH_3Br	10.3	10.2	1.0	11.5	11.5	—	12.9	13.2	−2.3
CH_2Br_2	13.2	13.1	0.8	14.9	14.7	1.4	16.5	16.3	1.2
$CHBr_3$	16.8	17.1	−1.7	18.5	18.5	—	20.1	19.9	1.0
$CHBr_2F$	15.3			17.1	17.1	—	18.9	18.7	1.1
$CHBrCl_2$	15.9			17.7	17.7	—	19.5	19.3	1.0
$CHBrClF$	15.0	15.1	−0.7	16.9	16.7	1.2	18.7	18.4	1.6
$CHBr_2Cl$	16.3			18.1	18.1	0	19.8	19.5	1.5
CF_2Br_2	18.0	18.5	−2.7	19.9	20.0	−0.5	21.6	21.6	0

* The statistically calculated heat capacities are from the following sources: references 3, 6, 8.

$CHBrF_2$ at 373.1°K to be

$$C^0_p = 7.948 + (0.0026 + 1.284 + 2\times 0.595) + 5/6(0.825 + 1.503 + 2\times 0.438 + 2\times 1.622),$$

$C^0_p = 15.8$ cal./°K/mole.

In Table III a comparison is made between values calculated by Eq. (2) in which constant stretching and empirical deformation frequencies have been used and those calculated by the more rigorous statistical method involving experimentally determined frequencies. A mark (−) on the percent deviation column indicates that this value was used in evaluating the deformation frequencies in Table II. The largest deviation (excepting CH_3F) is 2.7 percent, while the average deviation is ±0.9 percent. It has been shown[7] that heat capacities calculated statistically and corrected to finite pressures by the usual methods are accurate to ±5 percent. Table III indicates that the use of Eq. (2) and Table II will yield results accurate to 8 percent in the temperature range $T = 250$ to 550°K. This is more reliable than most of the meager data available at present.

It should be emphasized that Eq. (2) does not apply to molecules of the type CX_4.

Evidence for a Rigid Multilayer at a Solid-Liquid Interface

W. G. Eversole and Paul H. Lahr
Division of Physical Chemistry, State University of Iowa, Iowa City, Iowa

(Received March 20, 1941)

The assumption of an immobile hydrous multilayer at a wall of fixed potential was used in deriving equations relating zeta potentials, concentrations of univalent salt solution, wall potential, and thickness of the immobile layer. Calculations were made using data taken from published papers of various experimenters. Values of 8A to 63A were obtained for the thickness of the immobile layer. The values of wall potential and film thickness were considered sufficiently consistent for each set of data to justify the original assumption.

THE theory of Freundlich[1] on the variation of electrokinetic (ζ) potentials with concentration of electrolyte involved the hypothesis of an immobile layer of electrolytic solution at the solid-liquid interface. More recently, Müller[2] has considered the Freundlich rigidity layer as "probably monomolecular" and treated the interface involved in ζ potential phenomena as only an adsorbed monolayer containing ions.[3] It is the purpose of this paper to show evidence in favor of a rigid multilayer.

The ζ potential may be defined as the electrical potential at an interface which is responsible for the experimental phenomena of streaming potential, cataphoresis, and electro-osmosis. Zeta potentials are obtained from the experimental data by means of a formula by Helmholtz and von Smoluchowski.[4] The formula for streaming potential (E) is $E=\zeta DPR/4\pi\eta$ where D is the dielectric constant, P the pressure forcing liquid through a capillary, R the specific resistance of the liquid, and η the viscosity.

Abramson and Müller[3] derived an equation $\sigma=2\alpha(c)^{\frac{1}{2}}\sinh\zeta/\beta$ for the charge, σ, at the interface required to produce the ζ potential in a concentration, c. (α and β are constants.) A similar derivation utilizing different boundary conditions results in equations for charge density and interface potentials based upon the postulate of a rigid multilayer.

Let ψ be the potential at a distance X from a flat surface in contact with a dilute solution of simple salt (see Fig. 1). ψ_0 is the potential of the wall with its adsorbed ions. ψ_N is the Nernst potential of the wall. ψ_0 will be influenced by changes in ψ_N and by adsorption of non-potential determining ions having high specific adsorption potentials. It will be assumed that monatomic ions of low polarizability have a negligible specific adsorption potential and therefore ψ_N and ψ_0 are not changed by the addition of small amounts of alkali halides. Outside the ψ_0 plane only Coulomb forces will be considered.

The potential, ψ, will decrease with distance, X, from the wall as a result of a diffuse double layer or Gouy "ion atmosphere" in a manner as shown in Fig. 1. Let ζ be the potential at a distance, t, from the wall, t being the thickness of the solution which is assumed not to take part in viscous flow during streaming potential determinations. Then, according to the Boltzmann distribution equation, the excess charge density Π of ions in solution near the charged wall will be:

$$\Pi=-nz\epsilon[\exp(z\epsilon\psi/KT)-\exp(-z\epsilon\psi/KT)], \quad (1)$$

where n = number of ions per unit volume of solution
z = valence of the ions (only symmetrical valence considered)
ϵ = unit charge
K = Boltzmann's constant
T = absolute temperature.

More compactly,

$$\Pi=-2nz\epsilon\sinh\epsilon z\psi/KT. \quad (2)$$

Π can be eliminated from the equation by the use of Poisson's differential equation (for a flat

[1] H. Freundlich, *Kapillarchemie* (Akademische Verlagsgesellshaft m.b.H., Leipzig, 1922), p. 342.
[2] H. Müller, *Cold Spring Harbor Symposium Quant. Biol.* (1933), Vol. 1, p. 7.
[3] H. A. Abramson and H. Müller, *Cold Spring Harbor Symposium Quant. Biol.* (1933), Vol. 1, p. 29.
[4] Graetz, *Handbuch der Elektricitat und des Magnetismus* (Barth, Leipzig, 1921), Vol. II, p. 366.

surface),

$$\frac{\partial^2\psi}{\partial X^2}=-\frac{4\pi}{D}\Pi. \tag{3}$$

Then

$$\frac{\partial^2\psi}{\partial X^2}=\frac{8\pi nz\epsilon}{D}\sinh\frac{\epsilon z\psi}{KT} \tag{4}$$

and

$$2\frac{\partial^2\psi}{\partial X^2}\frac{\partial\psi}{\partial X}=\frac{16\pi nz\epsilon}{D}\sinh\frac{\epsilon z\psi}{KT}\frac{\partial\psi}{\partial X}. \tag{5}$$

Integrating,

$$\left(\frac{\partial\psi}{\partial X}\right)^2=\frac{16\pi nKT}{D}\cosh\frac{\epsilon z\psi}{KT}+I, \tag{6}$$

where I is the constant of integration, or

$$\frac{\partial\psi}{\partial X}=\pm\left(\frac{16\pi nKT}{D}\cosh\frac{\epsilon z\psi}{KT}+I\right)^{\frac{1}{2}}. \tag{7}$$

If $\partial\psi/\partial X$ is negative, approaching zero at infinite distance where ψ is zero,

$$\frac{\partial\psi}{\partial X}=-\left[\frac{16\pi nKT}{D}\left(\cosh\frac{\epsilon z\psi}{KT}-1\right)\right]^{\frac{1}{2}}. \tag{8}$$

Letting $(8\pi nz^2\epsilon^2/DKT)^{\frac{1}{2}}=$ Debye's κ and

$$a=\epsilon z/KT$$

$$\frac{a\partial\psi}{(\cosh a\psi-1)^{\frac{1}{2}}}=-\sqrt{2}\kappa\partial X. \tag{9}$$

This equation can be rearranged into a standard form for integrating.

$$\frac{a\sinh a\psi\partial\psi}{(\cosh a\psi-1)^{\frac{1}{2}}(\cosh^2 a\psi-1)^{\frac{1}{2}}}=-\sqrt{2}\kappa\partial X. \tag{10}$$

$$\int\frac{a\sinh a\psi\partial\psi}{(\cosh a\psi-1)(\cosh a\psi+1)^{\frac{1}{2}}}=-\int\sqrt{2}\kappa\partial X. \tag{11}$$

$$-2\kappa x=\ln\frac{(\cosh a\psi+1)^{\frac{1}{2}}-\sqrt{2}}{(\cosh a\psi+1)^{\frac{1}{2}}+\sqrt{2}}+\ln\frac{1}{p}. \tag{12}$$

When $X=0$, $\psi=\psi_0$ and

$$p=\frac{(\cosh a\psi_0+1)^{\frac{1}{2}}-\sqrt{2}}{(\cosh a\psi_0+1)^{\frac{1}{2}}+\sqrt{2}}$$

or

$$2\kappa x=\ln\frac{\cosh a\psi_0/2-1}{\cosh a\psi_0/2+1}-\ln\frac{\cosh a\psi/2-1}{\cosh a\psi/2+1}. \tag{13}$$

When $X=t$, $\psi=\zeta$ and

$$2\kappa t=\ln\frac{\cosh a\psi_0/2-1}{\cosh a\psi_0/2+1}-\ln\frac{\cosh a\zeta/2-1}{\cosh a\zeta/2+1}. \tag{14}$$

σ, the charge density on the wall is the negative of the integral of the excess charge density from the wall to infinity. Or, from Gauss' law,

$$\frac{\partial\psi}{\partial X}=-\frac{4\pi}{D}\sigma \quad \text{and Eq. (8)} \tag{15}$$

$$\frac{4\pi\sigma}{D}=\left[\frac{16\pi nKT}{D}\left(\cosh\frac{\epsilon z\psi_0}{KT}-1\right)\right]^{\frac{1}{2}}. \tag{16}$$

$$\sigma=\frac{4nz\epsilon}{\kappa}\sinh\frac{a\psi_0}{2}, \tag{17}$$

or

$$\sigma=35{,}300c^{\frac{1}{2}}\sinh 19.5\psi_0 \tag{18}$$

for water solutions if $T=298.2$ and $D=78.8$. Formula (18) is strictly true only if the charge giving rise to the potential ψ_0 lies in the ψ_0 plane. Now if ψ_0 is not a function of concentration, it may be eliminated from Eq. (14) in terms of ζ for two concentrations.

$$2t(\kappa_2-\kappa_1)=\ln\frac{(\cosh a\zeta_1/2-1)(\cosh a\zeta_2/2+1)}{(\cosh a\zeta_1/2+1)(\cosh a\zeta_2/2-1)}. \tag{19}$$

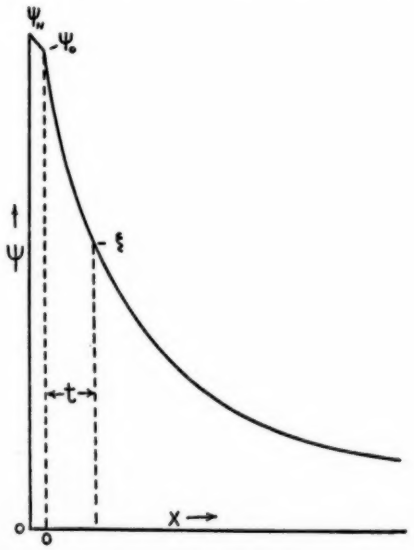

FIG. 1. Variation of potential with distance from a solid-liquid interface.

TABLE I. *Calculations from published zeta potential data*

EXPERIMENTER	ELECTROLYTE	METHOD	SOLID	MOLARITY $c\times10^2$	VOLTS ζ	VOLTS ψ_0	σ_0 IN e.s.u.	t IN cm $\times10^6$
Schönfeldt[1]	KCl	Electro-osmosis	Ceramics	0.03	0.0327	0.0391	510	
	"	"	"	.05	.0309	.0390	658	0.29
	"	"	"	.07	.0298	.0390	779	
Velisek and	"	"	"	10	.015	.053	13700	
Vasicek[2]	"	"	"	1	.035	.054	4320	.115
	"	"	"	.316	.042	.054	2470	
	NaCl	"	"	31.6	.010	.042	24300	
	"	"	"	10	.024	.056	13700	.075
	"	"	"	3.16	.036	.060	7680	
	"	"	"	1	.040	.053	4320	
	KI	"	"	10	.006	.052	13400	
	"	"	"	1	.029	.061	4200	.2
	"	"	"	.1	.041	.051	1340	
Baborovsky and	KCl	Streaming	"	1	.0057	.028	1980	
Burgl[3]	"	Potential	"	.75	.0066	.026	1710	
	"	"	"	.5	.0104	.032	1390	
	"	"	"	.25	.0113	.025	988	.469
	"	"	"	.1	.0156	.026	624	
	"	"	"	.05	.0189	.027	441	
	"	"	"	.01	.0228	.027	198	
	"	"	"	.005	.0262	.029	139	
Monagham and	"	Electro-osmosis	Pyrex	1	040	.135	3040	
White[4]	"	"	(spheres)	.1	.066	.097	1860	.257
	"	"	"	.01	.095	.111	1100	
	"	"	Pyrex	1	053	.107	4330	
	"	"	(capil-	.1	.083	.108	2700	.15
	"	"	laries)	.01	.098	.107	1160	
DuBois and	"	"	Glass	.1	.049	.130	1230	
Roberts[5]	"	"	"	.05	.052	.104	1060	.626
	"	"	"	.01	.079	.113	780	
	"	Streaming	"	.1	.040	.048	960	
	"	Potential	"	.05	.044	.050	855	.16
	"	"	"	.01	.045	.048	350	

[1] N. Schönfeldt, Zeits. f. Elektrochemie **37**, 734 (1931).
[2] J. Velisek and A. Vasicek, Collection of Czechoslovak Chem. Commun. **4**, 428 (1932).
[3] J. Baborovsky and B. Burgl, Collection of Czechoslovak Chem. Commun. **3**, 563 (1931).
[4] Monagham and White, J. Phys. Chem. **39**, 935 (1935).
[5] R. DuBois and A. H. Roberts, J. Phys. Chem. **40**, 543 (1936).

Using Eq. (19) and published data of various experimenters, the value of t was calculated. The average value of t was substituted back in Eq. (14) to determine ψ_0. The average value of ψ_0 was then used in Eq. (18) to calculate σ. The results are shown in Table I.

As is evident from the table, it is possible by proper choice of a value for t to fit these equations to experimental zeta-concentration data. The failure of experimental data to fit exactly the derived equation may be due in part to errors in the data itself and partly to the assumption of a constant ψ_0 in deriving the equations used.

It is of interest to note that in data from Monagham and White's work, ψ_0 is the same for both methods of measurement while both ζ and t are different. It may be that the flow of liquid had a more destructive effect upon the water layer in the capillary than in the diaphragm of Pyrex spheres. Also, the data from Velisek and Vasicek for a ceramics diaphragm show nearly the same value (0.05 volt) for sodium chloride, potassium chloride and potassium iodide, while again ζ and t differ for the three salts.

At least to some degree, the assumption of a rigid multilayer which incloses part of the counter ions of the ion atmosphere at an interface makes it possible to account for observed variations of ζ with concentration of simple ions. Evidence which would seemingly contradict such an assumption may be found in a paper by Abramson and Müller.[3] They applied the formula (20), $\sigma=2\alpha(c)^{\frac{1}{2}}\sinh\zeta/\beta$, which corresponds to Eq. (17), to determine the charge at the interface of solid and solution necessary to produce the ζ potential. For a large variety of electrolytes, their curves relating surface charge (σ) to concentration (c) for concentrations up to 0.01

molar closely resemble a Langmuir adsorption isotherm for adsorption of gas molecules on an inert surface. The adsorbed charge on the negative glass surface proves to be negative, whereas counter ions in a layer near a negative surface would have a predominantly positive charge.

However, several observations throw some doubt on the validity of this evidence. As Abramson and Müller pointed out, at concentrations above 0.01 molar "σ might conceivably decrease." According to the formula for σ, the charge would be zero for zero ζ at any finite concentration. Such a decrease in σ at higher concentrations is foreign to a Langmuir isotherm. Moreover, in the specific case of potassium chloride adsorption on glass, Abramson and Müller's $\sigma - c$ curve shows an increasing negative charge on the negative glass surface whereas a large difference in specific adsorption potentials of two ions so nearly alike in ionic weight and volume is not to be expected. Finally, a careful analysis of the equation for σ will reveal that σ may consist very largely of charges other than ions of the added electrolyte.

The equation $\sigma = 2\alpha(c)^{\frac{1}{2}} \sinh \zeta/\beta$ involves the assumption that the entire charge on the wall is in the single ζ potential plane. Verwey[5] considers the charges on the wall to be scattered in a finite layer, consisting of potential-determining ions in the wall, adsorbed ions on the wall and, perhaps, counter ions inclosed in an immobile water layer along the wall. If the only force holding ions in or near a glass surface were electrostatic (obviously not strictly true), if the dielectric constant of the solution were unchanged near the surface, and if all the potential determining ions of a glass electrode were in one plane, an equation similar to Eq. (17) could be derived to give $\sigma_N = 4nz\epsilon/\kappa \sinh a\psi_N/2$. Using Abramson and Müller's constants, this would become $\sigma_N = 2\alpha c^{\frac{1}{2}} \sinh \psi_N/\beta$. In this case ψ_N would be the Nernst potential of the glass as an electrode, σ_N would be the charge in the potential plane, and c would be as before the concentration of ions of all kinds in the bulk solution. The Nernst potential of glass in pure water would be expected to be the same sign and perhaps larger in magnitude than the ζ potential of glass in pure water. It follows from the above equation that an increase in concentration of the solution must result in an increase in σ_N if ψ_N is to remain constant. Unless the electrolyte added in ζ potential measurements contains potential-determining ions, ψ_N should remain nearly constant. According to the equation, the $\sigma - c$ curve for a constant ψ_N would be a parabola of increasing negative charge resulting from a transfer of potential-determining ions. The reason for an increase in σ_N in this case is clear if the electrode and its double layer are considered to be two plates of a charged condenser. If the plates are moved closer together, a greater charge on the plates is necessary to maintain the original potential. An increase in the concentration of a solution results in a greater κ, the reciprocal of which is Debye's measure of the effective thickness of a double layer. That is, an increase in c results in a decrease in the effective thickness of the double layer.

Even though the assumptions necessary to derive an equation for σ_N are not strictly valid, it is evident that the σ in the ζ potential plane which could represent all the charges in the finite wall surface is in a large measure representative of the adsorbed potential-determining ions rather than ions of the added electrolyte. The first approximation of the charge of adsorbed potassium and chloride ions might be obtained by subtracting Abramson and Müller's curve (Eq. (20)) from a true parabola (Eq. (17)), (see Fig. 2). The resulting σ for adsorbed counter ions would be positive instead of negative and would comprise the part of the positive ion

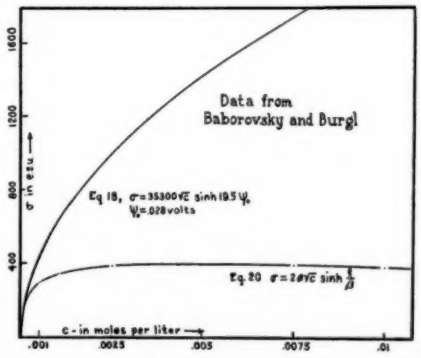

FIG. 2. Variation with concentration of effective charge density.

[5] E. J. W. Verwey, Chem. Rev. **16**, 363–411 (1935).

atmosphere in the immobilized layer between the ψ_0 and ζ planes. This σ might not necessarily follow a Langmuir adsorption isotherm.

SUMMARY

(1) Equations have been derived for the relations between wall potential, zeta potential, and concentration of univalent salt solutions, assuming an immobile hydrous layer of finite thickness was attached to a wall of fixed potential.

(2) When published ζ potential-concentration data for simple salt solutions are substituted in an equation relating film thickness to ζ potential for a constant wall potential, values of 8A to 63A are obtained for the rigid layer thickness.

(3) The results show that ζ potential-concentration curves for simple univalent ions can be explained without attributing such large specific adsorption potentials to the ions as the $\sigma-c$ curves of Abramson and Müller might indicate.

(4) The hypothesis of a rigid or viscous water multilayer at a solid-water interface, though not proved, is at least tenable in the light of its ability to fit certain ζ-potential data.

JULY, 1941 JOURNAL OF CHEMICAL PHYSICS VOLUME 9

The Spreading of Oils on Water

Part I. Ionized Molecules Having Only One Polar Group

W. A. ZISMAN
Naval Research Laboratory, Anacostia Station, Washington, D. C.
(Received March 31, 1941)

The spreading phenomena on water of drops of mineral oils containing a wide variety of organic acids and amines having but one polar group have been studied under conditions where dissociation at the oil-water interface could most readily occur. Particular emphasis is placed on the homologous series as an aid in separating the variables involved. Various phenomena of edge diffusion are described and a qualitative theory is presented. Edge diffusion is shown not to be a serious source of error in measuring the cross-sectional areas of the adsorbed molecules if there are over 13 carbon atoms per straight chain. The different types of film spreading and break-up effects are described and the various physical and chemical factors involved are discussed. The changes in the spreading effects due to varying the pH and to the presence in the water of Ca^{++}, Cu^{++}, Pb^{++}, Fe^{+++}, Al^{+++}, La^{+++}, and Th^{++++} on the interfacial film are described. It is shown that only the long chain monobasic saturated acids form rigid films when affected by metallic ions, while other acids are either condensed somewhat or are unaffected. Short chain metallic salts of these fatty acids are often oil soluble and have brief lifetimes of adsorption. An experimental proof is given that dissociated long chain acids and amines have infinite lifetimes of adsorption. Evidence is given for concluding that the lifetime is short for molecules having less than 14 carbon atoms. The effect of Ca^{++} on the spreading of oleic-stearic acid mixtures is given in some detail and also a theory of the results. Reasons are given for concluding that the adsorbed acid molecules form two-dimensional film complexes with hydrocarbon molecules derived from the oil.

1. INTRODUCTION

IT has long been known that highly purified mineral oils such as medicinal petrolatum do not spread on the clean surface of water but form lenses having well defined contact angles with the water. Such lenses were studied by Hardy,[1] Coghill and Anderson,[2] Lyons,[3] and more recently by Langmuir.[4] Harkins and Feldman[5] have shown that a drop of a pure liquid would not spread on water if its spreading coefficient F_S were negative; and in agreement with this, values of F_S for mineral oils, calculated from surface tension data, range usually between -11 and -14 dynes per centimeter.

When such oils are either heated or radiated with ultraviolet light in the presence of air they

[1] W. B. Hardy, Proc. Roy. Soc. **A86**, 610 (1912).
[2] W. H. Coghill and C. O. Anderson, Tech. Paper 262, U. S. Bureau of Mines, 1924.
[3] C. G. Lyons, Trans. J. Chem. Soc. (London) 623 (1930).
[4] I. Langmuir, J. Chem. Phys. **1**, 756 (1933).
[5] W. D. Harkins and A. Feldman, J. Am. Chem. Soc. 44, 2665 (1922).

develop the ability to spread on water and the colored films due to the spreading of oxidized engine oils are a familiar sight on wet city streets and around waterfronts. Langmuir[6] pointed out years ago that such spreading was probably due to the presence of polar molecules developed in the oil as oxidation products, and that acid molecules must be particularly effective. Later optical properties of thermally oxidized lubricating oils were described by Blodgett[7] and their value for use as "indicator" or "piston" oils was subsequently shown by Langmuir and Schaefer.[8]

An extensive literature exists[9] covering various physical and chemical properties of monolayers adsorbed at the air-water interface, but comparatively little is known about the monolayers adsorbed at the oil-water interface. Yet adsorption phenomena at the oil-water interface are technologically and biologically more common.

In recent years there has been an increasing amount of research on the interfacial adsorption of polar molecules initially in solution in one of the two liquid phases, employing interfacial tension techniques, but due in part to the experimental difficulties encountered in separating the numerous variables involved, much remains to be learned before there will be a satisfactory understanding of the fundamental phenomena involved. Particularly pertinent to the subject matter presented here is the well-known study of the adsorption of short chain acids by Harkins and his pupils,[10,11] the work on the effect of *p*H and buffers by Peters[12] and by Danielli,[13] and of Alexander and Teorell[14] as well as of Alexander and Schulman[15] on the equation of state of interfacial films.

In the past decade in three stimulating papers, Langmuir and Blodgett[4,16,17] have presented their results on the properties of interfacial films of stearic acid obtained by quantitative studies of the spreading on water of drops of a solution of that acid in mineral oil. They also described the remarkable sensitivity of the oil drop spreading to the presence of polyvalent metallic ions as well as to the effect of the *p*H of the aqueous substrate. They concluded that every stearic acid molecule was eventually adsorbed at the oil-water interface at alkaline *p*H, while at acid *p*H the solubility in oil of the stearic acid prevented spreading until a critical concentration was exceeded.

Ford, McBain and Wilson[18] described the spreading of oleic acid in mineral oil and reported that the edge of the disk was preceded by a monolayer of the acid. This was ingeniously done by the use of rapid motion pictures of the spreading drop of oil.

Stenstrom and Vigness[19] described experiments on the spreading of oil drops containing stearic, oleic and linoleic acids on alkaline water and found that oil drops containing either oleic or linoleic acids spread on alkaline water, but unlike stearic acid would also spread on alkaline water containing calcium ions.

Allen, Grant and Burdon[20] have investigated, using a motion picture camera, the rate of spreading on water of oil drops which had previously been irradiated with ultraviolet light. They found that in the latter stages of spreading the diameter of such an oil disk was accurately proportional to the square of the time.

Of particular interest here are Mercer's[21] experiments on the spreading on alkaline water of oil drops containing stearic acid. It was demonstrated that during the spreading of an oil drop there was shed or given off from the boundary of the disk a monolayer of stearic acid. Raising the temperature was found to cause this effect to become more prominent.

---

[6] I. Langmuir, Trans. Faraday Soc. **15**, 62 (1920).
[7] K. B. Blodgett, J. Opt. Soc. Am. **24**, 313 (1934).
[8] I. Langmuir and V. Schaefer, J. Am. Chem. Soc. **59**, 2400 (1937).
[9] N. K. Adam, *Physics and Chemistry of Surfaces* (Oxford University Press, 1938), second edition.
[10] W. D. Harkins and H. King, J. Am. Chem. Soc. **41**, 970 (1919).
[11] W. D. Harkins and H. McLaughlin, J. Am. Chem. Soc. **47**, 1610 (1925).
[12] R. A. Peters, Proc. Roy. Soc. **A133**, 140 (1931).
[13] J. F. Danielli, Proc. Roy. Soc. **B122**, 155 (1937).
[14] A. Alexander and T. Teorell, Trans. Faraday Soc. **35**, 727 (1939).
[15] A. Alexander and Schulman, Trans. Faraday Soc. **36**, 960 (1940).
[16] I. Langmuir, J. Frank. Inst. **218**, 143 (1934).
[17] I. Langmuir, Science **84**, 382 (1936).
[18] Ford, McBain and Wilson, Kolloid Zeits. **78**, 1 (1937).
[19] W. Stenstrom and I. Vigness, J. Phys. Chem. **43**, 531 (1939).
[20] Allen, Grant and Burdon, Trans. Faraday Soc. **33**, 1531 (1937).
[21] E. H. Mercer, Proc. Phys. Soc. London **51**, 561 (1939).

Recently Askew and Danielli[22] have studied the aqueous state of the adsorbed interfacial monolayers using a barrier arranged at the liquid-liquid interface, but due to experimental difficulties this more fundamental approach has been limited to a few materials. However, they came to one conclusion of interest here, that is, trimethyl cellulose and alpha-amino palmitic acid had adsorption areas per molecule considerably higher at the brombenzene-water interface than at the air-water interface. Murray[23] has investigated the effect of varying the polar content and nature of the oil used in the spreading of oils with emphasis on their use for mosquito control. Measurements were made of their spreading pressure and durability after spreading.

2. Outline of Work to be Presented

The plan of attack here adopted for the study of the spreading of oil drops on water was first to work entirely with one pure mineral oil while varying the nature of the polar additive compound dissolved in it (with emphasis on the employment of the homologous organic series as a tool to aid in unraveling the various chemical and physical factors involved in the mechanism of spreading), and second, to study each of the various factors so found as they are affected by altering the nature of either the mineral oil or the pure hydrocarbon compound employed.

Accordingly, unless otherwise stated, the mineral oil used will be understood to be a USPX1 light petrolatum manufactured by L. Sonneborn Sons Company, Inc., of New York City, and having a density varying from 0.839 to 0.841 and an absolute viscosity of 19.72 centipoises at 25°C. This oil does not spread on water. Employing both a Cenco duNouy interfacial tensiometer and a drop weight apparatus and applying the Harkins and Jordan corrections,[24] surface tension measurements on this oil gave for the interfacial tension oil-water at 25° the value of 53.5 dynes/cm, and for the surface tension oil-air 29.8 dynes/cm. Using 71.97 dynes/cm for the surface tension air-water, one obtains for the Harkins spreading coefficient, F_s, the value of -11.3 dynes/cm.

If one regards the spreading of oil drops as a means of studying interfacial films, it is evident that it is restricted to studying those polar compounds capable of being dissolved in the mineral oil used. As mineral oils oxidize rapidly at temperatures around 100°C, and as it is so often true that a polar compound dissolves little in oil unless heated close to its melting point, it has not been found possible here to study additive compounds whose melting points exceed 90° to 100°C. It is also a restricted technique in the sense that with it the films can only make their presence noted when the surface film pressure is equal to or greater than the compression due to surface tension forces inherent in the existence of a floating drop, i.e., for the above-mentioned mineral oil it is 11.3 dynes/cm.

3. Technique

The oil drops were spread on water held in Pyrex trays while Pyrex barriers were used for scraping clean the surface of the water. All aqueous solutions were handled entirely in Pyrex containers which had previously been well cleaned with chromic acid and aged in hot distilled water. The distilled water was collected from a metal still which was designed to give unusual protection from spattering and entrainment, and had a solid tin condenser thus largely eliminating contamination from traces of copper so serious in film research. For some experiments an all-quartz still was used to redistill the water.

The amount of oil in each disk was measured by weighing it in Pyrex droppers using a chainomatic balance good to 0.1 milligram; hence the error of measuring the quantity of oil used in forming a spreading film was never greater than 0.5 percent for the smallest disk studied and proportionately less for the larger disks.

All measurements, unless otherwise noted, were made with the water at 25°C±0.2° while the room air temperature was usually maintained within 0.5° of that.

The hydrophil tray was arranged inside of a metal box having a glass top in order to prevent air currents from distorting the circular spreading

[22] F. Askew and J. Danielli, Trans. Faraday Soc. **36**, 785 (1940).
[23] D. Murray, Bull. Entomological Research **30**, 173 (1939).
[24] W. Harkins and H. Jordan, J. Am. Chem. Soc. **52**, 1751 (1930).

oil disks. Two thin metric rulers arranged at right angles close to but above the plane of the water in the tray permitted measurement of two mutually perpendicular diameters of the oil disk whenever air or water currents caused a slight distortion from a circular shape.

The obtaining of the wide variety of polar compounds necessary for these experiments was a most serious problem, particularly since in the course of the early experiments it was found that certain of the phenomena studied were sensitive to the presence of organic polar impurities.

The pentadecanoic, nonadecanoic and eicosanoic, also a remarkably complete series of branch chain acetic acid derivatives having from 14 to 20 carbon atoms per molecule, and the chaulmoogric acid and the 13-hydroxy stearic acid, many of them being of unusual purity, were furnished this laboratory by Dr. Roger Adams of the Department of Chemistry of the University of Illinois. The oleic and elaidic acids were of exceptional purity (for example, the oleic acid was colorless and odorless and had an iodine number of 88.3) were newly prepared by Dr. J. P. Kass of the Department of Botany of the University of Minnesota. The ricinelaidic acid was a purified specimen prepared by Professor St. Elmo Brady of the Department of Chemistry of Fiske University and has been described elsewhere.[25] The phenylstearic, ethylphenylstearic, xenylstearic, and tetrahydronaphthylstearic acids were obtained from Messrs. Stirton, Peterson and Groggins of the Bureau of Agricultural Chemistry and Engineering, Department of Agriculture, and have been described elsewhere.[26] The normal octadecyl, hexadecyl, tetradecyl, dodecyl, and the mixed octadecenyl and octadecendienyl amines were obtained from the Chemistry Division of Armour & Company, while the heptadecyl amine was prepared in this laboratory using pure heptadecyl amine hydrochloride made with great care by the Varlacoid Chemical Company of New York City. The cooperation and generosity of these individuals and organizations are gratefully acknowledged.

The ricinoleic acid was obtained freshly prepared from the City Chemical Company of New York City, the trioctyl amine was obtained from the Sharples Solvents Corporation, and the dioctyl amine was obtained from the Carbide and Carbon Chemicals Corporation. The remaining chemicals used for the work presented here were newly obtained Eastman Chemical Company preparations.

[25] St. Elmo Brady, J. Am. Chem. Soc. **61**, 3464 (1939).
[26] Stirton, Peterson and Groggins, Ind. Eng. Chem. **32**, 1136 (1940).

4. Edge Diffusion

The escape of stearic acid molecules from a spreading oil drop previously described[18, 21] was found to be a common phenomenon. Mercer's technique of using aluminum powder, though suitable for photographic purposes, was discarded in order to avoid the consequent metallic contamination of the water and use was made of either grease-free talc or clean, precipitated and washed sulfur powder which was spread on the water from a previously flamed platinum mesh bag. The escaping molecules push the talc particles away from the disk forming thereby a circular ring which encloses the escaped monolayer. The greater the rate of escape of the polar molecules, the more rapid the rate of increase of diameter of the ring of talc.

If the escaped monolayer is insoluble in water, the talc ring does not contract when the oil disk ceases emitting polar molecules. If there is no reaction between the adsorbed molecules and polyvalent metallic impurities, the edge loss continues as long as there are adsorbed molecules present. If the escaped monolayer is soluble in water, the ring rarely spreads more than a few centimeters from the disk and remains so. There is then an equilibrium between the rate of escape of the molecules from the oil disk and their rate of subsequent solution in the water. This can readily be shown by dropping a few talc particles in the space between the ring and the oil disk and observing the still rapid motion of the talc away from the edge of the disk even though the circular talc boundary still maintains itself at a fixed distance from the disk.

The existence of rapid edge diffusion can often be detected by observing the difficulty of making two oil disks join each other. If there is edge diffusion they will appear to repel one another, sometimes with considerable speed.

Experiments with the normal saturated acids from hexanoic acid (C_6) to eicosanoic acid (C_{20})

using equimolal concentrations in the petrolatum demonstrated that each showed edge diffusion, but whereas in the case of the C_{20} acid the effect was barely detectable, it was so pronounced for the C_8, C_7 and C_6 acids as to be the most evident spreading effect caused by their presence in oil. In fact, if a weight concentration of from 10^{-4} to 10^{-3} was used, the oil drop did not spread on the water but skated about while the nearby talc particles were propelled violently away from the disk. Now, when a drop of pure hexanoic or octanoic acid was held in the air just above the surface of the talc-covered water, the acid vapor from the drop also caused spreading of the talc. It therefore might be concluded as in the classic study of the propulsion of camphor particles on water[27] that the edge diffusion effect of such acids dissolved in oil drops is entirely due to the vapor spreading from the oil disk through the air followed by condensation on the water. However, upon employing decanoic acid (C_{10}) or higher homologs, no vapor spreading could be observed by the simple tests described above, and, consequently, it was concluded that this mechanism, though contributory in the case of the short chain length acids, was of minor consequence with the longer chain length molecules.

It was found that equimolal solutions in oil of alcohols, esters, ketones, amines, phenols, phosphates, and ethers all showed edge diffusion effects which decreased in intensity as the chain length of the hydrocarbon portion of the molecule increased. In fact, the effect for all the straight chain molecules containing the same number of carbon atoms per molecule seems roughly to be of the same intensity whatever the polar group. In a polar molecule containing several branch chains the length of the longest branch and not the total number of carbon atoms in the molecule seemed to determine the intensity of edge diffusion. Thus, either dioctyl or trioctyl amine caused a much more intense edge loss than did hexadecyl amine and either dibenzylacetic or di-*n*-heptylacetic acid much more than hexadecanoic acid. Again using a series of branched chain acetic acid derivatives, each having 17 carbon atoms per molecule ranging from methyltetradecylacetic acid to heptyloctylacetic acid, it was found that the rate of edge diffusion increased rapidly as the length of the largest branched chain decreased. Many more such illustrations could be given.

Although the greatest intensity of edge loss is shown by short chain molecules, and although it is true that the shorter the chain length the lower the melting point and the higher the vapor pressure of a molecule, it is not true that a simple melting point rule can be used for predicting relative rates of edge loss, for the molecular configuration is too important. Thus oleic acid with an 18 carbon chain has a melting point below 20°C while dibenzylacetic acid with 16 carbon atoms per molecule has a melting point around 81°C. Yet the former exhibited a barely noticeable edge loss while the latter showed a most pronounced effect. Here the low melting point of oleic acid is due to its *cis*-configuration, which, however, does not cause increased edge diffusion, while the intense edge loss of dibenzylacetic acid is due to its being a branch chain aromatic molecule having only 7 carbon atoms in its longest chain. However, it is true that the rate of edge loss increases as the melting point decreases for any homologous series of molecules containing only one straight chain per molecule.

It is concluded that edge diffusion is essentially a kinetic phenomenon, a 2-dimensional evaporation occurring across a lineal boundary and requiring the presence of two liquids, one more polar than the other. Its mechanism in the case of long chain polar molecules presumably involves the adsorption of the polar molecule at the oil-water interface, followed by thermal agitation while adsorbed there and a certain amount of associated diffusion in the interface, and finally in the case of the adsorbed molecules nearest the rim of the oil disk, a more frequent breaking away of the hydrocarbon ends of the molecules from the oil during which time the polar end of the molecule continues to adhere to the water phase. The longer the chain length the slower the rate of two-dimensional diffusion in the interface and the less the frequency of breaking away of the hydrocarbon chains of the polar molecules nearest the rim or edge of the disk, since the rupture of a number of hydrogen

[27] A. Marcelin, *Solutions Superficielles*, (1931), Chapter X.

bonds is necessary for such an event to occur. It is possible that this effect varies with the nature of the hydrocarbon in the oil used.

5. Some Factors Controlling the Stability of Oil Films

It was found from a comparative study of the breaking up of oil films that if the amount of the polar molecules dissolved in the oil was sufficient just to cause spreading as a thin disk, i.e., a weight concentration of 10^{-5} in case of the long chain molecules and 10^{-3} in case of the short chain ones, the mode of breaking up of the disk was qualitatively indicative of the greatest chain length of the polar molecule. Compounds with but 6 to 9 carbon atoms per molecule spread in a second and at once burst into hundreds of tiny drops, each of which exhibited a considerable contact angle with the water while skating about for a period 20 seconds or less, depending on chain length. But if there were approximately from 10 to 13 carbon atoms per molecule, the disk spread in a few seconds and then broke up by a streaming of small flat disks from the periphery of the central disk leaving a constantly contracting central disk. These disks initially spread to a larger diameter, broke off more slowly, and after breaking off, contracted more slowly, the greater the chain length of the molecule. Finally, if there were 14 or more carbon atoms per molecule, the disk spread more slowly and to a greater diameter (exhibited surface oil flow effects described below) and broke up more slowly. These break-up effects can be of remarkable regularity and are fascinating to observe.

The mechanism operating to cause such a variety of break-up effects, of course, cannot be simple. However, the use of a wide range of concentrations has made it possible to distinguish four factors responsible for these phenomena. They are: first, the rapid increase in the speed of diffusion through the volume of the oil disk of the polar molecules as their chain length decreases; second, the rapid increase in the rate of edge diffusion as the chain length decreases; third, the inertia of the oil in the upper layer of the oil in a spreading disk; and fourth, the viscosity of the oil in causing a dampening effect on any inertia flow or surging in the upper oil layer of the disk.

The first factor is evident, since the rate of diffusion of a long chain molecule should increase as the chain length decreases. The fewer carbon atoms per chain the fewer bonds to be made and broken with the hydrocarbon solvent and also the less the probability of collision with other molecules. To illustrate this, if solutions of the same molal concentration are used corresponding to $w=0.90\times10^{-5}$ stearic acid (i.e., 3.18×10^{-8} gram molecule per gram oil), then the time, T_M, required for the disk to spread to its maximum diameter on alkaline water free from polyvalent metallic ions is found to be approximately 3 minutes for tetradecanoic, 5 minutes for hexadecanoic, $6\frac{1}{2}$ minutes for octadecanoic, 8 minutes for nonadecanoic, and $9\frac{1}{2}$ minutes for eicosanoic acid. Since the time required for the actual adsorption at the interface must be extremely small, and since for a given molal concentration the total spreading area on such a substrate is approximately the same independent of chain length (see Section 8 below), this progressive increase in T_M can only be due to a corresponding decrease in the speed of molecular diffusion with increased chain length in a homologous series. Again, using the same molal concentrations of various 18 carbon aliphatic acids, it was found that stearic, oleic, and elaidic acids had the same value of $T_M=6.5$ min., whereas ricinoleic and ricinelaidic acids each had the large value of $T_M=50$ min. Hence the double bond in the first case was of no influence, but the hydroxy group in the second case was of great influence, and, in fact, may have caused association.

The second factor, edge diffusion, has already been described. It was always evidenced by the behavior of the smaller oil disks formed after the break-up, for the disks so formed had a greater contact angle, showed more skating, were smaller in diameter, and contracted more quickly, the greater the rate of edge diffusion. Where thin disks exhibited considerable edge diffusion, the disks gradually contracted in diameter as a beaded rim formed. This was a common phenomenon.

The third and fourth factors were made most evident by observing the spreading of oil disks of different viscosities containing acids of 16 or

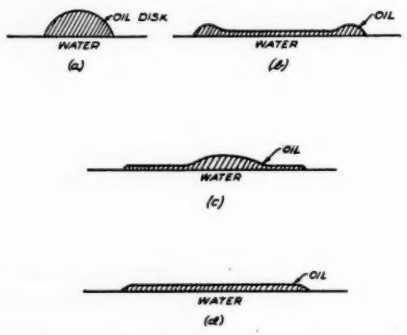

FIG. 1. Damped oscillation of a spreading oil disk.

more carbon atoms per molecule and present in weight concentrations in the range 2×10^{-5} to 5×10^{-5}. Using light petrolatum and this range of concentrations, the spreading oil drop required from 8 minutes to a few seconds to spread to its maximum diameter. Under these circumstances the inertia of the upper oil layer caused it to pile up at the circumference so that at maximum spreading the disk exhibited a uniform rim bounding its circumference. This rim was narrower and higher the greater the speed of spreading (i.e., the greater the value of w) and the less viscous the oil. If $w=1\times10^{-5}$, the rim could not be seen, whereas if w was around 5×10^{-5} it could not be missed. At the low range of spreading speeds after the rim formed, it slowly subsided so that the final result was a critically damped oscillation (see Fig. 1 (a), (b), (c) and (d). At the high range of spreading speeds the flow of oil from the center of the disk caused a hole to form there; the hole grew rapidly until only a thin oil ring remained. Finally, there developed a necking-in or narrowing at various points on the internal circumference, and finally at these points necking-in progressed until these had caused the formation of a number of oil disks, see Fig. 2 (a), (b), (c), (d), (e) and (f). If a much more viscous oil like Squibbs heavy petrolatum is used with $w=5\times10^{-5}$, spreading though slower, resulted in the formation of a low and wide oil rim. After the disk had reached its maximum diameter, if air currents did not distort the disk enough to start a breaking-up process, the rim gradually became transformed into a border of oil mounds which in time became fewer in number and shallower until eventually the disk was flat.

As an oil drop spreads, the thickness of the oil layer will decrease and the polar molecules in solution will have less oil through which to diffuse in reaching the oil-water interface. Therefore, they will arrive at the interface at a rapidly accelerated rate until the maximum spreading area of the disk is approached. Hence, T_M will increase with great rapidity as the initial concentration of the polar molecules is increased. It was found in the case of stearic acid in mineral oil that T_M was 6.5 minutes when w was 0.85×10^{-5}, 1.5 minutes when w was 2×10^{-5}, and 25 seconds when w was 2.5×10^{-5}. Again in the case of a ricinoleic acid, T_M was 40 minutes when w was 1×10^{-5} and 7 minutes when w was 2×10^{-5}. These are in reasonable accord with Langmuir's theoretical conclusion[16] that the initial rate of spreading of the oil disk should increase exponentially with time and with the square of the initial concentration.

At still higher spreading speeds the various factors operating are no longer readily discernible. If the speed of diffusion is considerable, the spreading effect of the polar molecules in the oil of the inertia layer as it flows towards the circumference is an important part of the whole and tends to nullify the trend to form a high rim. Hence at concentrations in the range $w=10^{-4}$ to 10^{-3} rims are not usually evident. Since under such circumstances the break-up is by a streaming of small disks away from the circumference, it is possible that a border of oil mounds formed and in breaking off were the origin of these small disks; however, that is a conjecture. At the highest speeds, such as are obtained with long chain acids when w exceeds 10^{-3}, there is an additional phenomenon, a bursting of the oil film in its center to form a large hole, as if due to the tearing of a tight membrane.

In addition to these causes of film instability, there are two due to solubility effects. First, if the interfacial film is so soluble in one of the liquid phases as to be forced to leave the interface, the oil film will contract from its maximum area. Second, if any polar material is undissolved in the oil, the oil disk in spreading will develop numerous holes due to the increased local spreading occurring whenever particles of that polar material reach the interface. This phenomenon can

be used to indicate the attainment of the solubility limit of polar substances in oils. Measurements of this type will be described in Part II.

6. Method of Measuring Area Per Molecule

Langmuir and Blodgett[16,17] found the maximum area of spreading of an oil disk on alkaline water to be the same whatever the volume of the oil so long as the same total number of stearic acid molecules were present in the disk, and hence concluded that every stearic acid molecule had been adsorbed at the oil-water interface. Mercer[21] came to the same conclusion upon finding that after spreading had occurred oil obtained by sucking up some of the upper oil layer of the disk and in turn placing it on alkaline water no longer had the ability to spread. Assuming the correctness of their conclusion, if the average area occupied by each adsorbed molecule at the oil-water interface is A, if M is the gram molecular weight of the polar substance, present in a weight concentration w, and if the mass of the oil in the disk is m, then the total area S of the interface between oil disk and water is given by $S=6.06\times10^{+23}(mw/M)A$. For very thin circular disks of radius R evidently $S=\pi R^2$. For thicker disks $S>\pi R^2$ since it is no longer a good approximation to treat the interface as a plane surface.

The procedure used here was to calculate an apparent area per molecule A' obtained by the use of the above formula and the assumption that $S=\pi R^2$. If w was not too low, a plot of A' as a function of m revealed that A' increased with m until a certain value m_0 was reached, after which A' became constant and equal to the true area per molecule. For example, in the case of stearic acid ($w=0.9\times10^{-5}$) in oil spread on 0.02 N NaOH $+0.02$ N Na_2CO_3, it was found that if m_0 exceeded 4.6×10^{-2} gram, then $A'=106\times10^{-16}$ cm^2; if $m=2.5\times10^{-2}$ gram, then $A'=95\times10^{-16}$ cm^2; and if $m=0.8\times10^{-2}$ gram, then $A'=84\times10^{-16}$ cm^2.

In handling the more dilute oil solutions of polar molecules adsorption upon the walls of the glass containers employed can be a source of error. A simple calculation shows that for solutions having a weight concentration of 10^{-5}, the maximum possible error will be 2 percent; for higher solution concentrations the maximum possible error will be proportionately less.

In order to obtain accuracy in measuring A, it is essential to choose carefully the value of w employed. If w ranges from 2×10^{-4} to 4×10^{-4}, the disk spreads in a circle but does it so rapidly and breaks up so quickly at the edges after completing the spreading that a rapid measurement of the diameter is necessary. If w is less than 1×10^{-5}, the curvature error involved in assuming that the interfacial area equals πR^2 becomes serious and also the edge loss error increases, since under such circumstances T_M is large. The best results obtained were with either of the ranges $w=1\times10^{-5}$ to 5×10^{-5} and 2×10^{-4} to 4×10^{-4}. The effect of the polyvalent metallic ions on the maximum diameter of spreading was less the smaller T_M and so unless the water was very carefully freed from traces of metallic ions, it was found best to use the higher concentration range. However, using either range and properly purified water, the same values of A were obtained.

7. The Effect of pH

The spreading areas of oil drops containing long chain acids vary with the pH of the aqueous

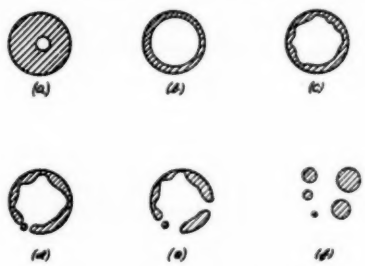

Fig. 2. Mechanism of break-up of oil disk; formation of 5 disks.

solution used. In Fig. 3, A gives the change in the diameter with pH of oil drops containing $w=0.890\times10^{-5}$ stearic acid, the pH having been varied by adding to distilled water in equilibrium with the CO_2 of the air a suitable amount of HCl, $KHCO_3$, or NaOH. Practically all of the increase in the spreading occurred in the pH range from pH 9 to pH 10.5. The value of this upper limit agrees with Langmuir and Schaefer's results[28]

[28] I. Langmuir and Schaefer, J. Am. Chem. Soc. **58**, 284 (1936).

on the effect of *p*H in converting to the calcium or barium soap a monolayer of stearic acid at the air-water interface. A similar study of the effect of *p*H on the diameter of oil drops containing $w = 0.865 \times 10^{-5}$ oleic acid is given in Fig. 3, *B*, where it is seen that the maximum effect is also at *p*H 10.5. This is in agreement with the results of Danielli[13] on the effect of *p*H on the interfacial tension lowering due to oleic acid adsorbed at the brombenzene-water interface.

The obvious conclusion to be made is that of the molecules in adsorption equilibrium at the interface, some are ionized by the water and remain permanently adsorbed. As the *p*H rises, the higher concentration of hydroxyl ions increases the number of ionized molecules present, and for values of *p*H exceeding 10.5 all are ionized and maximum spreading results. The fact that the same *p*H range is effective in causing maximum spreading of either the oleic or the stearic acids is evidence for inferring that this also is true for all long chain acid molecules. It need not be assumed that all of the permanently adsorbed acid molecules remain ionized, but instead that they have been converted to the undissociated sodium soap. However, it is theoretically more reasonable to assume practically complete ionization of the sodium soap. The electrical attraction which then must exist between the two portions of the double layer consisting of the negatively charged ionized carboxyl groups adhering to the oil disk and the corresponding sheath of sodium ions in the substrate immediately beneath will give rise to forces of attraction responsible for the infinite lifetime of adsorption of fatty acids at high *p*H.

Similar results on the effect of *p*H were obtained with the other long chain saturated straight chain acids, the unsaturated acids, oleic, elaidic, linoleic, linolenic, and erucic; the aryl stearic acids, phenylundecylic, phenylstearic, ethylphenylstearic, diethylphenylstearic, xenylstearic, and tetrahydronaphthylstearic; chaulmoogric and hydnocarpic acids; dibenzylacetic and di-*n*-heptylacetic acid; and finally with a variety of so-called naphthenic acids.

Oil drops containing acids in a weight concentration of less than $w = 10^{-3}$ and having less than 13 carbon atoms per molecule showed edge diffusion mainly. As has already been described, at higher concentrations they spread so rapidly as to seem to spread and burst into hundreds of tiny drops in the space of a few seconds, the speed being greater the shorter the chain length.

In the case of such molecules the effect of varying the *p*H was difficult to study, but roughly speaking, it was found that there was less change in oil drop spreading with the *p*H the shorter chain length. Only a decrease in the rate of edge loss with increased *p*H was noticed with the 6, 7 and 8 carbon acids. Evidently the film pressure due to these acid molecules is not sufficient to overcome the -11.3 dynes/cm compression of the oil disk unless w considerably exceeds 10^{-3}. Therefore dodecanoic acid is the shortest molecule of the series readily to exhibit disk spreading. But the shorter the chain length the greater the film pressure for constant area of packing per molecule. Hence the conclusion seems inevitable that for straight chains of less than 12 to 14 carbon atoms per molecule, the lifetime of adsorption is not infinite but is less the shorter the molecule.

Acids containing more than one polar group such as hydroxy acids behaved quite differently with respect to changes in *p*H, and for the sake of a logical order of presentation will be discussed in Part III.

8. The Effects Due to Polyvalent Metallic Ions

Langmuir and Blodgett[17] have described the remarkable ability shown by small traces of calcium ions in alkaline water to prevent any spreading of oil drops containing stearic acid. The simple expedient of probing such an oil disk with a clean thin glass rod or a platinum wire will show that the disk is floating as if on a rigid island. A systematic qualitative study was made of the effects of ions of Ca, Pb, Cu, Fe, Al, La or Th upon the interfacial films of the acids mentioned above. The metallic salts were either the chloride or the nitrate and were employed in concentrations of 10^{-3} to 10^{-4} molal. The *p*H was used as high as possible without causing complete precipitation of the metallic ions. The procedure used was to observe the rate of spreading and subsequent contraction of oil drops containing the fatty acid while talc and

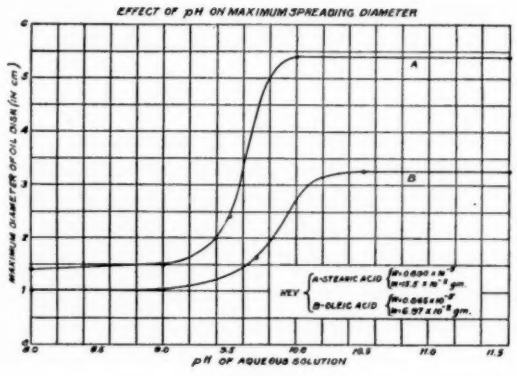

FIG. 3.

probe tests were also made for edge loss and film rigidity. Drops containing the acid in weight concentrations of 10^{-5}, 10^{-4} and 10^{-3} were tested. As is to be expected, the amount of the metallic salt necessary to cause rigidity was found to depend on the *p*H but it also depended on the concentration of the acid in the oil. When there was doubt as to the rigidity of the interfacial film, the interfacial surface tension of the oil solution was studied in a Cenco duNouy tensiometer, and it was then easy to test the physical state of the film. In every case a simple probe test gave the same results.

The following conclusions resulted from these experiments:

(1) Of the monobasic acids studied only those having one saturated straight chain formed rigid interfacial films.

(2) Of the saturated single straight chain acids, none having less than 14 carbon atoms per molecule was made rigid by any of the metallic ions, while those having 16 or more carbon atoms per molecule were made rigid by all the polyvalent metallic ions used. The acids having 14 or 15 carbon atoms per molecule were made rigid only by metallic ions of high valence. Thus, only thorium and lanthanum made both acids rigid. However, these polyvalent metallic ions probably make many of the acid interfacial films studied more condensed or more viscous, and as evidence may be mentioned the effect of calcium ions in considerably decreasing the adsorption area per molecule for oleic acid (to be described below).

(3) Certain hydroxy acids, ricinoleic, ricinelaidic, and 13-hydroxy stearic acids have interfacial areas per molecule which are unaffected by *p*H or by the presence of any polyvalent metallic ions. For the sake of logical presentation these acids will be discussed in Part III.

The effect of the highly charged ions on the spreading of acids in oil was simply studied and furnished results of interest. Thorium, being tetravalent, showed the most marked results as one would expect. In the following experiments thorium nitrate dissolved in distilled water in a concentration of 3×10^{-3} mole per liter was used. Such a solution will be briefly referred to here as thorium water and it has a *p*H of approximately 3.5.

The shorter chain-length saturated acids spread much more readily on the thorium water than on water (*p*H 2.0–*p*H 6.0) which had been acidified with HCl. In all cases the hexanoic acid showed edge loss and disk skating for $w=10^{-5}$ and $w=10^{-4}$ and spread and burst in an instant if $w=10^{-3}$. On the other hand, octanoic acid in acid water acted approximately the same as hexanoic with slightly less violent edge loss and skating, while on the thorium water it spread as a thick disk when $w=10^{-4}$ and as a thin colored disk when $w=10^{-3}$. Decanoic acid on thorium water showed the same behavior but the spreading effects happened more slowly, were more pronounced, and if $w=10^{-3}$, the disk did not burst but contracted rapidly immediately after spreading as a colored film. Dodecanoic acid behaved similarly but the initial spreading was slower and the maximum diameter attained was greater. In all these cases the interfacial films formed were not rigid. On the other hand, as mentioned earlier, tetradecanoic and its higher homologs became rigid on the thorium water.

The rapid contraction of the decanoic and dodecanoic acids on the thorium water was studied quantitatively. A disk of $w=1.023\times10^{-4}$ dodecanoic acid weighing 13.53×10^{-2} gram spread to a maximum diameter of 8 cm and then rapidly contracted while a disk of $w=1.096\times10^{-4}$ decanoic acid weighing 7.26×10^{-2} gram spread to a diameter of 6 cm and then also rapidly contracted as shown in Fig. 4. Now the spreading was due to the presence of the thorium ions; hence it is assumed it occurred because the thorium reacted with the acid molecules reaching the interface to form a fatty acid salt. Assuming that each straight chain molecule while at the

interface and combined with the thorium occupies a cross-sectional area A at the time of maximum spreading, and that at the maximum spreading area every molecule in the drop was adsorbed at the interface, then a simple calculation leads to a value of $A = 12 \times 10^{-16}$ cm² for the dodecanoic and $A = 10 \times 10^{-16}$ cm² for the decanoic acid chains. However, the cross-sectional area of each straight chain cannot be less than 18.5×10^{-16} cm². Hence the conclusion seems inevitable that every molecule was not adsorbed at the time of maximum spreading, for in the brief time required for such spreading far too few polar molecules could have escaped by edge loss (as shown by talc test) to have accounted for such a large difference. Therefore, if each adsorbed chain occupied approximately (18 to 20) $\times 10^{-16}$ cm², only 60 percent of the molecules in the drop were adsorbed in the case of the dodecanoic acid and 50 percent in the case of the decanoic. Since the interfacial film at maximum spreading was not rigid, a more reasonable assumption is that the adsorbed molecules occupied an area of around (25 to 35) $\times 10^{-16}$ cm² in which case around 34 percent and 29 percent were adsorbed, respectively.

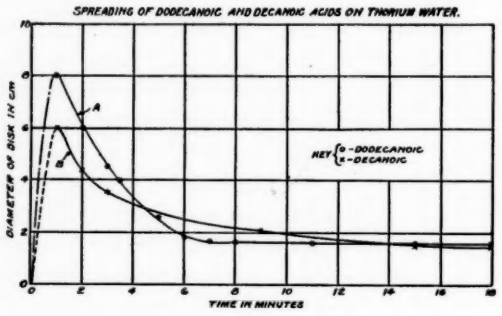

FIG. 4.

The subsequent rapid contraction of the oil disk could not have been due to a decrease in the area per molecule as the thorium ions bound the adsorbed chains together, for even though the area had decreased to 5 percent of its maximum value, the finally contracted disk was not rigid. Talc tests showed that the edge loss could not have caused this rapid contraction. Hence the conclusion is inevitable that the contraction was largely due to the dissolving back into the oil drop of a large part of the undissociated thorium salt of the fatty acid formed. Such an adsorption equilibrium due to the short life of adsorption of the undissociated salt is quite reasonable in terms of results to be presented in another connection in Part II.

If a hydrophil tray containing thorium water is first covered with an oxidized indicator oil and an extremely small amount of any one of the various fatty acids of interest is spread in the center, a circular monolayer of the acid is formed and its boundary is outlined by the colored indicator oil. The indicator oil can be so chosen and calibrated as to exert on thorium water from 2 to 15 dynes/cm pressure on the monolayer.[8] The rigidity of this monolayer due to its reaction with the thorium can be observed by cutting pie-shaped islands out of the circular monolayer. The persistence of the shape of each piece after cutting it away can be easily seen because its shape is well defined by the surrounding indicator oil. By employing this technique, it was found that at the air-water interface, the straight chain saturated acids from hexanoic up all contracted and then became rigid even when a low film pressure of 2 dynes/cm was used, the time required decreasing from 5 to 15 minutes as the chain length varied from 6 to 10 carbon atoms per molecule.

The fact that on the same aqueous solution oil disks containing the same fatty acids under a greater film pressure (11.3 dynes/cm) and exposed to the chemical reaction a greater length of time do not become rigid can most simply be interpreted to mean that at the oil-water interface either the thermal agitation of the acid molecules caused by the nearby oil molecules, or the separation of the adsorbed acid molecules by molecules of the solvent to form a mixed film, prevents cross-binding forces from forming a rigid film. The latter mechanism makes it possible to give a simple explanation of why after the undissociated compound was formed there resulted a considerable oil disk contraction yet did not form a rigid film. The thorium compound formed, no longer being ionized, and unbound by cohesional forces due to adjacent and similar molecules had a short lifetime of adsorption and so dissolved back into the oil drop until an adsorption equilibrium was reached. The same conclusion of the existence of mixed films is reached later on the basis of other experimental

facts concerning acid and amine molecules, containing 14 or more carbon atoms each.

The effect of calcium ions on the spreading of oil drops containing stearic or oleic acids has been studied in some detail. However, it is difficult to do accurate quantitative work here because of the unknown and variable amounts of polyvalent metallic ions present in the distilled water and glass apparatus used. If chemicals to eliminate these metals are employed they make the results regular but then prevent it from being possible to study the effects of adding small quantities of calcium. If buffers are used they affect the calcium concentration also. The repeatability of the results obtained in the following experimental work was good and although the true polyvalent metallic ion concentration is not accurately known, they help to establish certain qualitative points of interest.

Alkaline solutions 0.02 N in NaOH were used to which had been added 10^{-3} molal $KHCO_3$. Then oil disks containing $w=0.890\times10^{-3}$ stearic acid were spread on this solution, and the effect on the diameter *vs.* time curves of adding various amounts of calcium chloride was studied. In Fig. 5 are given the results obtained with oil disks weighing 15.52×10^{-2} gram, each curve being for a different calcium concentration (by calcium concentration is meant only the apparent concentration added since the value initially present in the water is not known). In Fig. 6 is given the area per stearic acid molecule as a function of apparent concentration. The dotted portion indicates the effect of eliminating the last of the polyvalent metallic impurities by chemical methods described in the next section.

Since all the changes caused by the calcium were made by less than 200 parts of calcium per 10^8, it is of interest to calculate approximately the effect of the HCO_3^- ions and OH^- ions on the calcium ion concentration. Since 2×10^{-2} gram molecule per liter of $Ca(OH)_2$ will dissolve in one liter of water, it is easy to show that the concentration of hydroxide ions present will not complete any precipitation of as little as 200 parts of calcium per 10^8. However, since the second dissociation constant of $KHCO_3$ is 6×10^{-11}, a concentration of 10^{-3} molal in HCO_3^- will furnish approximately 2.4×10^{-4} molal CO_3^{--} ions. $[Ca^{++}][CO_3^{--}]=0.9\times10^{-8}$; the calcium ion concentration present in solution cannot exceed 150 parts per 10^8. Hence the $KHCO_3$ concentration used may somewhat affect the calcium concentration but certainly not to a serious extent.

Returning to Fig. 5 and Fig. 6, certain conclusions of interest can now be drawn. In the case of curve A the first acid molecules reaching the water have been close packed by the calcium ions, and have become rigid so preventing any further spreading being caused by the later arrival of acid molecules yet in the oil drop. On the other hand, in curve D, since much less calcium was present, every molecule was able to adsorb at the interface and the film formed was liquid. Here $A=105\times10^{-16}$ cm^2. The further elimination of the calcium and other polyvalent ions present led to the value $A=125\times10^{-16}$ cm^2. The slight but definite decrease in diameter after reaching the maximum spreading was in part due to a slow rate of edge loss, which sulfur powder tests showed still continued, and the greater part of the contraction due to the condensing effect of the traces of calcium. In this case if the contraction was followed long enough it was found that A approached the value $(15\text{ to }17)\times10^{-16}$ cm^2. From curve D it is seen that about $6\frac{1}{2}$ minutes

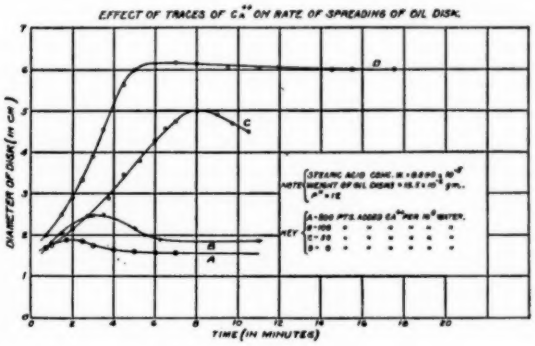

FIG. 5.

were needed for all acid molecules to reach the interface. The longer time needed at C to reach maximum diameter is presumably due to the slow rate of migration of the later arriving molecules through the partially condensed interfacial film. The more rapid rate of decrease of curve C than of curve D is almost entirely due to the increased rate of condensation of the adsorbed film made possible by the higher concentration of calcium ions.

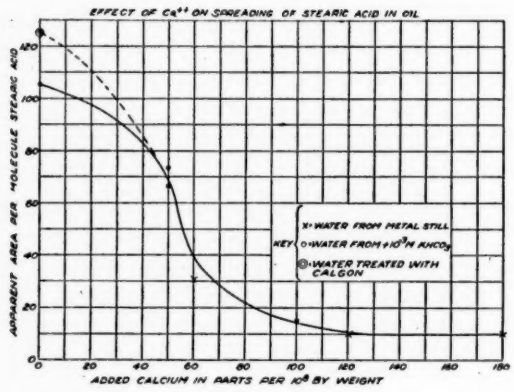
EFFECT OF Ca^{++} ON SPREADING OF STEARIC ACID IN OIL
APPARENT AREA PER MOLECULE STEARIC ACID
ADDED CALCIUM IN PARTS PER 10^6 BY WEIGHT
KEY
X-WATER FROM METAL STILL
O-WATER FROM $\frac{1}{2}10^{-3}$ N $KHCO_3$
⊙-WATER TREATED WITH CALGON

FIG. 6.

9. Results of Eliminating the Polyvalent Metallic Ions

Because of the important influence shown by polyvalent metallic ions on the spreading of the oil disks, and since the best distilled water obtainable has enough of such metals when used in a Pyrex tray to have appreciable influence on the results, in some experiments resort was made to chemicals to precipitate or render less effective these metals. Like Langmuir and Blodgett,[17] use was made of a solution of 0.02 N NaOH and 0.02 N Na_2CO_3, and it was found that such a solution aged overnight helped matters considerably. Using still higher concentrations of Na_2CO_3 is of little advantage since adding the Na_2CO_3 also brings with it an increase in metallic impurities. To illustrate the results obtained using 0.02 N NaOH alone, values of A of from (90 to 105)$\times 10^{-16}$ cm^2 were obtained for stearic acid while using 0.02 N NaOH+0.02 N Na_2CO_3 solution resulted in values of from (105 to 110) $\times 10^{-16}$ cm^2. Following Langmuir and Schaefer[8] use was made of about 6×10^{-4} gram of Calgon per liter of the above solution to remove polyvalent metallic ions. The result was that A ranged from (120 to 125)$\times 10^{-16}$ cm^2 (see dotted portion of Fig. 6). Such an alkaline solution was adopted as a standard and for convenience will be called Calgon water.

In Table I are listed the values found for A employing Calgon water. Differences in the values between any two acids greater than ± 5 percent need not be taken seriously since it is entirely possible that they are due to error or to accidental metallic impurities. In the case of the dodecanoic and tridecanoic acids, to minimize the error due to edge loss, A was measured using a weight concentration of $w=2\times 10^{-4}$, thus making T_M short.

Summarizing these results: with the exception of the long chain hydroxy acids, A is always in the range 100 to 125 square angstroms for all acids whose chain lengths are greater than 14 carbon atoms per molecule. The apparent progressive decrease in the area per molecule with chain length for values of N less than 14 is so rapid that one infers the existence of a corresponding decrease in the lifetime of adsorption, but the error in the value of A due to the effect of edge loss is unknown and hence this cannot be considered the only logical conclusion. Since most of these molecules occupy, when close-packed at the water-air interface, an area of around (20 to 35)$\times 10^{-16}$ cm^2, it is apparent that at the oil-water interface they occupy an area of from $3\frac{1}{2}$ to 6 times as great.

10. Proof of 100 Percent Adsorption

An experimental technique was developed to directly prove the correctness of Langmuir and Blodgett's conclusion regarding the infinite lifetime of adsorption of stearic acid on alkaline water and where necessary to extend the result to other adsorption problems. When the oil disk had spread to its maximum diameter, a device named for convenience a "multiple dropper" was used to cause droplets of "piston oil" (usually either castor oil or oleic acid) to touch the surface of the water simultaneously at 16 equally spaced points arranged in a circle external to but concentric with the oil disk. The piston oil spread simultaneously from the 16 points of contact and squeezed the disk from 16 directions at once, so compressing it under a pressure equal to the equilibrium spreading pressure of the piston oil used. With careful centering the contracting disk was not driven off to one side against the hydrophil tray wall. The oil disk contracted under the equilibrium pressure of the piston oil and the area per molecule decreased to a smaller value. The advantage of such a device is that the oil disk was permitted to spread to its maximum area in the absence of any piston oil or external

polar monolayer, thus minimizing the danger of contamination of the interfacial layer. After the spreading was complete the disk compression was so rapid that a measurement of the new value of the area per molecule was obtained before any appreciable error from contamination had resulted. The method has the disadvantage of inflexibility if one wishes to obtain a series of measurements of A as a function of external piston oil pressure.

To illustrate the results obtained, the experiment was performed with $w=1\times10^{-5}$ stearic acid on Calgon water. This disk usually spread to a diameter of around 6 or 7 cm. Then the castor oil caused that disk to contract immediately to a diameter of around 3 cm corresponding to $A=(27 \text{ to } 32)\times10^{-16}$ cm² and in 2 or 3 minutes more it had decreased to a minimum diameter of 2.6 cm corresponding to $A=(18 \text{ to } 24)\times10^{-16}$ cm². In the course of another 3 to 5 minutes it stayed close to that minimum diameter and thereafter it gradually increased with time. Simple tests demonstrated that this subsequent increase was due to the dissolving of the castor oil in the oil disk. It was not due to the effect of the alkali on the castor oil since it was found that the piston pressure of the castor oil, initially 20 dynes/cm on such an alkaline solution, decreased to 19 dynes/cm in 35 to 40 minutes. The effect was reversible to a certain extent for if the castor oil was scraped from the water surface the disk spread out again, while upon again adding castor oil it contracted to the same minimum area. If oleic acid was used for the piston oil its initial pressure on alkaline water was around 38 dynes/cm, decreasing to 31 dynes/cm in 35 to 40 minutes. This higher pressure caused the oil disk to contract at once to a value corresponding to $(15 \text{ to } 19)\times10^{-16}$ cm², but immediately after that the disk continued to contract; in short, this pressure caused collapse of the interfacial monolayer.

A large number of such measurements resulted in a mean value for the compressed stearic acid interfacial film of $A=20.6\times10^{-16}$ cm²±5 percent.

When a solution of oleic acid in light petrolatum was compressed in the same way, the value of A under the pressure of castor oil decreased immediately to $(30 \text{ to } 34)\times10^{-16}$ cm², which is nearly the same value found at the air-water interface on acid water at that same film pressure. However, using oleic acid for the piston oil caused the disk to contract further to a minimum area corresponding to $A=20.5\times10^{-16}$ cm²±5 percent. Hence, the higher piston oil pressure of oleic acid was needed to close-pack the oleic acid molecules, presumably as a result of its *cis*-configuration.

From these experiments it is evident that all of the stearic acid or oleic acid molecules originally present in the oil drop had migrated and remained at the oil-water interface. From the fact that all of the other long chain acids of Table I showed the same range of values of A on Calgon water, one concludes that all these long chain acids have infinite lifetimes of adsorption on alkaline water.

11. Origin of Large Values of A

Langmuir and Blodgett[17] inferred from their work on stearic acid in Squibb's petrolatum that their large value of $A=90\times10^{-16}$ cm² was due to a considerable hydration of the carboxyl group of the molecules. From experiments on compressing such disks they concluded that the relation

Table I. *Area per molecule of fatty acids at the interface between Calgon water and oil.*

Acid	No. of Carbon Atoms per Molecule	$A\times10^{16}$ cm²
Dodecanoic (lauric)	12	35*
Tridecanoic	13	70*
Tetradecanoic (myristic)	14	95
Pentadecanoic	15	104
Hexadecanoic (palmitic)	16	110
Heptadecanoic (margaric)	17	115
Octadecanoic (stearic)	18	125
Nonadecanoic	19	117
Eicosanoic (arachidic)	20	122
Octadecenoic (oleic)	18-*cis*	123
Octadecenoic (elaidic)	18-*trans*	123
13-docosenoic (erucic)	22	96
12-hydroxy-9 octadecenoic	18-*cis*	57.5
12-hydroxy-9 octadecenoic	18-*trans*	57.5
13-hydroxyoctadecanoic	18	62.5
Chaulmoogric	18	97.0
Di-*n*-heptylacetic	16	66.0*
Methyltetradecylacetic	17	110–120
Propyldodecylacetic	17	117
Phenylstearic	24	91
Ethylphenylstearic	26	103
Xenylstearic	30	114
Tetrahydronapthylstearic	28	117

* Edge diffusion loss too great for an accurate measurement of A.

$F(A-A_0)=kT$ held true for such an interfacial film and that $A_0=57\times10^{-16}$ cm². It seems quite unlikely that enough water of hydration adheres to each carboxyl group so tenaciously as to cause A_0 to be that much greater than the value 22×10^{-16}, particularly when it is remembered that the interfacial monolayer is under a compression of between 11 and 14 dynes/cm due to the large negative spreading coefficient F_s of the oil disk. If the water of hydration were responsible, the castor oil piston pressure experiment described above would cause the total film pressure to rise from between 11 and 14 dynes/cm to between 19 and 20 dynes/cm; and since the first pressure would not brush off all the water of hydration, one would not expect the second pressure to do so. Yet the fact is that A under the higher pressure is 20.6×10^{-16} cm².

In the above experiment with the castor oil, a definite time interval was found to occur before the interfacial film was compressed to the minimum area corresponding to close-packing. This suggests that the acid molecules are separated by hydrocarbon molecules of the oil and that under the external pressure of the piston oil the hydrocarbon molecules were forced up and out of the interfacial film, thus eventually permitting close-packing of the acid molecules. If this were true, then the results of Table I would mean that all these long chain acids when adsorbed form 2-dimensional complexes or solutions with hydrocarbon molecules from the oil. The large value of A and the fact that it is nearly the same for all acids are then quite understandable. The existence of oil molecules in the adsorbed film is not an unimportant point since it is reasonable to assume that the hydrocarbon molecules present between the adsorbed acid molecules will have a certain amount of bonding with them. If this were not the case, thermal agitation would eventually cause these hydrocarbon molecules to be worked out of the interfacial film and eventually they would be replaced by adsorbed acid molecules, thus leading to a system of lesser energy. Entirely independent evidence for this conclusion will be presented later in Part II.

The above-mentioned value of $A_0=57\times10^{-16}$ cm² obtained by Langmuir and Blodgett may be given a simple molecular interpretation: The electrical repulsion between adjacent dissociated stearic acid molecules acts counter to the net surface tension force of -11 to -14 dynes/cm and hence more than one hydrocarbon molecule can insert itself and be weakly bound between each pair of acid molecules. Their difference $(90-57=33)\times10^{-16}$ cm² suggests that there are two hydrocarbon molecules per acid molecule in the complex film, and that under the action of small external pressures, the disk readily contracts until one of the two hydrocarbon molecules is forced out of the film. However, the remaining hydrocarbon molecule is much more strongly held in the film, and a greater external pressure than was used in their experiments is needed to force it out. One would then be led to the conclusion that the true area per acid molecule is 57×10^{-16} cm². But it has here been shown that a greater external pressure will cause the area to decrease to approximately 21×10^{-16} cm². It will be noted that $(57-21=36)\times10^{-16}$ cm² which is in reasonably good agreement with the above deduced value of 33×10^{-16} cm² for the area occupied by each of the hydrocarbon molecules in the complex film.

The above hypothesis as to the relative abilities of 1 : 1 and 1 : 2 film complexes to stand external pressure, and also the resulting inferred area per hydrocarbon molecule are in good agreement with the results of the recent study by Davis, Krahl and Clowes[29] of two-dimensional complex films formed at the air-water interface by various mixtures of sterols and aromatic hydrocarbons.

12. Behavior of Mixed Films of Oleic and Stearic Acids

When drops of oil containing various proportions of both oleic and stearic acids were spread on Calgon water, the observed area per molecule was the same as for the pure acids; i.e., 120×10^{-16} cm². This was to be expected since they each occupied the same area when pure and also, being so far, apart the acid molecules showed little interaction. When drops of the same mixed acids were placed on 0.02 N NaOH to which 2.5×10^{-4} molal $CaCl_2$ was added, the results given in Fig. 7 were found. The method of

[29] W. Davis, M. Krahl and G. Clowes, J. Am. Chem. Soc. **62**, 3080 (1940).

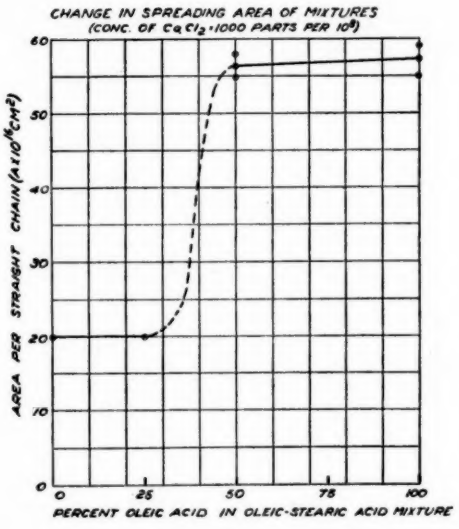

FIG. 7.

obtaining the values given requires some explanation. The 100 percent oleic and the 50–50 percent oleic-stearic mixture spread on the calcium water without trouble. Using the multiple dropper with castor oil as described above, it was possible to prove there was no serious error from edge diffusion and that in each case every acid molecule in a drop had been adsorbed at the interface. Hence within the experimental error indicated by the scattering of points on the graph, the value of A, the area per acid chain, was really the same for the 100 percent oleic or the 50–50 percent oleic-stearic mixture. In the case of the 25 percent oleic 75 percent stearic mixture, the disk required from 3 to 5 times longer to spread to its maximum diameter but eventually spread to an area per molecule of $(16 \text{ to } 19) \times 10^{-16}$ cm². Allowing for the edge loss of so long an experiment, the correct value of A was assumed to have been around $(18 \text{ to } 22) \times 10^{-16}$ cm², indicating close-packing. The spreading area of 20×10^{-16} cm² indicated on the graph for the 100 percent stearic acid is a reasonable assumption although the actual spreading is negligible, for that lack of spreading is due to the formation of a rigid interfacial form in which A must have a value between $(18 \text{ to } 22) \times 10^{-16}$ cm².

Before interpreting these results, it is of interest to note that the calcium ions cannot cause close-packing in interfacial films containing pure oleic acid. In fact, thorium ions also are unable to close-pack interfacial films of oleic acid at either the oil-water or the air-water interface. The value of $A = 57 \times 10^{-16}$ cm² is much greater than that to be expected from the results of studies at the air-water interface for there under film pressures of 11 to 14 dynes/cm, A has a value of around $(32 \text{ to } 34) \times 10^{-16}$ cm². It might be thought that this value of 57×10^{-16} cm², is due to the adsorption of the double bond of oleic acid at the oil-water interface. However, Marsden and Rideal[30] have shown from their studies of oleic and elaidic acids at the air-water interface that the lack of close-packing for oleic acid is due to the *cis*-configuration. Only that conclusion made understandable their result that elaidic acid, the *trans*-isomer, formed much more condensed films. In agreement with their result, experiments performed here using oleic and elaidic acids at the air-water interface and employing thorium water showed that whereas the elaidic acid was made rigid by these highly charged ions, the oleic acid was not.

The use of the hypotheses of Section 11 concerning the formation of mixed film complexes also permits a simple molecular explanation of these observations on oleic-stearic acid films. A calcium ion reacts with two dissociated acid chains, and because of the strong electrical binding effect of a divalent metallic ion, the resulting molecules are little dissociated. Hence, the acid chains are no longer repelled by electrical forces and hence, as in Section 11, the film is acted on only by the compression effect of the surface tension forces (from -11 to -14 dynes/cm). This forces out some of the hydrocarbon molecules of the original mixed acid-hydrocarbon film until only one hydrocarbon molecule is left per acid chain. The result is a complex made up of four-leaf-clover-like aggregates of two acid chains and two hydrocarbons. Apparently the cross-binding forces due to Ca ions are not sufficient to force all the hydrocarbon molecules out of the film to form a rigid interfacial monolayer. The area per acid chain can reasonably be taken to be around $(30\text{–}35) \times 10^{-16}$ cm², since that is the area per oleic acid molecule at the air-water interface in acid water at a compression of 11 to 14 dynes/cm. This reasonable assumption

[30] J. Marsden and E. Rideal, J. Chem. Soc. London, 1163 (1938).

leads to the conclusion that the area per hydrocarbon molecule still left is $(57-33=24)\ 10^{-16}$ cm², which is a good approximation to the area occupied by a straight chain paraffin hydrocarbon molecule or by many types of aromatic hydrocarbons.

However, the 0–25 percent mixture causes interfacial film freezing because a large enough percentage of these salt molecules are calcium stearate for there to exist considerable cross-binding due to the added effect of the van der Waals forces between the stearic acid hydrocarbon chains. In the case of 25–50 percent mixture such freezing apparently goes on in small patches between which places that are not close-packed are left permitting the newly arriving acid molecules to reach the interface. Hence the adsorption is slow but complete.

13. Effect of High Acid Concentration

Oil disks containing more than $w=10^{-3}$ of long chain acids spread even on acid water and the mechanism and quantitative relations involved will be discussed in Part II.

14. The Spreading of Amines When Ionized

The long chain primary normal amines, like the long chain acids, spread to a remarkable extent when ionized and very much less when not. The behavior of solutions of heptadecyl amine in mineral oil is typical. In Fig. 8 is plotted the diameter of spreading as a function of pH of the water for oil disks weighing 1.7×10^{-2} gram and containing the amine in a weight concentration $w=1.204\times10^{-4}$. The solutions were made up with hydrochloric acid, $KHCO_3$ or NaOH. It is evident that for pH values exceeding 6 there is practically no spreading, while it is complete for values more acid than pH 2. The small diameter attained for pH greater than 6 is precisely the same as that of the same volume of oil free from the presence of amines. This behavior is quite general for all amine concentrations below roughly 10^{-3}. This result is qualitatively in agreement with that obtained by Peters[12] in connection with his study of the effect of pH on the benzene-water interfacial tension lowering caused by hexadecyl amine dissolved in benzene. The spreading behavior of amines on alkaline water for higher values of w than 10^{-3} will be discussed in Part II in connection with the discussion of the spreading of acids in similar concentrations on acid water.

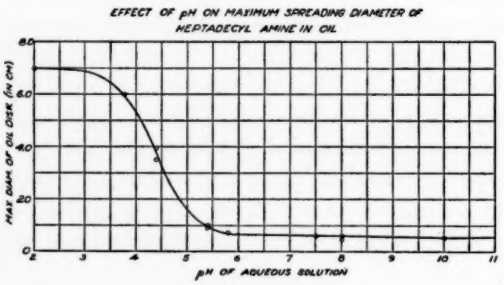

FIG. 8.

As is well known, a primary amine such as heptadecyl amine reacts in dilute aqueous hydrochloric acid to form heptadecyl amine hydrochloride, which then dissociates to form a long chain positively charged complex ion and a chloride ion. Or in general,

$$R:\underset{\underset{H}{\vdots}}{\overset{H}{\vdots}}{N}: + H^+Cl^- \rightleftharpoons \left[R:\underset{\underset{H}{\vdots}}{\overset{H}{\vdots}}{N}:H\right]^+ + Cl^-.$$

Hence the spreading of the oil disk on acid water was caused by the migration to the interface of heptadecyl amine followed by a dissociation reaction and adsorption which was complete if pH was less than 3.

Since dissociated acid molecules were found to have infinite lifetimes of adsorption, one would expect the dissociated amine molecules to behave likewise. Such was found to be the case when the multiple dropper technique was used to close-pack the fully spread oil disk containing heptadecyl amine, and a contraction to an area per molecule of $(18\text{ to }20)\times10^{-16}$ cm² was observed.

Measurements of the area per adsorbed molecule A carried out by methods entirely similar to those already described for acids, but using distilled water 10^{-2} N in HCl, furnished the results of Table II. Only a brief study was made of the effects of various negative polyvalent ions on the value of A, and although the ions CO_3^{--} PO_4^{---} and $Fe(CN)_6^{----}$ did not cause rigidity of heptadecyl amine at the oil-water or air-water interface, it is possible that some condensation of

the film resulted. The molecular meaning of the data of Table II cannot be stressed too much for that reason. However, it appears that the mutual repulsions between the dissociated amine hydrochlorides is less than between the corresponding dissociated acids, and A increases linearly with N, the number of carbon atoms per molecule.

The rate of edge loss was found to be greater for a primary amine than for the corresponding single chain aliphatic acid, and as a result the error in measuring A due to edge loss was more serious. The observed decrease of A with decreased chain length may be partly due to this cause.

The time, T_M, for the disk to reach its maximum diameter was found to be approximately the same for heptadecyl amine as for heptadecanoic acid at the same molal concentration. Hence the rate of diffusion of these two types of polar molecules through the oil is approximately independent of the nature of the polar group.

The fact that the value of A is so much greater than the true molecular cross-sectional area (18.5 to 24) $\times 10^{-16}$ cm^2 as in the case of the acids can also be interpreted to mean that the adsorbed amine film at the oil-water interface is a 2-dimensional solution in oil.

A study was made of the spreading of oil drops containing the secondary and tertiary amines, di-*n*-octyl amine and di-*n*-amyl amine, as well as tri-*n*-octyl amine and tri-*n*-amyl amine. The octyl amines behaved like the primary amines with regard to the effect of *p*H but the oil drops spread with greater rapidity and showed even more edge diffusion. The amyl amines either spread so rapidly as to appear to burst, or simply skated over the surface of the water while exhibiting intense edge diffusion. Since these triamines have either 24 or 15 carbon atoms per molecule, respectively, it is again evident that the rate of edge diffusion is not controlled by the total molecular weight but the length of the longest chain present.

TABLE II. *Area per molecule of amines on acid water.*

AMINE	NUMBER OF CARBON ATOMS PER MOLECULE	$A \times 10^{16}$ cm^2
Octadecanoic amine	18	84.2
Heptadecanoic amine	17	75.3
Hexadecanoic amine	16	68.5
Tetradecanoic amine	14	55.3
Octadecenyl and octadecendienyl amine	18	59.4

Oil solutions of diphenyl amine and triphenyl amine were tested similarly but neither showed any spreading variation with *p*H, and in fact spreading occurred only if w considerably exceeded 10^{-3}. On the other hand, dibenzyl amine and tribenzyl amine showed more spreading on acid than on alkaline water, but the amount of spreading was negligible unless w also considerably exceeded 10^{-3}. These results agree with the well-known dissociation rule that a phenyl group attached directly to the nitrogen atom of an amine group cuts down its degree of dissociation, while the further away the point of attachment of the phenyl group from the nitrogen atom, the less it affects the dissociation constant. The fact that the *p*H has effect on only the benzyl amines is therefore understandable. The difficulty in causing disk spreading is merely due to the fact that the longest chain length present in the molecule is still so short that edge diffusion is the most pronounced spreading effect unless high concentrations are used.

ACKNOWLEDGMENTS

Without the constant encouragement of Dr. Parry Borgstrom, this work, the first of a series of studies on polar molecules in hydrocarbon fluids, could neither have been undertaken nor completed.

A General Thermodynamic Theory of the Spreading of Liquids to Form Duplex Films and of Liquids or Solids to Form Monolayers

WILLIAM D. HARKINS
George Herbert Jones Laboratory, University of Chicago, and the Universal Oil Products Company, Chicago, Illinois

(Received March 21, 1941)

A comprehensive thermodynamic theory is developed for the spreading of any liquid or solid b over the surface of any liquid a. Spreading is considered to occur by two types of processes: (A) duplex film or D spreading, and (B) non-duplex or M spreading. A duplex film is always unstable, and transforms into a non-duplex film and a lens. Every non-duplex film of known structure is a monolayer (M). Either type of film may spread if its formation involves a decrease of free energy. The free surface energy of mercury at 20°C is 476 erg cm^{-2}, and the spreading of water or any organic liquid on the surface as either a duplex film or a monolayer, gives a decrease of free surface energy, so all such liquids spread on mercury. On water all organic liquids spread as monolayers; an organic solid also spreads as a monolayer unless it is too non-volatile in the two-dimensional system. A liquid b will spread over the surface of a liquid a as a duplex film if the initial spreading coefficient $S_{b/a}=W_A-W_{Cb}$ is positive, that is if the work of adhesion W_A between the two liquids is greater than the work of cohesion (W_{Cb}) in b. If b is saturated with a, then $S_{b'/a}$ is designated as the semi-initial spreading coefficient, which has almost the value of the initial coefficient. If the liquids are mutually saturated the final spreading coefficient, $S_{b'/a'}$, is *always negative*. Thus a liquid b will never spread over its own monolayer, and if the whole surface of water in any vessel is covered by a duplex film, it is certain that a monolayer has not spread over any part of it. After a definite period, the length of which is dependent on many factors, a duplex film begins to segregate into a monolayer, patches of thicker duplex film, and lenses, and finally into a monolayer and a lens. The film pressure π_e of a monolayer of b in equilibrium with a lens of b is equal to the difference between the semi-initial and the final spreading coefficient, or $\pi_e=S_{b'/a}-S_{b'/a'}$. Since $S_{b'/a'}$ is always negative, the equilibrium film pressure is always greater than the semi-initial coefficient. Hydrocarbons of not too high molecular weight are found to spread on water as either duplex films or monolayers. Thus many nonpolar oils spread on water to form either type of film. Benzene, which according to one of the most prominent theories does not spread at all, spreads readily, and exhibits the following values, which are almost the same as those for isopentane: initial coefficient 8.94, semi-initial 8.90, and equilibrium film pressure 10.6, in erg cm^{-2}. Carbon disulfide (nonpolar) and methylene iodide (highly polar) have initial coefficients -7.3 and -23.8, and therefore do not give duplex films, but they vaporize in the two-dimensional surface, and give equilibrium film pressures of 2.3 and 0.6 dyne cm^{-1}, respectively. Presumably their monolayers are gaseous. In general for liquids which spread as duplex films, it takes less work (i.e., the increase of free energy is less) to pull a liquid away from its equilibrium monolayer than to pull it away from itself. For benzene the difference is 1.7 and for n-heptyl alcohol, 5.4 erg cm^{-2}. An oil which is non-spreading in the sense of duplex film formation, may be caused to spread as a duplex film by the addition of an oil of sufficiently high initial spreading coefficient. This also increases the equilibrium film pressure of the monolayer. The oils added for this purpose are, in general, of the polar-nonpolar type, such as stearic acid. With such mixtures the values of the thermodynamic spreading coefficients, or the free energy levels, are highly dependent upon the nature and the concentration of the oil added. If the aqueous subphase is alkaline, stearic, or another similar acid is converted into a salt, and if the positive ions have a charge of two or higher, this has a pronounced effect upon the spreading coefficients and the film pressure.

SYMBOLS

A, Helmholtz free energy.
a, The liquid phase a.
a', Phase a saturated with b.
b, The liquid phase b.
b', The phase b saturated with a.
γ, Surface tension; or free surface energy for 1 cm^{-2}, γ_f, free surface energy of the film covered surface, and γ_e, equilibrium value of γ_f.
γ_{ab}, γ_{ow} or γ_i, Interfacial tension or free energy.
d, Duplex film, D spreading as a duplex film.
δ, Non-exact differential.
E, Internal energy.
ϵ, Internal energy for unit area (molecular potential energy).
F, Gibbs free energy.
f, (subscript) denotes a film.
f, free surface energy per sq. cm.
G, Gravitational potential, g, acceleration of gravity.
h, enthalpy per cm^2.
L, liquid. l, (subscript) denotes a lens.
m, Monolayer or mass. M, Spreading as a monolayer.
o, Oil.
p, Pressure in dyne cm^{-2}.
π, Film pressure in dyne cm^{-1}.
ρ, Density, ρ_v density of vapor phase.
S, Entropy.
Σ, Summation of terms.
$S_{b/a}$, Initial spreading coefficient of b on a.

$S_{b'/a}$, Semi-initial spreading coefficient of b on a.
$S_{b'/a'}$, Final spreading coefficient of mutually saturated b on a.
T, Temperature, Kelvin scale.
v, Volume.
W_{C_b}, Work of cohesion for the liquid b.
W_A, Work of adhesion for the interface ab.
w, Water.

1. Introduction

SOME of the most fundamental relations of surface chemistry are those involved in the spreading of a liquid phase over a subphase to form a duplex film and a monolayer. Nevertheless there is no branch of the subject which is in a more confused state in both the earlier and the more recent literature. This is probably due to the fact that there have been not only contradictory theories of the spreading of duplex films, but also their further transformation to monolayers has not been treated from the thermodynamic standpoint, nor from that of statistical mechanics.

The term duplex, as used here, does not refer to any application of a double film theory to a monolayer, in which case the upper and lower surfaces of a single molecular layer are treated as having almost independent interfaces. According to the definition of the term as used here a duplex film is a phase so thin as to have properties which are practically independent of the force of gravitation, but which is sufficiently thick to allow the interfacial energy, both free and total, of each of its interfaces to be the same as when both liquids are present in bulk, so that each interface is independent of the other. In this particular sense of the term a monolayer cannot be a duplex film.

2. Theories of Spreading

All of the divergent views concerning spreading may be considered as included in the three theories outlined below.

1. According to the theory of Lord Rayleigh,[1] as based upon the work of Marangoni,[2] Van der Mensbrugghe,[3] and Quincke,[4] (A) All liquids spread on water: (B) Lenses of a liquid do not form upon water unless the surface of the water is contaminated by some foreign substances. The Neumann triangle of forces is imaginary and there cannot be equilibrium between a lens and its own film or water. "No such equilibrium, and no such triangle, is possible if the materials are pure; when it occurs it can only be due to the contamination of one of the surfaces."

2. The theory of Langmuir[5] is extremely simple, and on this account has exerted a wide influence. It may be stated as follows: Liquids whose molecules contain polar groups spread on water; if polar groups are not present the liquid will not spread. In a recent paper Langmuir applies this theory to the spreading of hydrocarbons. Thus he states:[6] "Pure hydrocarbons and other substances whose molecules are wholly hydrophobic do not mix with water, *nor do they spread*, but remain on the surface as a globule. The only substances which spread are those whose molecules contain *both hydrophylic* and *hydrophobic parts*." Again on p. 182: "*A pure hydrocarbon does not spread.*" The italics have been introduced to emphasize the points under discussion.

3. In the present paper a comprehensive thermodynamic theory of spreading is presented. This is not restricted to oils on water, but is a general theory which includes the spreading of liquids on the surface of solids, and of solids on the surface of liquids.

The relations of the phenomena involved are much more clearly understood if it is considered that there are two types of spreading. These are: (A) Duplex (or D) spreading: a liquid spreads as a duplex film. The thermodynamic relations indicate that this is unstable. (B) Non-duplex (or M) spreading: a non-duplex film may spread directly from a three-dimensional liquid or solid, or it may be formed by the transformation of a duplex film. All non-duplex oil films on water, whose structure is known, are monolayers.

The thermodynamic theory developed in this paper establishes the conditions which determine the spreading of material, initially in the form of a liquid or a solid phase, over the surface of a liquid. It applies also to the spreading over the

[1] Lord Rayleigh, *Scientific Papers*, Vol. III (1887–92), pp. 351, 397, 513, 562, 572.
[2] Marangoni, Pogg. Ann. **118**, 348, 1871 (1865).
[3] Van der Mensbrugghe, "Essai sur la Theorie Mécanique de la Tension Superficielle," Bull. Acad. roy. Belgique, [3] 9, 12 (1885).
[4] Quincke, Wied. Ann. **2**, 145 (1877).
[5] I. Langmuir, J. Am. Chem. Soc. **39**, 1864 (1917).
[6] I. Langmuir, *Cold Spring Harbor Symposia on Quantitative Biology*, Vol. 6 (1938), pp. 173, 182.

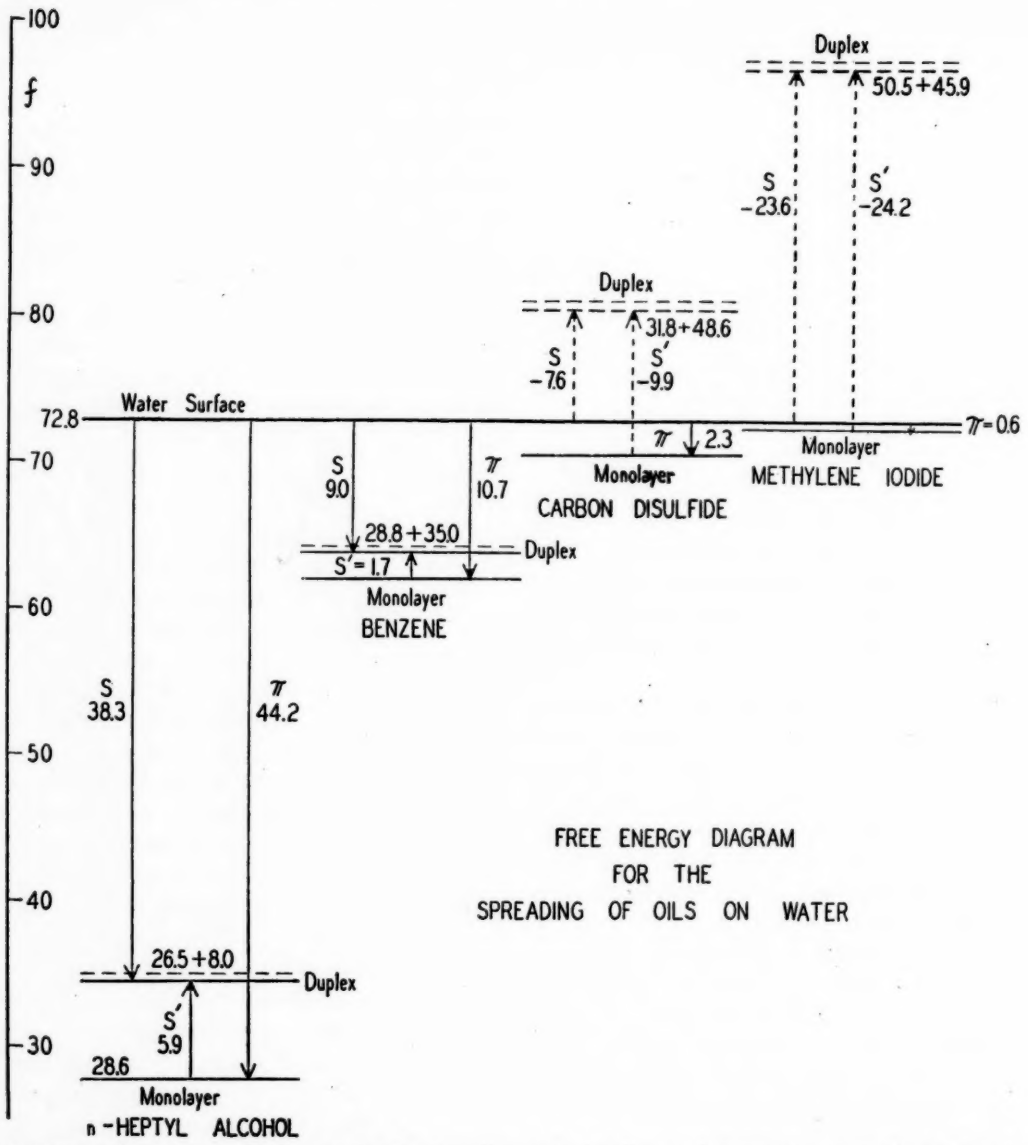

FIG. 1. Free surface energy (f) diagram for the spreading of duplex films and of monolayers on the surface of water. The free surface energy of a duplex film is the sum of that for the interface (γ_{wo}) and for the surface of the oil ($f_d=\gamma_{wo}+\gamma_o$). The lower of the two energy levels of a duplex film represents oil saturated with water, while the upper level is that when no water is in the surface of the oil. S designates the semi-initial spreading coefficient $S_{b'/a}$ which may be positive (arrow pointing downward) or negative (arrow pointing upward). S', which represents the final coefficient ($S_{b'/a'}$) *is always negative*. Obviously if the free energy of a duplex film is above that of water, it will not form: if below that of water it may spread, *but is always unstable with reference to the formation of a monolayer (and a lens)*. For the spreading of water on an oil the free energy levels for the duplex film are above that for water (usually by 40 to 110 erg cm^{-2}) so water does not spread on an oil as a duplex film. Thus, except for the greater height of the duplex level the diagram is like that for methylene iodide.

surface of a solid, insofar as this can be considered to have a uniform, instead of a periodic, surface field.

The only condition which determines whether spreading of a particular type may or may not occur, is the change of free energy involved.

3. Free Energy Diagram for the Spreading of Oils on Water

The amount of work which must be done to form one sq. cm of the plane surface of water is, at 20°C, 72.8 ergs. Thus in a diagram (Fig. 1) the surface of water may be represented as existing

at a free energy level of 72.8 erg cm^{-2}. *Any oil which can reduce this free energy level by spreading to give any particular type of film, may spread to give such a film.* If the particular type of oil film lies at a higher free energy level than that of water, it will not spread spontaneously, and if it could be spread by any mechanical means, would be unstable.

It is apparent from the figure that all four of the liquids represented spread on water to form monolayers. The spreading coefficient, that is the decrease in free energy involved when a lens of the oil spreads to form its equilibrium monolayer, is given by the value of the film pressure π_e. The values in erg cm^{-2} are as follows: *n*-heptyl alcohol, 44.2; benzene, 10.7; carbon disulfide, 2.3, and methylene iodide, 0.6. Thus this diagram appears to justify that part of Rayleigh's theory which considers that all liquids spread on water. However the equilibrium film pressure of a non-polar liquid oil of very high boiling point, such as octadecane is presumably very low (at 30°C). The film pressure of a solid *n*-paraffin of very high molecular weight is extremely small and would be difficult to detect.

With respect to their spreading as duplex films all liquids fall into two classes, those for which the free energy of the duplex film is (1) below, and those for which it is (2) above, that of the subphase. The free energy level of any duplex film is equal to the sum of its two interfacial energies, or $f=\gamma_o+\gamma_{wo}$. Thus for benzene, saturated with water, $f=28.8+35.0=63.8$, while for dry benzene $f=28.9+35.0=63.9$. Thus the duplex film does not exhibit a single free energy level, but its different levels are close together.

The decrease of free energy for the spreading of a duplex film of benzene on water is 9.0 erg cm^{-2}, and for isopentane 9.4 erg cm^{-2}, which indicates that not only aromatic compounds, but also lower *n*-paraffin oils, spread readily on water to form duplex films.

While carbon disulfide and methylene iodide spread as monolayers, it is evident that they do not form duplex films.

The relations between spreading coefficients and spreading involves the thermodynamic relations presented in the next section.

The theory of (A) duplex film spreading as presented here is an elaboration of the preliminary theory of the writer,[7] which was based on the earlier considerations of Dupré[8] and Hardy.[9]

Non-duplex, presumably monolayer, spreading is found to occur with all liquids which are not too non-volatile with respect to the two-dimensional system which consists of the clean surface of the liquid used as the subphase. To this extent there is agreement with (A) of Rayleigh's theory. It is found, however, that (B) of Rayleigh's theory is not valid, since a lens of oil is found to be stable in the presence of its *own* monolayer.

The lower hydrocarbons are found to spread *both as duplex films and monolayers*, while *those of higher* (but not too high) *molecular weight give monolayers alone.*

4. Thermodynamics of the Spreading of Duplex Films

The maximum work (δW) done by a surface when its area (σ) is increased by $d\sigma$ is

$$\delta W=-\gamma d\sigma+pdv. \qquad (1)$$

The value of the free energy of Gibbs is defined by the equation

$$F=E-ST+pv \qquad (2)$$

and the Helmholtz free energy by

$$A=E-ST. \qquad (3)$$

It follows that

$$F=A+pv \qquad (4)$$

and

$$dF=dA+pdv+vdp. \qquad (5)$$

If a process is reversible and isothermal, $T\Delta S=Q$ is the heat adsorbed and

$$dA=-dW, \qquad (6)$$

so

$$dF=-dW+pdv+vdp. \qquad (7)$$

From (7) and (1)

$$dF=\gamma d\sigma+vdp, \qquad (8)$$

so that at constant pressure and temperature

$$(\partial F/\partial\sigma)_{p,T}=\gamma \qquad (9)$$

and for a saturated surface γ is a function of p

[7] W. D. Harkins and A. Feldman, J. Am. Chem. Soc. **44**, 2665 (1922); W. D. Harkins, Sixth Colloid Symposium Monograph (1928), p. 31.
[8] Dupré, *Theorie Mécanique de la Chaleur*, p. 368.
[9] W. Hardy, Proc. Roy. Soc. **A88**, 313 (1913).

and T only, so

$$\Delta F=\gamma\Delta\sigma, \tag{10}$$

$$f=\gamma. \tag{11}$$

The condition that a liquid b shall by itself spread on a liquid a, at constant temperature, is thus that the summation of the terms $(\partial F/\partial\sigma)_{p,T}$ must be negative, that is less than zero. Thus, if b spreads on a, a certain area of the surface of a disappears and certain areas of the surface of b and of the interface ab, appear. The increase of free energy is

$$dF=\left(\frac{\partial F}{\partial\sigma_b}\right)_{p,T}d\sigma_b+\left(\frac{\partial F}{\partial\sigma_{ab}}\right)_{p,T}d\sigma_{ab}+\left(\frac{\partial F}{\partial\sigma_a}\right)_{p,T}d\sigma_a. \tag{12}$$

For a film of appreciable thickness the effects of gravitation must also be considered; but they may be neglected here.

The condition for spreading to occur starting from any given condition, is

$$dF<0, \tag{13}$$

and for non-spreading

$$dF>0. \tag{14}$$

If it is assumed that

$$d\sigma_b=d\sigma_{ab}=-d\sigma_a, \tag{15}$$

which is practically valid for a very thin layer, then

$$(dF/d\sigma)_{p,T}=\gamma_b+\gamma_{ab}-\gamma_a. \tag{16}$$

Let $-dF/d\sigma$ be designated as the final spreading coefficient $(S_{b'/a'})$ then

$$S_{b'/a'}=\gamma_{a'}-(\gamma_{b'}+\gamma_{a'b'}) \tag{17}$$

(p, T=constant, the surfaces are saturated as is designated by the primes).

It will be shown later that

$$S_{b'/a'}<0. \tag{18}$$

That is, the final spreading coefficient is always negative.

Now if a drop of the *pure* liquid b is put on the surface of the pure liquid a, and the surfaces of these liquids are considered to be still uncontaminated with each other, then the initial coefficient of spreading $S_{b/a}$ is given[7] by the equation

$$-(dF/d\sigma)_{p,T}=S_{b/a}=\gamma_a-(\gamma_b+\gamma_{a'b'}). \tag{19}$$

If b is saturated with a, but the surface of a is clean, the initial coefficient may be designated as the semi-initial spreading coefficient $(S_{b'/a})$, which, on account of the small effect of water on the surface tension of an organic liquid, is not very different from $S_{b/a}$ when these are the liquids involved.

Now

$$S_{b'/a}=\gamma_a-(\gamma_{b'}+\gamma_{a'b'}). \tag{20}$$

The work (W_A) required at constant T and p to pull the interface ab apart to give clean surfaces of a and b, is, for unit area of interface, given by:

$$W_A=\gamma_a+\gamma_b-\gamma_{a'b'} \tag{21}$$

and the work of cohesion (Wc) for the liquid b is[7]

$$Wc_b=2\gamma_b \tag{22}$$

or

$$W_A-Wc_b=\gamma_a-(\gamma_b+\gamma_{a'b'}). \tag{23}$$

From (19) and (23) the initial spreading of the liquid b over the clean surface of a is given by

$$-(\partial F/\partial\sigma)_{p,T}=S_{b/a}=W_A-Wc_b\gtreqless 0. \tag{24}$$

Thus spreading to form a duplex film occurs if $S_{b/a}$ is greater than zero, while b remains as a lens if it is less than zero.

5. Transformation of a Duplex Film to Form a Non-Duplex Thin Film (Presumably a Monolayer)

If a non-duplex thin film or a monolayer of b is present on the surface of the liquid a, the pressure (π) of the film is *defined* as:

$$\pi=\gamma_a-\gamma_f, \tag{25}$$

where γ_a is the surface tension of the pure liquid a and γ_f is its surface tension when covered with a film of b. While there is nothing in the thermodynamics which indicates that such a thin non-duplex film is always a monolayer, certain relations, presented later, seem to indicate that this is true.

What is now desired is the relation between the film pressure and the spreading coefficient.

TABLE I. *Equilibrium film pressures* (π_e), *and initial* ($S_{b/a}$), *semi-initial* ($S_{b'/a}$), *and final* ($S_{b'/a'}$) *spreading coefficients of oils on water at 20°C.* ($H_2O = 72.75$.)

	γ_e	π_e	γ OF DRY OIL	γ OF WET OIL	γ_i	$S_{b/a}$	$S_{b'/a}$	$S_{b'/a'}$
Methylene iodide	72.20	0.55	50.68	50.52	45.87	−23.80	−23.64	−24.19
Carbon disulfide	70.49	2.26	32.35	31.81	48.63	− 8.23	− 7.69	− 9.95
Benzene	62.36	10.39	28.88	28.82	35.03	8.84	8.90	− 1.49
n-Heptyl alcohol	28.53	44.22	26.97	26.48	7.95	37.83	38.32	− 5.90
Isoamyl alcohol	25.92	46.83	23.73	23.56	5.00	44.02	44.19	− 2.64

In the treatment of the transformation of a duplex film into a monolayer it is essential to consider the semi-initial spreading coefficient ($S_{b'/a}$; Eq. (20)).

Equation (17) may be written

$$S_{b'/a'} = \gamma_e - (\gamma_{b'} + \gamma_{a'b'}), \qquad (17')$$

where γ_e is the equilibrium value of γ_f and Eq. (20)–Eq. (17′) gives

$$S_{b'/a} - S_{b'/a'} = \pi_e. \qquad (26)$$

Thus π_e, the pressure of the monolayer in equilibrium with a lens of b, is equal to the semi-initial minus the final spreading coefficient.

With an oil on water *the final spreading coefficient is always negative, so the film pressure* (π_e) *is always larger than the semi-initial coefficient* ($S_{b'/a}$), which has nearly the value of the initial coefficient ($S_{b/a}$).

6. Discussion of the Theories of Spreading

As a basis for a discussion of the validity of the three theories of spreading, the values of the film pressure π_e, and of the semi-initial and final spreading coefficients of five oils on water are presented in Table I. They are calculated from surface and interfacial tension values obtained earlier in this laboratory[10] by a special modification of the drop weight method. The determinations of γ_e, the surface tension of the water covered by the equilibrium monolayer, were made on a water surface in the presence of the saturated vapor of the oil. The most likely error in such a method is that due to undersaturation of the film, which would give too high a value of γ_e and too low a value of π_e, which for benzene $= 10.8$ dyne cm^{-1} as determined by the ring method by L. E. Copeland. In a preliminary experiment at room temperature (26.5°C) H. F. Jordan[11] by the use of the ring method, found π_e for CS_2 to be 2.6 dyne cm^{-1}.

The five liquids are chosen in such a way that:

A. Three of the liquids have positive initial and semi-initial spreading coefficients, and thus should exhibit duplex film spreading, as is shown to be true by direct experiments on spreading. Of the three liquids benzene is a nonpolar hydrocarbon, and two are polar-nonpolar alcohols. Isopentane, a paraffin, has an initial spreading coefficient of 9.4, so its spreading is much the same as with benzene,

B. Two of the liquids, methylene iodide and carbon disulfide have negative initial spreading coefficients, and so exhibit only non-duplex or monolayer spreading. Methylene iodide is chosen as a *highly polar liquid which does not spread as a duplex film on water.*

Carbon disulfide exhibits very interesting relations, since it does not spread to a duplex film, but has a high vapor pressure at 20°. The molecules are adsorbed from the vapor upon the surface of the water. If this adsorbed film were to exhibit a higher equilibrium film pressure than that from the lens of the liquid, the material would at constant temperature and pressure continually evaporate to form a three-dimensional vapor, which would condense into a two-dimensional gaseous film on the water. This film would condense into the one-dimensional edge of the lens, and the carbon disulfide would complete its cycle by returning to the lens. Thus the system would exhibit perpetual motion of the second kind. Actually a gaseous film spreads rapidly from the edge of the lens until the equilibrium film pressure of 2.3 dyne cm^{-1} is attained. With methylene iodide, which has a very large negative value for its initial spreading coefficient as a duplex film, the positive film pressure for the gaseous film is smaller (0.55 dyne cm^{-1}).

7. The Instability of Duplex Films and Their Transformation Into Monolayers

Up to the present time no evidence has been presented to show that any stable truly duplex (uniform polymolecular) film has ever been

[10] W. D. Harkins and B. Ginsberg, Colloid Symposium Monograph, Vol. 6 (1928), p. 20.

[11] H. F. Jordan, Thesis, University of Chicago, 1927.

prepared. Such films have always changed into a more stable system which consists of lenses and a monomolecular film. The closest approach to a stable film of this type ever seen by the writer, was obtained by spreading an extremely old, and therefore partly oxidized, lubricating oil on water. For a period of about half an hour, white light reflected at about 15° from the plane of the surface, gave a uniform color, dependent on the thickness, over the whole area which was about 4×10^3 sq. cm. Finally, however, the film developed a large number of striations and islands of varying color.

An interesting experiment on the spreading of any oil which has a positive initial spreading coefficient, may be made in a very simple way.

A large crystallizing dish is made overfull with very pure water, and the surface is cleaned thoroughly by any one of several well-known methods. If the form of the surface of the water is correct for the purpose, a layer of the oil may be spread so that it covers the surface of the water near the edge of the dish, leaving a practically circular hole of any desired size, smaller than the area of the surface. The instability of a uniform layer of benzene of a thickness of 1 mm, or somewhat more, may be illustrated by a modification of this experiment.

The benzene, initially present as a layer several mm thick, may be allowed to evaporate. At some certain thickness, usually over 1 mm, a hole appears in the center of the layer. The non-duplex film (monolayer) in this hole expands, causing a thickening of the layer, which is now a large lens. If the surface of the water is below the top of the crystallizing dish, the shape of the meniscus is such as to cause the hole, or holes, to appear close to the edge of the surface of the water, instead of in the center. Suppose the hole to appear in the center of a duplex film, of large area, instead of in a thick layer as described above. The duplex film may be considered as exerting a film pressure ($\pi_d = S_{b'/a} = 8.9$ dyne cm^{-1}, $\pi_m = ca.$ 10.4 dyne cm^{-1}).

On account of its higher pressure the monolayer enlarges its area at the expense of the area of the duplex film, which changes into a lens. As the lens becomes thicker it gains gravitational energy, which causes a greater pressure against the monolayer. As a result of this the pressure (π_m) of the monolayer is slightly increased until it becomes π_e. The theory is treated later. H. F. Jordan[11] finds that a lens of benzene 24.9 cm in diameter ($v = ca.$ 14.5 cm^3) is 0.257 cm thick, while one 16.9 cm in diameter ($v = ca.$ 6.35 cm^3) is 0.212 mm thick. Thus a large sheet of a benzene phase on water must be several mm thick before it becomes stable, and without the effect of gravitation it is not stable at greater thicknesses. Presumably a sheet 2 mm thick will not rupture unless there is considerable vibration. If a circular ring of circular wire is pulled from the surface of this hole, the pull in the case of benzene (Fig. 1) at 20° is found to correspond to a film pressure of 10.6 dyne cm^{-1}, or a free surface energy of 62.15 erg cm^{-2}. A very large lens or layer of benzene on the water has a free energy of 28.8 erg cm^{-2} in its surface, and of 35.05 erg cm^{-2} in the interface parallel to the surface, or a total of 63.85 erg cm^{-2}. If this lens could be made so thin as to give a duplex film, then, since $63.85 - 62.15 = 1.7$, there would be a decrease of free energy of 1.7 ergs for every sq. cm of area lost by the duplex film and gained by the monolayer. But this is the numerical value of the final spreading coefficient. Thus if it were not for the work done against gravitation in the piling up of a part of the material into lenses, the monolayer would grow continually at the expense of the duplex film. Actually, if the surface of the water is completely covered by a duplex film, this transforms itself into a monolayer while the remainder of the material of the duplex film changes to a layer, lens, or lenses. As the lenses thicken the rate of decrease of area of their upper

TABLE II. *Some lower hydrocarbons which spread on water to form duplex films.*

LIQUID	$t°$	$S_{b/a}$			
		Paraffins			
Isopentane	20°	9.40			
n-Hexane	30°	3.37			
	40°	2.81			
n-Octane	10°	0.48			
	40°	0.16			
Di-isoamyl	20°	3.71			
		Aromatics			
Benzene	10°	8.40	Liquid	$t°$	$S_{b'/a}$
	20°	8.89	*o*-Xylene	20°	6.80
	30°	9.23	*m*-Xylene	20°	6.14
	40°	9.47	Mesitylene	20°	5.54
Toluene	20°	6.80	*p*-Cymene	20°	10.05

and lower surfaces becomes less than the rate of increase in area of the monolayer. This reduces the drop in total *free* surface energy until the rate of decrease becomes equal to the rate of increase of the gravitational work done, which, obviously, gives an equilibrium state.

Thus if the final coefficient of spreading is negative for all oils, as it seems to be, the monolayer is always more stable than the duplex film. This explains why uniform polymolecular oil films on water have not been found to exist for any considerable time.

Whether the velocity of spreading of the monolayer is greater or less than that of the duplex film is not a question of the free energy decrease, but of the rate at which each type of film spreads. In an experiment with oxidized Nujol it was found that the oil spreads first as a duplex film, and that later this breaks up into lenses and a monolayer. One thin duplex film of this oil which was observed had a life of 90 seconds, after which it exhibited segregation. This life seemed to decrease as the duplex film was made thicker.

8. Adhesion Between Benzene and a Monolayer of Benzene on Water

It is important to learn how far the attraction due to molecules of water penetrates into benzene at an interface between water and benzene. The work of adhesion between the two pure liquids at 20° is 66.60 erg cm^{-2}, or if the benzene is saturated with water, 66.55 erg cm^{-2}. However, if the water is already covered by the equilibrium monolayer, the work of adhesion between this and the benzene, is only 56.20 erg cm. The fact of interest is that this work of adhesion is 1.7 erg cm^{-2} *less* than the work of cohesion in the benzene. Thus the presence of the water *lowers* the increase in free energy when benzene is pulled apart between the first and second layers. In the case of heptyl alcohol it requires 6 erg cm^{-2} *less* work to pull this from its monolayer on water than to pull heptyl alcohol apart. This is presumably due to the orientation of the heptyl molecules in the film so that the paraffin chains in the first monolayer, are oriented toward the alcohol. Thus the intermolecular forces between the hydrocarbon chains and the alcohol, are weaker on the average than those in the alcohol.

Unfortunately the increase in *molecular potential* energy (ϵ_A = increase in internal energy) in the separation of a liquid from its first monolayer on water is not known, since, although the free energy has been determined, the latent heat of the process has not been obtained.

9. The Spreading of Hydrocarbons on Water as Duplex Films

It has been shown that thermodynamics predicts that liquids with a positive initial spreading coefficient may spread on clean water to form duplex films, and that these transform themselves into lenses and a monolayer. In Table II it is shown that hydrocarbons, either paraffin or aromatic compounds, exhibit positive initial spreading coefficients, provided their molecular weight is not too high, and that these liquids actually spread is shown if they are tested as described in the last section.

This table shows definitely that hydrocarbons of not too high molecular weight spread on water, so Langmuir's theory (3) that polar groups are necessary for spreading, is not adequate, since it often leads to conclusions which are not in accord with the facts of observation.

The idea that hydrocarbons do not spread on water has part of its origin in the fact that, prior to the publication of this paper, there seem to have been no values of their film pressures in the literature. This is partly because the ordinary horizontal type of film balance cannot be used to determine this pressure, since the volatility of the compound causes it to be adsorbed on the water behind the float.

The explanation of the fact that film pressures have always been determined by the use of oils whose molecules contain at least one polar group, is that this group anchors the molecule to the water and lowers the volatility. This not only allows the ordinary film balance to be used, but what is more important, it makes it possible to know how many molecules are present in the surface; which would be true of the higher hydrocarbons also, but they exhibit negative initial spreading coefficients and so will not spread. Even tetradecane, a non-spreading oil, is bound so lightly to the water and in the film, that it escapes too rapidly, as from mixed films, to give good measurements.

10. Lower Hydrocarbons Form Monolayers on Water

The geometrical relations of thin non-duplex films of oleic acid and other polar-non-polar oils, indicate that they are monomolecular, when spread from a liquid or a solid three-dimensional phase. It is assumed by the writer that the thin non-duplex film formed by transformation from the duplex film of a lower hydrocarbon, is also monomolecular.

According to Table I the free energy level for the monolayer of *n*-heptane on water is 28.6, while that of the duplex film is 34.5 erg cm^{-2}. Thus the duplex film will not spread ($S_{b'/a'} = -5.9$) over the non-duplex film, which is a monolayer. The relations for benzene differ in magnitude only.

The values show that the work required to pull *n*-heptyl alcohol from its monolayer on water is 5.9 erg cm^{-2} less than that required to pull the alcohol from itself. This difference is evidently due to the orientation of the alcohol in the first monolayer. As a result of this the alcohol has to be pulled away from only the hydrocarbon chains of the first monolayer, so the work involved is less than when the alcohol is pulled apart, since some polar groups of the alcohol must be separated from each other. While the orientation of the benzene does not involve so large an amount of energy, nevertheless the most active part of the benzene molecule is turned toward the water, with its more powerful field, that is the least active part of the benzene molecules in the first layer is turned toward the second layer.

As a result of this the smallest molecular interaction in the water-benzene system is that between the first and the second monolayers of benzene.

From our knowledge of the range of intermolecular forces it is evident that above the third benzene layer there can be only a negligible attraction of the water at the interface. If this is true there is no source of energy which can keep the material of the benzene lens, which may have a thickness of as much as 2.7 mm. from flowing over a film of four molecules in thickness by the action of gravitation. However from the discussion in the preceding paragraph it is evident that the greatest difference in the energy of interaction in the benzene phase is not between the layers 3 and 4, or 2 and 3, but between 1 and 2. Thus it seems practically certain that the stable hydrocarbon film is monolayer.

It may be assumed that if a monolayer of benzene, in equilibrium with a lens, is present on the surface of water, a second layer may begin to deposit upon it. A molecule in the second layer will not be bound as tightly as if in the first layer. Therefore $(t_2)_{evap} < (t_1)_{evap}$, where t_2 and t_1 are the life periods if molecules can only escape from each layer by evaporation. However, a molecule in the second layer can also escape into the first layer, where it is held more firmly. This makes $(t_2) < (t_2)_{evap}$, where t_2 is the mean life with respect to both methods of escape. A molecule of the second layer which escapes into the first layer replaces a molecule in this layer, and causes a molecule in the first layer to move into the lens. This last step is accompanied by an increase in free energy, but this increase is less than the decrease of free energy which is involved in the movement of a molecule from the second into the first layer. Thus a double film of benzene is not stable and only the monolayer remains.

The "hole" in a hydrocarbon lens disappears in a slightly supersaturated vapor of the hydrocarbon, not by a deposition of a second and a third layer on the monolayer, but by an increase in the amount of the hydrocarbon liquid phase, and a consequent closing in of the walls of the hole.

11. Changes of Free Energy Involved in the Spreading of a Lens into a Duplex Film and a Monolayer

If a drop of an oil which spreads is put on the surface of water it forms a transient lens. If the area of the water surface replaced by the lens is σ_l, the area of the surface of the oil by σ_o, and that of the interface by σ_{wo}, then the decrease in free surface energy *for this area* σ_l when the lens spreads completely to form a duplex film is*

$$-\Delta F_{p,T} = \gamma_o(\sigma_o - \sigma_l) + \gamma_{wo}(\sigma_{wo} - \sigma_l) \qquad (27)$$

* If the lens, which has an area σ_o for its oil surface and σ_{wo} for its interface with the water spreads to form a duplex film of total area σ, the increase of free energy may be listed as follows:

Oil:	$\gamma_o(\sigma - \sigma_o)$
Water:	$-\gamma_w\sigma$
Interface:	$\gamma_{wo}(\sigma - \sigma_{wo})$.

or for unit area

$$\frac{-\Delta F_{p,T}}{\sigma_l}=\frac{\gamma_o\sigma_o+\gamma_{wo}\sigma_{wo}}{\sigma_l}-(\gamma_o+\gamma_{wo}). \quad (28)$$

There is also a decrease of gravitational potential (G), which may be expressed for the whole conversion into a duplex film, as

$$G=g\cdot f(m,\ \gamma_a,\ \gamma_{b'},\ \gamma_{a'b'},\ \rho_a,\ \rho_{b'}\ \rho_v), \quad (29)$$

The oil of the lens, other than that which remains on the area σ_l, may also be considered as spreading to form a duplex film. The decrease in the free energy per unit area of the surface of the subphase covered in this process is, for the spreading of b' on a

$$-\Delta F/(\sigma_d-\sigma_l)=\gamma_a-(\gamma_{b'}+\gamma_{a'b'})=-S_{b'/a}, \quad (30)$$

where σ_d is the area of the duplex film. Thus the lowering of the free energy per unit area is given by the semi-initial spreading coefficient.

If a duplex film is formed over the whole of a restricted area, the next process which occurs is the formation of "holes" in the duplex film. As has been shown earlier, the surface of the water in these holes is covered by a monolayer of the oil. In the formation of the monolayer the free energy is again decreased, as follows:

$$-\Delta F/\sigma_m=-S_{b'/a'}. \quad (31)$$

If the total available area is sufficiently small the duplex film of area σ_d changes completely into a monolayer of area σ_m and a lens of area σ_l'. This area is not that (σ_l) of the initial lens, but

$$\sigma_m+\sigma_l'=\sigma_d. \quad (32)$$

In an experiment of limited duration either one lens or many lenses may be formed. It is obvious that, in the process in which a duplex film is changed into a monolayer and a lens, there is an increase of gravitational potential (Eq. (29)).

The free energy of the surface of the water covered by the monolayer is per unit area

$$(\partial F/\partial\sigma_m)_{p,T}=\gamma_w-(S_{b'/a}-S_{b'/a'})=\gamma_w-\pi_e, \quad (33)$$

where π_e is the film pressure of the equilibrium monolayer.

Thus

$$-\Delta F=\gamma_w\sigma-\gamma_o(\sigma-\sigma_o)-\gamma_{wo}(\sigma-\sigma_{wo}). \quad (27+30)$$

Unless the lens is extremely small σ_o and σ_{wo} are negligible in comparison with the total area σ, so

$$-\Delta F/\sigma\approx\gamma_w-(\gamma_{o'}+\gamma_{w'o'})=-S_{o'/w} \quad (30')$$

which is Eq. (30) except for the minute difference in area.

If the area available is just that occupied by all of the oil in a monolayer at the equilibrium pressure, no lenses are left, and no work is done against gravitation.

If a very much larger area than this is available the monolayer spreads over it, with a concomitant decrease of film pressure and increase of γ_f. While the free energy per unit area of the film-covered surface is thus increased in a spontaneous isothermal, isopiestic process, the free energy (F) of the area as a whole is decreased. That is, while the free energy of that part of the surface of the water covered by the film is increasing, the free energy of the clean water is decreasing even more rapidly, as the film spreads over it.

If a monolayer, with the free surface energy γ_e is not in contact with a duplex film or lenses, the rate at which γ_f increases with increase of area at constant temperature depends upon the state of the monolayer,[12] which may be, for example, the liquid expanded (L_1) state or the gaseous state. If in the former of these two states the monolayer at a certain stage of expansion undergoes a change of the first order in which there is a transition to a two-dimensional gas. Throughout the extensive area change through which this transition occurs the pressure remains constant as the area increases. It is obvious that the pressure (π_f) of the gaseous film approaches zero, and the value of γ_f approaches that of water as the monolayer expands to very large areas.

Thus the history of the expansion of a lens and a duplex film involves two steps in each of which the free surface energy decreases sharply (Fig. 1). The first, and usually the greatest, decrease is due to the spreading of the duplex film over the water surface, and the second, to the conversion of the duplex film into a monolayer and a lens, if the area is limited, or if sufficient area for its formation is available, into a monolayer alone. Further spreading of the equilibrium monolayer produces an increase in the free energy of that part of the surface covered by the oil.

12. The Spreading of Mixed Oils

A non-polar oil, which has a negative spreading coefficient ($S_{b/a}$ or $S_{b'/a}$) may be converted into an oil which spreads to form a larger lens or to a

[12] W. D. Harkins and E. Boyd, J. Phys. Chem. **45**, 20 (1941).

duplex film by the addition of a polar-non-polar substance, such as stearic acid. For tetradecane on water at 25° Langmuir[13] finds $S_{b/a}$ to be -7.6, while the value for a sample of Squibb's petrolatum at 20° was -11.4. In the relation $S_{b/a}=\gamma_a-(\gamma_b+\gamma_{ab})$ the values are:

tetradecane: $-7.6=72.0-(26.9+51.3)$ and
petrolatum: $-11.4=72.75-(31.1+53.0)$.

If myristic acid or another polar-nonpolar material is present in the oil, it is partially adsorbed by the interface. This lowers $\gamma_{a'b'}$, which gives a temporary value of the spreading coefficient which is closer to zero, or may be positive. This causes the lens to expand with a reduction of the contact angle. As the lens expands the amount of acid adsorbed is increased on account of the increase of interfacial area, and this lowers the concentration of acid in the oil. This reduces the adsorption of the acid and thus increases the interfacial tension (decreases $\gamma_{a'b'}$). As a result the lens would attain a definite larger area with a value of $S_{b'/a}$ closer to zero, if no myristic acid were to spread from the lens to give a monolayer. If the surface of the water has a limited area any acid which escapes gives a film pressure, which depends on the concentration of the acid in the monolayer. This decreases γ_a, which, in turn, decreases the value of the spreading coefficient, and causes the lens to become smaller.

In the non-equilibrium processes associated with changes in the area of the lens, the rate at which the monolayer spreads from the lens, through the linear region at its boundary, is a very important factor, which is not always kept in mind. This rate is often very small.

When equilibrium is finally attained the relative concentrations of the polar-non-polar substance in the interface (ab) and the surface of the water (a) should be constant, or $C_a/C_{ab}=k$. In the few cases for which values of k have been determined it has been found to be much larger than unity. Thus Harkins and King[14] found that many more molecules of butyric acid are adsorbed at the surface of water than at the interface water-benzene at a given concentration in the water, provided the film is not so tightly packed as to have its concentration determined by geometrical considerations. The value of k for trimethyl cellulose or α-amino-palmitic acid at the water-brombenzene interface was also found to be much larger than unity (Askew and Danielli). In all instances in which $k>1$, it is evident that, after equilibrium is attained between an oil lens and water, the concentration of the solute should be greater on the surface outside the lens than in the interface under it.

If an acid, such as myristic acid, is present in the lens its spreading is highly dependent upon the pH of the aqueous subphase, and, if this is alkaline, upon the extent to which bivalent, trivalent, and quadrivalent positive ions are present.

It was found by Mercer[15] that a monolayer escapes from the edge of a non-polar oil in which stearic acid is dissolved, even when the subphase is alkaline. Langmuir[16] finds that if more than 0.006 g stearic acid per g of Squibb's petrolatum is present the oil spreads on water to a film so thin as to show interference colors, and that the molecular area of the stearic acid at the interface is 64A^2. With more than 0.010 g of stearic acid the duplex film is too thin to exhibit interference colors.

When duplex films are formed in this way the free energy diagram is of the type exhibited by benzene in Fig. 1. The general relations are unchanged, but the free energy level of the duplex film is now dependent upon the concentration of the polar-non-polar solute as well as upon the nature of the oil. The concentration of the solute depends upon the area to which the oil has spread. If the solution is basic, calcium ions reduce the molecular area of the acid at the interface to about a third of 64A^2. Preliminary measurements in this laboratory by B. Adinoff show that Ca^{++} ions reduce the area on the surface of water from a value of 24.4 to 21.15A at zero pressure (extrapolated).

The duplex mixed film is always unstable, and breaks up into the final state of a monolayer and a lens. A drop of oil of the composition of this equilibrium lens will not spread over the surface of the monolayer in equilibrium with the lens.

[13] I. Langmuir, J. Chem. Phys. **1**, 763 (1933).
[14] W. D. Harkins and H. H. King, J. Am. Chem. Soc. **41**, 982 (1919); F. Askew and J. Danielli, Trans. Faraday Soc. **36**, 785 (1940).
[15] E. H. Mercer, Proc. Phys. Soc. London **51**, 561 (1939).
[16] I. Langmuir, J. Frank. Inst. **218**, 165 (1934).

Thus the general relations for spreading as duplex films are the same as when a pure oil is involved, except that the free energies and the related spreading coefficients are made variable by the changing composition of the oil of the lens.

13. Non-Equilibrium Interference Patterns Exhibited by Duplex Films, and Other Non-Equilibrium Phenomena

The phenomena associated with the non-equilibrium state of the duplex film and of its conversion into a monolayer are very complex, and remarkably beautiful interference patterns of extremely varied shapes and colors may be obtained in ordinary white light. On account of the fact that the light reflected by the surfaces of the layer is partially elliptically polarized, it is instructive to view the film through a Wollaston or a Nicol prism, when the electric vector is parallel and when it is perpendicular to the plane of the surface.

If a fine stream of benzene is allowed to flow slowly upon the clean surface of water in an open vessel, the benzene may be seen to advance over the surface as a duplex film, at the edge of which there appear narrow colored interference fringes, which exhibit as many as four or more orders of the spectrum. For a short distance beyond this the film is still duplex, but still beyond this spreads as a non-duplex film, presumably a monolayer. Islands of duplex film, which exhibit rapid, lifelike pulsating movements are formed if evaporation occurs at the proper rate. In some instances the motions resemble those of amoebae.

A duplex film too thin to give interference colors may be obtained by spreading one or two drops of an oxidized hydrocarbon oil (as oxidized Nujol) over a large water surface. On compression by a barrier of glass or metal, colors appear, and these are uniform over the whole area of the surface (about 4×10^3 cm² in the experiments). The colors appear in the sequence pale yellow, yellow, gold, orange, brown, red, purple, blue, pale blue, green, pale yellow, etc. Finally, in the highest orders of interference, red and green are the predominant colors.

On standing the duplex film of such a material may segregate into duplex films of different thicknesses. For example, a delicate lace pattern of interlocked fine curved lines of red on a field of green, has been observed frequently. Loose ends of the red lines are often coiled into spiral. The pattern seems to depend upon the chemical nature of the oil, its complexity of composition, and its viscosity.

Often there is a segregation into flat duplex islands of uniform color, except for small colorless holes or lakes of monomolecular thickness. Between the islands there are canals of a colorless monolayer, studded with colorless islets, which are actually very small lenses.

The patterns obtained with different oils are so manifold that it is impossible to describe them.

If such a nonhomogeneous colored duplex film is compressed further, it gives apparently flat colorless duplex islands, with lakes, canals, etc., just as when the film is colored. Finally, when equilibrium is attained, a monolayer and a lens remain.

Hardy[17] calls attention to an interesting phenomenon which he has observed with small lenses of carbon disulfide. This is exhibited by other highly volatile liquids whose lenses are imbedded in monolayers. Two small lenses, if they come within 1 or 2 cm, of each other, act as if violently attracted and move rapidly toward each other until close together, when they are just as violently repelled. However, if the velocity of approach exceeds a critical value, the two lenses fuse into one.

Monolayers may in general be compressed to higher values of π_f, that is lower values of γ_f, than corresponds to equilibrium with a lens or crystal of the material at the given temperature. For example, at 20°C an ordinary crystal of stearic acid gives an equilibrium film pressure of only 3.1 dyne cm^{-1}, but by rapid compression it is possible to obtain the pressure-area ($\pi\cdot\sigma$) relation without much error up to film pressures as high as 50 dyne cm^{-1}, that is, to a free surface energy level as low as 22.8 erg cm^{-2}. In fact, a considerable fraction of the data in the literature, which have been used to give $\pi\cdot\sigma$ diagrams, have been obtained in the regions of instability.

14. The Non-Spreading of Water on Organic Liquids

From the relation for the initial spreading coefficient

$$S_{b/a}=W_A-W_{C_b}=\gamma_a-(\gamma_b+\gamma_{a'b'})$$

it is found that water will not spread on any organic liquid for which the relations are known, and presumably not on any organic liquid. Here a is an oil and b is water. For isopentane $S_{w/o}=13.7-(72.8+49.6)=-108.7$, an extremely large negative value. For carbon disulfide $S_{w/o}=31.4-(72.8+48.6)=-90$. For water on primary isoamyl alcohol, $S_{b/a}=23.7-(72.8+5.0)=-54.1$. However the greater mutual solubility of a pair of liquids such as these, reduces greatly the value of the final spreading coefficient. Thus for this alcohol $S_{b'/a'}=23.6-(25.9+5.0)=-7.3$, which, while still negative, is very small for water on an oil. However, it is obvious that the smallness of this value is due to the great reduction of the free surface energy of the water which is caused by the oil.

15. The Spreading of Liquids and Solids on Mercury (Fig. 2)

The free surface energy of mercury in erg cm^{-2} is: 480 at 0°C; 476 at 20°C, and 467 at 60°C. The

[17] W. Hardy, Proc. Roy. Soc. **A88**, 560 (1913).

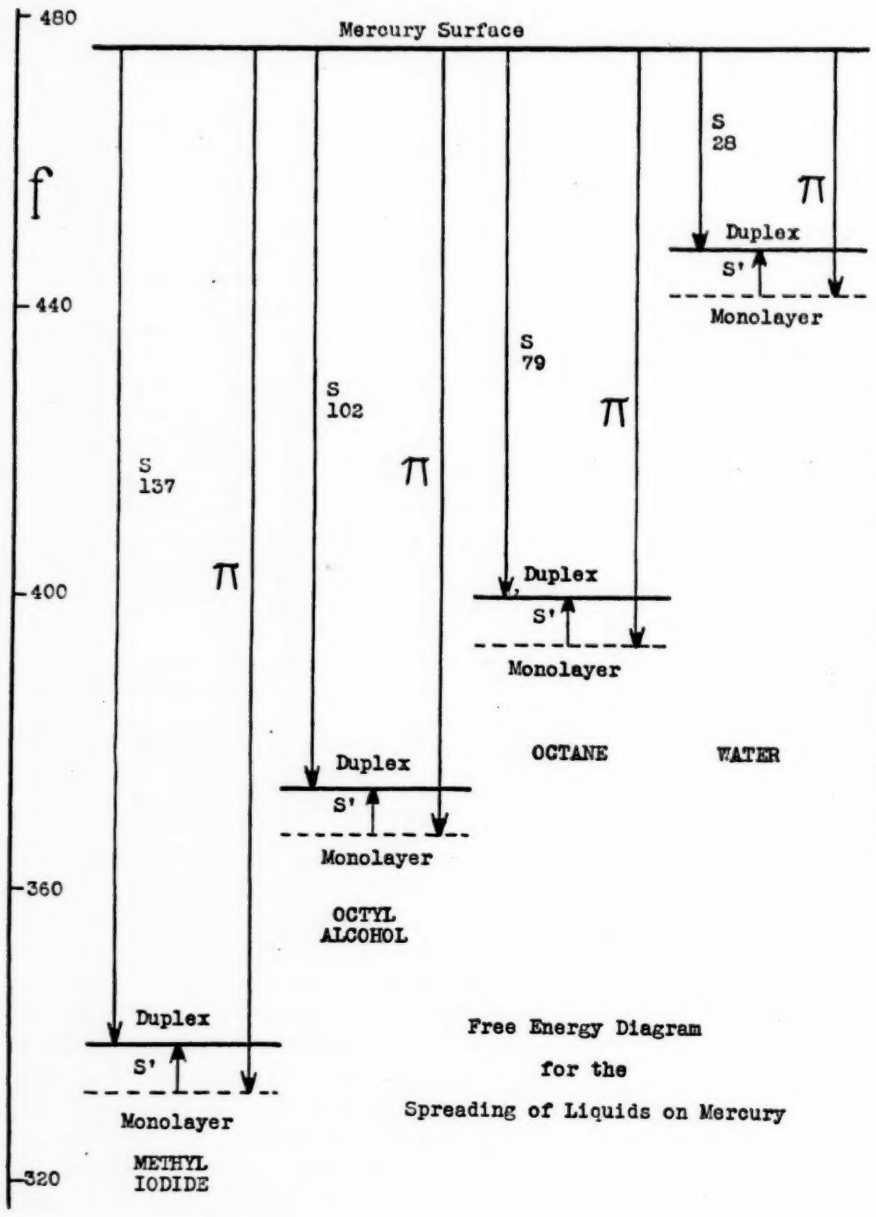

FIG. 2. Water and all organic liquids have positive initial spreading coefficients on mercury, and thus may spread to form duplex films. The monolayers lie at a lower free energy level, so the duplex film, if formed, transforms into a monolayer and a lens. The free energy levels of the duplex films are known and are properly placed in the diagram. Those for the monolayers have not been determined, so only the sign of the final spreading coefficient (S') is known. While the film pressure π_e is larger than the initial spreading coefficient $S_{b/a}$, it is probable that it is not very much larger, so the diagram gives the general location of the free energy level for each monolayer.

total surface energy (h or ϵ) is 540. Thus if a free energy diagram, similar to Fig. 1, is constructed for the spreading of liquids or solids on mercury, the level for the mercury surface at 20°C is very high (476). The result of this is that all duplex and all monolayer levels for water and for oils lie far below the mercury level. There is a large decrease in free energy if water or any liquid oil spreads as a duplex film on mercury. Thus water and all organic liquids spread on mercury.

There are no reliable determinations of the final spreading coefficient $S_{b'/a'}$ or of the equilibrium film pressure for any liquid on mercury. However the lenses which form on the non-duplex film, presumably a monolayer, indicate that this film pressure is somewhat greater than the initial spreading coefficient, $S_{b/a}$. In ergs per cm^{-2} this quantity has the values: water, 32; acetone, 60; hexane, 79; propyl alcohol, 85; carbon tetrachloride, 93; benzene, 90; chloro-

form, 97; octyl alcohol, 102; ethylene bromide, 116; ethyl iodide, 135; and methyl iodide, 137.

Many organic solids are found to spread on the clean surface of mercury.

16. The Spreading of Liquids on the Surface of Crystalline Solids

Insofar as the periodic surface field of a solid may be considered as a uniform field, the free energy relations involved in the spreading of a liquid over the surface of a solid are the same as when the subphase is a liquid, except that with inorganic solids of high melting point W_A is very much higher. The phenomena, however, are very different. In the atmosphere practically all inorganic solids are covered with a film of water, and if this is the case the spreading of another liquid or of more water is often prevented. Both the rigidity and the periodic electrical field of the surface of the solid, have a great influence on the rate of spreading.

The spreading of a pure liquid over the clean surface of a solid does not seem to occur, as it may on a liquid, by the pulling out of a duplex film from the lens, but by the spreading of a monolayer. The rate of formation of the monolayer by the process of spreading may, however, be less than its rate of formation from the vapor of the liquid. It is obvious that this condensation may form a polymolecular film on the surface of the solid, and, on account of the lack of mobility, neither the surface of the solid nor the first monolayer will move to make a place for the molecules of a second layer. Hardy[18] gives an interesting example of spreading on glass. A drop of anhydrous acetic acid remains drawn up as a lens on a clean dry glass plate, but if the atmosphere is admitted for even a moment, the slight amount of moisture causes the drop to flash over the whole surface.

It is now well known that films adsorbed on solid surfaces may be mobile, as shown by Volmer and collaborators,[19] or immobile. It is not the purpose of this paper to deal with immobile layers. It has been shown recently[20] that certain short chain organic acids, salts, alcohols, and amines, form gaseous adsorbed films at the interface between water and a solid, such as stibnite, graphite, talc, or paraffin.

The conclusion which may be drawn from the above relations is that the spreading coefficient relations presented in this paper are applicable to the spreading of mobile films over solids. If duplex films do not spread directly, it is obvious that the steps in which they are involved should be omitted.

With solids such as $BaSO_4$, TiO_2, $ZrSiO_4$, ZrO_2, and all other solids of high cohesion, the initial spreading coefficient is undoubtedly positive. That is, the spreading of the liquid film over the surface of any solids of this type gives a decrease of free energy. On solid paraffin however, the coefficient for water, as is well known, has a large negative value. This is true for many other organic solids.

17. The Principle of Independent Surface Action and the Spreading of Carbon Tetrachloride on Water

The extent to which the principle of independent surface action is correct is exhibited in

Table III. *Increase in molecular potential energy when a liquid is pulled apart (ϵ_C), or from another liquid (ϵ_A) (ergs for a bar of liquid 1 cm² in cross section, for the separation of the upper from the lower liquid) ($t = 20°C$).**

n-Octane	*n*-Octyl Alcohol	*n*-Heptylic Acid	*n*-Heptane
100	101	105	100
n-Octane	*n*-Octyl Alcohol	*n*-Heptylic Acid	*n*-Heptane
n-Octane	*n*-Octyl Alcohol	*n*-Heptylic Acid	*n*-Heptane
107	165	151	106
Water	Water	Water	Water

Effect of the Length of the Hydrocarbon Chain on the Cohesional Energy

n-Butane	*n*-Butyl alcohol	*n*-Propyl alcohol	Propane
92	97	96	68
n-Butane	*n*-Butyl alcohol	*n*-Propyl alcohol	Propane

* The shortening of the chain a paraffin hydrocarbon produces its first very marked effect in lowering the cohesional energy in the decrease from 4 to 3 carbon atoms in the hydrocarbon chain. Shortening the chain has little effect with the alcohols, which give 97 and 98 erg cm^{-2} for ethyl and methyl alcohols, respectively.

[18] W. Hardy, *Collected Papers*, p. 713.

[19] Volmer and Estermann, Zeits. f. Physik **7**, 13 (1921); Volmer and Adhikari, Trans. Faraday Soc. **28**, 359 (1932).

[20] W. D. Harkins and F. M. Fowkes, J. Am. Chem. Soc. **60**, 1511 (1938); F. M. Fowkes and W. D. Harkins, *ibid.* **62**, 3377 (1940).

the early work of the writer and his collaborators[21] on the free energy relations of surfaces and interfaces, but is shown even more perfectly by the magnitude of the increase of molecular potential energy when liquids are pulled apart,[22] at a plane inside the body of liquid. The relations are illustrated (Table III) by the numbers which give the increase in potential energy in ergs when a column of liquid 1 cm^2 in cross section is pulled into two parts.

It is remarkable that the increase of molecular potential (internal) energy which accompanies the separation of the polar-non-polar liquid (alcohol or acid) is only 1 or 5 percent higher than when the non-polar saturated liquid (*n*-octane or *n*-heptane) is involved. Since this amount of energy, of the order of 3 ergs per cm of interface, is surprisingly small for the energy of orientation of the molecules of octyl alcohol or heptylic acid, it is evident that the polar groups exert no appreciable effect on the energy of separation of the liquid when this separation occurs between the hydrocarbon chains only, that is after the molecules are oriented at the plane of separation (Fig. 3). This is not a surprising result, as the distance between the polar groups under these conditions is of the order of 22A and it is known that for a given relative orientation of a pair of dipoles, the interaction energy decreases as the cube of the distance between them.

Even though the dipoles in water molecules give a strong interaction with other permanent dipoles it is evident that only six or seven percent more energy is required to separate either heptane or octane from water than from itself. This indicates that the dipoles induced in the paraffin by the water are weak. Obviously the London dispersion forces are not the same when water constitutes one of the phases at the phase boundary, as when an oil is on both sides of an imaginary boundary.

If the acid or alcohol is pulled from water at the interface the close proximity of the polar groups results in a large increase in the energy of separation to 165 ergs for the alcohol and 151 ergs for the alcohol.

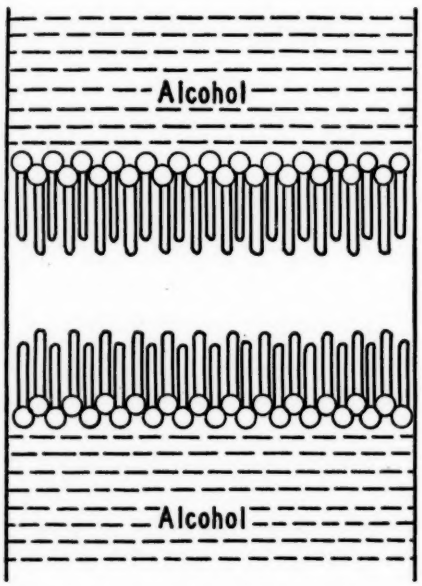

FIG. 3. Idealized diagram illustrating the separation of a bar of liquid alcohol into two parts. The molecules are represented as already oriented at the interface, since the break is well under way. This diagram indicates that in such an ideal case the energy of separation of a moderately long chain alcohol should be practically equal to that of a hydrocarbon of the same molecular size, except for the relatively small energy of orientation of the molecules at the interface before the actual separation has occurred.

The principle of independent surface action indicates merely that the behavior of surfaces and interfaces is in accord with the idea that the range of intermolecular forces is very small.

By the use of this principle Langmuir[23] reaches the conclusion that "in general the properties of the upper surface of an adsorbed monomolecular film are nearly the same as those of the substance in bulk."

As an example illustrating the correctness of this point of view he states: "Carbon tetrachloride vapor forms an adsorbed monomolecular film on water which tends to become nearly complete before the vapor becomes saturated. The properties of the upper surface of the film thus approximate to that of liquid carbon tetrachloride, so that the life of the molecules of CCl_4 which may condense on the film is about the same as that of molecules on liquid CCl_4. *Thus the film grows in thickness which means that* $F_s=0$."

[21] W. D. Harkins, F. E. Brown, and E. C. H. Davies, J. Am. Chem. Soc. **39**, 354 (1917); W. D. Harkins, E. C. H. Davies, and G. L. Clark, *ibid.* **39**, 541 (1917).

[22] W. D. Harkins, Zeits. f. physik. Chemie **A139**, 670 (1928).

[23] I. Langmuir, J. Chem. Phys. **1**, 775 (1933).

In contrast with this, all determinations of the initial spreading coefficient of CCl_4, $-(\partial F/\partial\sigma)_{p,T} = S_{b/a} = F_S$, give a small positive value, and a direct experiment shows that the film which spreads on a clean water surface from a lens of the liquid "pushes" talc powder in front of it to form a circular area free from talc. After the film has spread any excess of liquid remains as a lens, almost flat above and quite curved below. The stability of the lens indicates that the final spreading coefficient is negative.

The fact that the lens remains on the surface in a saturated atmosphere of the vapor indicates that the mechanism postulated by Langmuir is incorrect. Thus the film does not thicken beyond a monolayer by condensation of the vapor, and the spreading relations of CCl_4 are not changed, by its low value of $S_{b/a}$, from those postulated earlier in this paper for liquids which have higher positive initial coefficients. Even if the initial coefficient were exactly zero this would not allow the monolayer to become thicker, since the final coefficient ($S_{b'/a'}$) would still be negative. As pointed out earlier, this causes any molecules, which cannot be accommodated in the monolayer, to move into the lens.

18. The Spreading of a Solid as a Non-Duplex Film

Acids, alcohols, amines, and other substances of the polar-non-polar type spread readily on water if the molecular weight is not too large. This fact has given rise to the idea that the presence of a polar group or groups in the molecule always gives rise to spreading, but this is incorrect. What the polar group does, in general, is to make the adhesion of the oil for the water relatively greater, when compared with the work of cohesion of the oil itself, than if the polar group were absent.

However, if the nonpolar part of the molecule is a sufficiently large fraction of the whole the cohesion may become high enough to inhibit spreading. In the case of an oil a sufficient increase in cohesion causes the material to take on a solid, rather than a liquid state. The solid state does not, of itself, prevent spreading, but does eliminate spreading as a duplex film. Thus the films formed by the direct spreading of a solid are monolayers.

A monolayer formed by the direct spreading of a solid (e.g., an acid, alcohol, amine, etc.) may be in the solid state, or any one of the known liquid states. If the equilibrium film pressure is too low to give one of these more or less condensed states, the solid may, nevertheless, vaporize in the surface to give a two-dimensional gaseous film.

Crystals of myristic acid exhibit non-duplex or monolayer spreading on the surface of clean water. The type of monolayer which is in equilibrium with the crystals is dependent upon the temperature. Thus at 12.5°C a condensed liquid (L_2) monolayer is formed, at 16° the film is in the intermediate, and at 23° in the liquid expanded (L_1) state. At 30°C octadecyl alcohol spreads to give at equilibrium a monolayer which is in the solid state, with a film pressure (π_e) of 34 dyne cm^{-1}. The equilibrium pressure of an alcohol is much higher than that of an acid, if the hydrocarbon chain is the same in both.

As the length of the hydrocarbon chain is increased, the equilibrium film pressure, at a given temperature, decreases. As a result of this, acids with sufficiently long chains spread to give gaseous monolayers only. This seems to be true of arachidic acid, the normal acid with 20 carbon atoms per molecule, which, at 20°C, gives an equilibrium pressure of only a few tenths of a dyne per cm. If the number of carbon atoms is 19 or 21 the equilibrium pressure is considerably higher.

It is evident that if the length of the hydrocarbon chain of a polar-non-polar or a non-polar substance is increased sufficiently, the equilibrium pressure of the gaseous film will be so low that it cannot be measured or detected by a film balance of any sensitivity now employed. From the practical standpoint such a substance can be considered as non-spreading.

Thus non-spreading organic substances are not limited to those whose molecules are wholly non-polar. If a polar group is present, spreading may be attained by an increase in size of the non-polar part of the molecule.

19. The General Effect of the Type of Molecule Upon the Spreading of a Liquid on Water

Table IV shows how the stability of the duplex and monomolecular types of film depends upon the molecular nature of the liquid which

TABLE IV. *Effect of molecular constitution upon the formation of duplex films and of monolayers.*

MOLECULES OR GROUPS	ATTRACTION FOR WATER W_A	ATTRACTION FOR LIKE MOLECULES W_C	DUPLEX FILM[1]	STABILITY OF MONOLAYER
Hydrocarbons of high molecular weight	Weak 60	Weak 65	None	None or gaseous
$-CH_2I$, $-CH_2Br$, $-CH_2I$	Moderately strong 75	Strong 100	None	None or gaseous
Hydrocarbons of low molecular weight	Weak 45	Weak 40	Unstable	Gaseous
Esters	Strong 80	Weak 50	Unstable	Stable. Relatively high compressibility
$-CH_2OH$, $-COOH$, $-CN$, $-CONH_2$, $-C_6H_4OH$, $-NHCONH_2$, etc.	Very strong 100	Weak 50	Unstable	Stable liquid, solid and gaseous
$-SO_3H$, $-C_6H_4SO_3H$, $-SO_4H$	Extremely strong	Moderately weak	Forms if material liquid. Unstable	Form monolayers
Soaps (solids)	Extremely strong	Moderately weak	None	Form monolayers

[1] If the spreading material is a solid, a duplex film does not form, but only a monolayer spreads. See Section 12 for the spreading of a duplex film of an oil which, of itself, does not spread in this way, by the addition of a polar-non-polar oil as a second component.

forms the spreading or non-spreading phase. The free energy values listed represent typical magnitudes. It is obvious that these vary considerably with chain length and other factors which are not indicated with any completeness in the table.

JULY, 1941 JOURNAL OF CHEMICAL PHYSICS VOLUME 9

The Equation of State of Solid Helium

BROTHER GABRIEL KANE
Manhattan College, New York, New York

(Received June 6, 1941)

THE idealized crystal is one in which particles form a perfectly ordered array and execute small oscillations about equilibrium positions. This hypothetical picture may be used as a starting point to determine the equation of state of a solid and to establish a theory of fusion. The simplest case to consider is that of frozen rare gases. The only forces existing between two rare gas atoms are the Heitler-London forces of repulsion and the van der Waals forces of attraction. The potential energy of the crystal is determined by making a summation over the whole lattice of the potential energy of interaction between pairs. The elastic constants may be determined from the interatomic forces and the frequency of oscillation from the elastic constants. The total energy of the crystal is

$$U=N\Phi/2+\tfrac{3}{2}Nh\bar{\nu},$$

being made up of the lattice potential energy and the zero-point energy. The minimum of total energy should give the heat of sublimation at absolute zero and the lattice distance between atoms. The shift from minimum of potential energy to minimum of total energy, which is produced by the zero-point energy, causes a change in both lattice distance and heat of sublimation. This change is most noticeable with the lighter elements. For temperatures above absolute zero, the free energy is

$$A=U-TS.$$

TABLE I. *Energy is in kilojoules, r in angstroms, V in cm³, p in atmospheres. θ=hν/k in degrees Kelvin. Figures in column containing minimum pressures are italicized.*

	Calculated Values						Experimental Values
r	2.80	2.85	2.90	*2.93*	2.95	3.00	3.57
V	9.35	9.86	10.39	*10.65*	10.93	11.50	17.4
$\frac{3}{2}Nh\bar{\nu}$	1.004	0.852	0.682	*0.630*	0.584	0.439	
$-N\Phi/2$	0.918	0.880	0.839	*0.815*	0.793	0.747	
U	−0.086	0.028	0.157	*0.185*	0.209	0.308	0.050
θ	107.4	91.0	72.8	*67.4*	62.5	46.9	32
p_0	2020	2470	1440	*830*	1600	2500	25

From this, the equation of state may be established since

$$p=-(\partial A/\partial V)_T.$$

Each isotherm drawn on a pressure-volume diagram has a minimum. Since any state is unstable where pressure increases with volume, the crystal must break down at this minimum pressure. The temperature of the isotherm whose minimum pressure is zero is interpreted as the melting point.

Following this line of procedure, the calculations were made for frozen argon and helium by Herzfeld and Goeppert Mayer.[1] For helium, they used the formula derived by Slater and Kirkwood;[2]

$$\varphi=\{770e^{-4.60r}-1.49/r^6\}10^{-12}\text{ erg}.$$

They considered helium as a cubic face-centered crystal and calculated the lattice distance, melting point, and Debye temperature. The agreement with experimental results was poor. For argon, they used the form

$$\varphi=ABe^{-r/\rho}-A/r^6,$$

in which the coefficients A and B were to be determined so as to make the minimum of the total energy curve coincide with the experimental interatomic distance and heat of sublimation at absolute zero. Two values were chosen for ρ, one deduced theoretically for two neon atoms ($\rho=0.2091$A), and the other for alkali halide crystals ($\rho=0.345$A). Kane[3] made the calculations for neon, krypton, and xenon and recalculated the results for argon. The agreement with experimental melting point was fairly good but not remarkable. He showed also that the use of second-order van der Waals terms produced only slight changes.

In the present paper the equation of state is deduced for solid helium. For the potential energy of interaction between two helium atoms, the values determined by Margenau[4] have been used

$$\varphi=\{770e^{-4.60r}-560e^{-5.33r}-1.39/r^6-3.0/r^8\}10^{-12}\text{ erg}.$$

The crystal has been considered as hexagonal close-packed with an ideal axial ratio.[5] The summations for potential energy and those to be used in the frequency formula have been made by Kane and Goeppert Mayer.[6] The formula for the frequency has been derived directly from the equations of motion of a particle. It is difficult to interpret the terms of the formula as elastic constants,[7] but there is no doubt about the validity of the result. The other rare gases have cubic lattices and therefore the symmetry relations make it quite easy to identify the terms as elastic constants. In a previous paper[8] the author stated that the frequency formula that Herzfeld and Goeppert Mayer had used was valid only at the minimum of potential energy. It now appears that their formula was correct and, consequently, that Kane's was wrong. The error arose from using Born's[8] formula for frequency which does not hold for cases of displacement from equilibrium. Any change resulting should be greatest for neon. Therefore, the calculations were repeated for this element using one value of ρ ($\rho=0.2091$). It was found that the error was slight and that deviations in the pressure-volume curves were negligible.

[1] K. F. Herzfeld and M. Goeppert Mayer, Phys. Rev. **46**, 995 (1934). In Table V the values for the potential energy and zero-point energy should be interchanged.

[2] J. C. Slater and J. G. Kirkwood, Phys. Rev. **37**, 682 (1931).

[3] G. Kane, J. Chem. Phys. **7**, 603 (1939).

[4] H. Margenau, Phys. Rev. **56**, 1000 (1939).

[5] W. H. Keesom and K. H. Taconis, Proc. K. Acad. Amst. **41**, 95 (1938); Comm. Leiden No. 250e.

[6] G. Kane and M. Goeppert Mayer, J. Chem. Phys. **8**, 642 (1940). Summations for hexagonal lattice are slightly larger than for cubic face-centered.

[7] M. A. Biot, Phil. Mag. **27**, 468 (1939).

[8] M. Born, *Dynamik der Kristallgitter* (Leipzig, 1923), p. 648.

The results for the calculations on helium using Margenau's formula have been tabulated in Table I. The agreement with experimental values is rather poor in all cases. The difference between experimental interatomic distance and the positions of minimum total energy may be accounted for to some extent by the fact that what is measured experimentally is not the equilibrium distance but the time-average position. Since the vibrations of helium are very large and anharmonic it follows that there should be considerable difference between the two. There seems to be no method available for correlating these two positions, since the crystal breaks down completely shortly beyond the equilibrium point due to the fact that the elastic constants become negative.

The method of Lennard-Jones[9] with assumptions of order-disorder transitions, may be applied to the equation of state of helium. This has been done by Nagamiya,[10] using Margenau's potential energy formula. His agreement with experimental results is remarkably good. However, in using Margenau's results, he changes the sign before $560e^{-5.33r}$ from minus to plus. This change of sign invalidates his results.

---

[9] J. E. Lennard-Jones and A. F. Devonshire, Proc. Roy. Soc. **A169**, 317 (1939).
[10] T. Nagamiya, Proc. Phys. Math. Soc. Japan **22**, 492 (1940).

Letters to the Editor

THIS section will accept reports of new work, provided these are terse and contain few figures, and especially few halftone cuts. The Editorial Board will not hold itself responsible for opinions expressed by the correspondents. Contributions to this section should not exceed 600 words in length and must reach the office of the Managing Editor not later than the 15th of the month preceding that of the issue in which the letter is to appear. No proof will be sent to the authors. The usual publication charge ($3.00 per page) will not be made and no reprints will be furnished free.

The Restricted Rotation Potential and Frequency Assignment in Propylene

D. TELFAIR AND W. H. PIELEMEIER
Physics Department, The Pennsylvania State College, State College, Pennsylvania
June 5, 1941

THE assignment of the fundamental vibrational frequencies given by Pitzer,[1] and a potential restricting rotation of the methyl group in propylene of about 800 cal./mole are not in disagreement with the heat capacity measurements reported by Kistiakowsky and Rice.[2] However, Wilson and Wells'[3] frequency assignment and a potential restricting rotation of about 2000 cal./mole are also in accord with the reported values of the heat capacities.

The temperature range of heat capacity measurements has recently been extended in this laboratory by supersonic methods with results which make possible a choice between the two suggested potentials and frequency assignments. As shown in Fig. 1 the measured heat capacities at the higher temperatures (between 360 and 500°K) are still in excellent agreement with the Wilson-Wells assignment and a 200 cal./mole potential, but values calculated from Pitzer's assignment and an 800 cal./mole potential deviate considerably more than the limits of accuracy of the measurements.

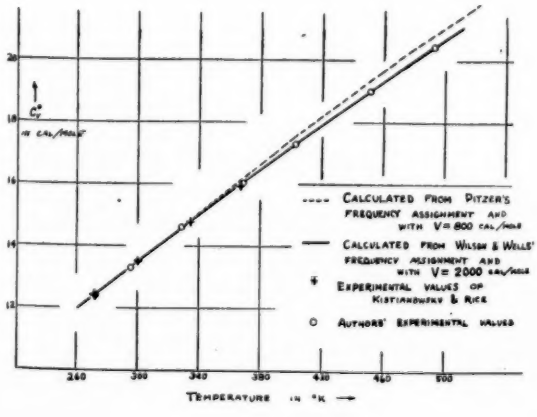

FIG. 1.

The entropy of propylene calculated on Pitzer's basis agrees with the measured values if one assumes an entropy of mixing due to the inability of the solid to distinguish between the two ends of the propylene molecule. However, Aston and his co-workers have recently found that cyclopentane is non-planar[4] by comparison of the third law entropies with the spectroscopic values. The five corners, although not all lying in the same plane, must resemble each other more closely than do the two ends of propylene. Aston's results show no entropy of mixing in the solid phase, and, therefore, an ordered arrangement in the crystal. Had the crystal not distinguished between the CH_2 groups in cyclopentane, the third law entropies would have appeared to correspond to a planar ring in spite of its non-planar structure.

Thus an entropy of mixing cannot be expected in propylene. Calculated on this basis, the Wilson-Wells frequency assignment and a 2000 cal./mole potential agree well with the measured entropy, whereas Pitzer's frequency assignment and an 800 cal./mole potential do not.

A description of the apparatus and justification of the methods used in the heat capacity measurements will appear later. We are indebted to the Pennsylvania State College Cryogenic Laboratory for furnishing the purified sample of propylene used for these measurements.

[1] K. S. Pitzer, J. Chem. Phys. **5**, 473 (1937); Chem. Rev. **27**, 39 (1940).
[2] G. B. Kistiakowsky and W. W. Rice, J. Chem. Phys. **8**, 610 (1940).
[3] E. B. Wilson and A. J. Wells, J. Chem. Phys. **9**, 319 (1941).
[4] J. G. Aston, private communication.

The Exchange Reaction between Gaseous and Combined Nitrogen

YOSHIO NISHINA, TAKEO IIMORI, HIDEO KUBO AND HIROMI NAKAYAMA
The Institute of Physical and Chemical Research, Komagome, Hongo, Tokyo, Japan
June 2, 1941

BY using heavy nitrogen gas Burris and Miller[1] have recently concluded that no exchange takes place between gaseous and combined nitrogen during the process of nitrogen fixation by *Azotobacter*. A possibility, however, cannot be excluded that in some other cases the exchange reaction of nitrogen may happen between nitrogen gas and some nitrogenous constituents of the plants. In fact, the following results of our experiments show quite clearly that the exchange reactions of nitrogen do occur to a certain extent between nitrogen gas and some nitrogen compounds, which are considered to exist in plant juices. Whether or not these exchanges are strong enough to be taken into account for the experiments of nitrogen fixation will be seen in the future.

Radioactive nitrogen N^{13} gas (half-life 10.5 min.) was obtained by bombarding amorphous carbon with 3-Mev deuterons from our cyclotron, the carbon being then heated in a closed vessel containing air. In order to get the gas completely freed from impurities NO, NO_2 and NH_3, it

TABLE I.

SUBSTANCE TESTED	CONCENTRATION MOLE/l	SUBSTANCE PRECIPITATED	RELATIVE INTENSITY OF RADIOACTIVITY
$NaNO_3$	1/10, 1/20	nitron nitrate	10
$NaNO_2$	1/20, 1/40	nitron nitrate	1
$NH_2OH \cdot HCl$	1/20	nitron nitrate	5
NH_4Cl	1/10	$(NH_4)_2PtCl_6$, Hg_2ONH_2I	<0.01
KCN	1/20	AgCN	<0.01
$N_2H_4 \cdot H_2SO_4$	1/10	benzalazine	<0.01
$Na_3Co(NO_2)_6$	1/20	$K_2NaCo(NO_2)_6$	3–5
8-hydroxyquinoline acetate	1/20	TiO-hydroxyquinolate	3
$CO(NH_2)_2$	1/10	(evaporated up)	~0.1

was vigorously shaken repeatedly with caustic soda solution containing potassium permanganate, and with dilute sulphuric acid. For the study of the exchange reaction mentioned above, the gas thus purified was introduced into a bottle containing aqueous solutions of various nitrogen compounds in question, and shaken for a few minutes. After the gas was carefully driven out of the solutions, the bottle was thoroughly evacuated in order to get rid of nitrogen gas absorbed by the solutions. Nitrogen compounds under consideration were then precipitated by the addition of appropriate reagents and the radioactivities of the precipitates were examined by a Geiger-Müller tube counter. Nitrite and hydroxylamine, before being precipitated, were oxidized to nitrate by adding excess of acidic permanganate and hypochlorite, respectively. The results are shown in Table I.

As is seen from the results, the exchange reaction of nitrogen occurs between gaseous nitrogen and nitrite, hydroxylamine, etc. The rate of exchange reaction in the case of nitrite was rather rapid, though not immeasurable. The concentration of the solution was proved to have a remarkable effect on the rate of the reaction. In the cases of nitrite or nitrate, for example, this rate was constant in dilute solutions, but decreased with the increase of concentration above 1/10 mole/l and no exchange was observed even in the solution of 2 moles/l. As it is difficult to conceive that the amount of nitrogen gas absorbed by such dilute solutions would differ according to compounds in such a marked degree, the effects observed are hardly to be ascribed to the phenomena of gas absorption by solutions. Some of the solutions, moreover, are all converted into nitrate before precipitation and the great difference still observed among these compounds confirms our conclusion.

The absolute rate of reaction together with the details of experiment will be published in the *Scientific Papers* of this Institute.

[1] R. H. Burris and C. E. Miller, Science **93**, 114 (1941).